การเตรียมตัวเร่งปฏิกิริยาไฮโดรเทอร์มอลคาร์บอนจากรำข้าวสกัดน้ำมันและน้ำตาลกลูโคสที่มีความเสถียรต่อการแปรสภาพชีวมวลเป็น 5-ไฮดรอกซีเมทิลเฟอฟูรอล

นางสาวปิยาภรณ์ วทานิยะกุล

วิทยานิพนธ์นี้เป็นส่วนหนึ่งของการศึกษาตามหลักสูตรปริญญาวิศวกรรมศาสตรดุษฎีบัณฑิต
สาขาวิชาวิศวกรรมเคมี ภาควิชาวิศวกรรมเคมี
คณะวิศวกรรมศาสตร์ จุฬาลงกรณ์มหาวิทยาลัย
ปีการศึกษา 2560

Preparation of Stable Hydrothermal Carbon-Based Catalyst from Defatted Rice Bran and Glucose for Biomass Conversion to 5-Hydroxymethylfurfural

Miss Piyaporn Wataniyakul

A Dissertation Submitted in Partial Fulfillment of the Requirements
for the Degree of Doctor of Engineering Program in Chemical Engineering
Department of Chemical Engineering
Faculty of Engineering
Chulalongkorn University
Academic Year 2017

Thesis Title	Preparation of Stable Hydrothermal Carbon-Based Catalyst from Defatted Rice Bran and Glucose for Biomass Conversion to 5-Hydroxymethylfurfural
By	Miss Piyaporn Wataniyakul
Field of Study	Chemical Engineering
Thesis Advisor	Professor Artiwan Shotipruk, Ph.D.

Accepted by the Faculty of Engineering, Chulalongkorn University in Partial Fulfillment of the Requirements for the Doctoral Degree

.....Dean of the Faculty of Engineering
(Associate Professor Supot Teachavorasinskun, Ph.D.)

THESIS COMMITTEE

.....Chairman
(Varun Taepaisitphongse, Ph.D.)

.....Thesis Advisor
(Professor Artiwan Shotipruk, Ph.D.)

.....Examiner
(Palang Bumroongsakulsawat, Ph.D.)

.....Examiner
(Associate ProfessorTharathon Mongkhonsi, Ph.D.)

.....External Examiner
(ProfessorNavadol Laosiripojana, Ph.D.)

ปิยาภรณ์ วทานิยะกุล : การเตรียมตัวเร่งปฏิกิริยาไฮโดรเทอร์มอลคาร์บอนจากรำข้าวสกัดน้ำมันและน้ำตาลกลูโคสที่มีความเสถียรต่อการแปรสภาพชีวมวลเป็น 5-ไฮดรอกซีเมทิลเฟอฟูรอล (Preparation of Stable Hydrothermal Carbon-Based Catalyst from Defatted Rice Bran and Glucose for Biomass Conversion to 5-Hydroxymethylfurfural) อ.ที่ปรึกษาวิทยานิพนธ์หลัก: ศ. ดร. อาทิวรรณ โชติพฤกษ์, 156 หน้า.

งานวิจัยนี้มีจุดมุ่งหมายเพื่อศึกษาการเตรียมตัวเร่งปฏิกิริยาไฮโดรเทอร์มอลคาร์บอนจากรำข้าวและน้ำตาลกลูโคสเพื่อใช้ในการแปรสภาพชีวมวลเป็น 5-ไฮดรอกซีเมทิลเฟอฟูรอล โดยพิจารณาผลของอุณหภูมิ (180-250 องศาเซลเซียส) และเวลา (1-8 ชั่วโมง) ในการคาร์บอไนเซชันต่อปริมาณและลักษณะทางเคมีของ HTC หลังจากนั้นทำการติดหมู่ซัลโฟนิก HTC ด้วยกรดซัลฟูริกเพื่อเตรียมตัวเร่งปฏิกิริยา HTC-SO_3H และทำการทดสอบความเสถียรของตัวเร่งปฏิกิริยาโดยพิจารณาปริมาณของผลิตภัณฑ์จากการแปรสภาพชีวมวลที่ถูกชะด้วยน้ำที่สภาวะการแปรสภาพชีวมวล จากการทดสอบพบว่า ไม่มีปริมาณ 5-ไฮดรอกซีเมทิลเฟอฟูรอลและเฟอฟูรอล และมีกรดลิวูลินิกและกรดฟอร์มิกปริมาณน้อย ถูกชะออกมาจาก HTCDRB-SO_3H ที่สังเคราะห์จาก HTCDRB ที่เตรียมจากการคาร์บอไนเซชันที่อุณหูมิ 220 องศาเซลเซียส เป็นเวลา 3 ชั่วโมง แสดงให้เห็นว่าสภาวะดังกล่าวเหมาะสมสำหรับการเตรียม HTCDRB-SO_3H เมื่อเปรียบเทียบเสถียรภาพของ HTCDRB-SO_3H และ HTCG-SO_3H ที่เตรียมที่สภาวะเดียวกัน พบว่า HTCG-SO_3H มีเสถียรภาพน้อยกว่า อย่างไรก็ตามยังมีการศึกษาการปรับปรุงเสถียรภาพของ HTCG-SO_3H โดยการเพิ่มเวลาในการคาร์บอไนเซชัน (6-24 ชั่วโมง) พบว่า HTCG ที่สภาวะต่างๆของการคาร์บอไนเซชันมีลักษณะทางเคมีและโครงสร้างเหมือนกัน ส่วนของเหลวที่ได้หลังผ่านไฮโดรเทอร์มอลคาร์บอไนเซชันสามารถบอกความเสถียรของ HTCG ได้ โดยสภาวะที่เหมาะสมในการเตรียมคาร์บอนจากน้ำตาลกลูโคสให้มีความเสถียร คือ ไฮโดรเทอร์มอลคาร์บอไนเซชันที่อุณหภูมิ 220 องศาเซลเซียสเป็นเวลา 6 ชั่วโมง นอกจากนี้ตัวเร่งปฏิกิริยาที่เตรียมจากสภาวะที่เหมาะสมมีความสามารถในการเร่งปฏิกิริยาไฮโดรไลซิสของเซลลูโลสและดีไฮเดรชันของน้ำตาลฟลุ๊กโตสได้ค่อนข้างสูง

ภาควิชา วิศวกรรมเคมี ลายมือชื่อนิสิต .....

สาขาวิชา วิศวกรรมเคมี ลายมือชื่อ อ.ที่ปรึกษาหลัก .....

ปีการศึกษา 2560

5671421121 : MAJOR CHEMICAL ENGINEERING
KEYWORDS: HYDROTHERMAL CARBONIZATION, HYDROTHERMAL CARBON-BASED CATALYST, DEFATTED RICE BRAN, GLUCOSE, BIOMASS CONVERSION, 5-HYDROXYMETHYLFURFURAL

PIYAPORN WATANIYAKUL: Preparation of Stable Hydrothermal Carbon-Based Catalyst from Defatted Rice Bran and Glucose for Biomass Conversion to 5-Hydroxymethylfurfural. ADVISOR: PROF. ARTIWAN SHOTIPRUK, Ph.D., 156 pp.

This research investigated the preparation of hydrothermal carbon-based catalysts (HTC-SO_3H) derived from defatted rice bran (DRB) and glucose for biomass conversion to 5-hydroxymethylfurfural (HMF). Firstly, the effects of hydrothermal carbonization conditions: temperature (180-250 °C) and time (1-8 h) on the yield and the chemical characteristics of the hydrothermal carbons (HTCs) were investigated. The HTCs were then sulfonated with sulfuric acid to obtain HTC-SO_3H catalysts. The stability of the catalysts was evaluated based on the amount of biomass conversion products leached into the water at a specified biomass conversion condition. Since no HMF and furfural, and only small amounts of levulinic acid and formic acid, were leached from DRB derived HTC-SO_3H (HTCDRB-SO_3H) catalyst synthesized from the DRB derived HTC (HTCDRB) prepared at the carbonization condition of 220 °C for 3 h, this condition was suggested to be a suitable carbonization condition for the preparation. Compared with HTCDRB-SO_3H, the glucose derived HTC-SO_3H (HTCG-SO_3H) prepared at the same condition showed the lower stability. The stability improvement of HTCG-SO_3H was then studied at the longer hydrothermal carbonization time (6-24 h). While glucose derived HTCs (HTCGs) prepared at all conditions exhibited similar chemical and structural characteristics, examination of liquid fractions from hydrothermal carbonization suggested the suitable hydrothermal carbonization condition to be at 220 °C and 6 h. Sulfonated catalysts prepared at the proposed conditions were shown to promote cellulose hydrolysis and fructose dehydration with relatively high reactivity.

Department: Chemical Engineering Student's Signature .....
Field of Study: Chemical Engineering Advisor's Signature .....
Academic Year: 2017

ACKNOWLEDGEMENTS

First and foremost, I would like to express my sincere thanks to my advisor, Prof. Artiwan Shotipruk, for her invaluable help and constant encouragement throughout the course of this research. I am most grateful for her teaching and advice, not only the research methodologies but also many other methodologies in life. I would not have achieved this far and this thesis would not have been completed without all the support that I have always received from her. My great appreciation goes to Prof. Tetsuya Kida, Assist. Prof. Armando T. Quitain, and Assoc. Prof. Mitsuru Sasaki for their warm regards during my stay in Kumamoto, Japan. I am grateful to Dr. Panatpong Boonnoun for continuous guidance, an enormous number of invaluable discussions, helpful suggestions, warm encouragement and patience to correct my writing.

Special thanks to thesis committees, Dr. Varun Taepaisitphongse, Prof. Navadol Laosiripojana, Assoc. Prof. Tharathon Mongkhonsi, and Dr. Palang Bumroongsakulsawat for their very useful guidance and comments, which made this thesis come to completion.

Sincere thanks are extended to Thai Edible Oil Co., Ltd. for supplying defatted rice bran used in this research. I greatly appreciate the financial supports from e-ASIA Joint Research Program (e-ASIA JRP), 100th Anniversary Chulalongkorn University Fund for Doctoral Scholarship, and the Japan Student Services Organization (JASSO) Scholarship.

I wish to thank all of Prof. Artiwan's lab members (Armmy, Tatto, Wee, Tang, Sine, View, On, Tae, Patty) and my lovely friends (Shower, Fern, Apple, Ayaka, Adrian, Nicholas, and Mus) for all the great help. In addition, I would like to thank all my friends at Chulalongkorn University and Kumamoto University for their assistance and friendly encouragement.

Finally, I would like to thank my parents and my family for their belief in me and the infinite love that means so much and fuels me to keep on accomplishing my goals.

CONTENTS

Page

Page

LIST OF TABLES

LIST OF FIGURES

CHAPTER I
INTRODUCTION

1.1 Motivation

Owing to increased world population, the energy demand for transportation and industries to produce various products has been rising and inevitably become an important societal issue. As a consequence, research on development of technology for effective processing and utilization of non-petroleum feedstocks for the production of biomaterials, fine chemicals and alternative fuels has now been under attention globally. Taking rice, the major food crop of Asian countries including Thailand, as an example, other than the edible milled rice, all other parts of rice are being extensively researched to provide the maximal benefits to human. Rice straws and rice husks are generally burned to produce heat (Kataki et al., 2017; Quispe et al., 2017). More recent researches have been focusing on their conversion into other high energy-density fuels and valuable chemicals such as production of ethanol, methane, acetic acid, sugar (glucose and xylose), 5-hydroxymethylfurfural (HMF), furfural, levulinic acid, and formic acid (Binod et al., 2010; Chandra et al., 2012; Karimi et al., 2006). Given its high silica content, rice husks have been used in silica synthesis, amine-modified silicon oxide (SiO_2) aerogel preparation, synthesis of belite cement, and development of refractory ceramic materials (Bakar et al., 2016; Cui et al.; Sinyoung et al., 2017; Sobrosa et al., 2017). Rice bran, due to the high oil content, is being extracted for edible oil (Hanmoungjai et al., 2001; Lakkakula et al., 2004; Mamidipally and Liu, 2004; Proctor and Bowen, 1996). Defatted rice bran, the residue from the rice bran oil industry, have been researched for extraction of protein (Adebiyi et al., 2009; Bandyopadhyay et al., 2012; Chittapalo and Noomhorm, 2009; Jongjareonrak et al., 2015) and phenolic compounds (Chiou et al., 2012; Devi and Arumughan, 2007; Wataniyakul et al., 2012) through various processes ranging from enzymatic extraction/hydrolysis to subcritical water extraction/hydrolysis by a number of research groups (Hata et al., 2008; Sereewatthanawut et al., 2008; Sunphorka et al., 2012; Viriya-Empikul et al., 2012)

In most industrial processes including those of bio-based nature, catalysts have for a long time played a key role. Research studies are being conducted to develop heterogeneous catalysts to replace the conventionally used homogeneous catalysts, due to their ease of separation and reusability. Owing to the low cost of raw materials, sulfonated carbon-based catalysts, have recently been developed from various carbon sources such as sugars, polycyclic aromatic compounds, polystyrene resins, activated biochar, and lignin (Mo et al., 2008; Toda et al., 2005; Yu et al., 2010), and have been applied to processes involving biofuel and biochemical production. Such catalysts can be produced via rather simple synthesis routes, either by carbonization of sulfopolycyclic aromatic carbons or sulfonation of carbonized inorganic/organic compounds (Boonnoun et al., 2010; Gao et al., 2007; Shu et al., 2009). Other advantages of this class of catalyst include high acid density and high thermal stability. Sulfonated carbon-based catalysts synthesized from various carbon sources such as glucose and biomass have been tested for the production of biodiesel by esterification and transesterification (T. Liu et al., 2013; Mo et al., 2008; Toda et al., 2005; Yu et al., 2010) and biomass conversion via processes in hot compressed water, particularly, hydrolysis of biomass to monomer sugars, and dehydration of the monomer sugars to furan compounds such as HMF and furfural (Daengprasert et al., 2011; Li et al., 2015). These furan compounds are not only the key intermediates for liquid fuels, but also the important biomass-derived platform chemicals for the production of fuels, furan-based polymers, as well as fine chemicals and pharmaceuticals (Antonetti et al., 2017).

Although various types of carbon sources such as glucose (Zong et al., 2007) and cellulose (Suganuma et al., 2010) can be used for the preparation of sulfonated carbon-based catalysts, the biomass derived carbon source offers additional advantages of being renewable and being available in abundance at extremely low cost. In this case, the first few steps for the synthesis of the biomass-derived catalysts are similar to those of the activated carbon preparation, involving removal of water (dehydration) and conversion of the organic matter to elemental carbon, driving off the non-carbon portion with heat (carbonization), followed optionally by pore enlargement (activation). Then in order to make the carbon suitable for catalyzing a specified reaction, the surface chemical properties of the carbon may be further modified by chemical or physical

functionalization. Nevertheless, a major bottleneck of this preparation process is the use of high carbonization/pyrolysis temperatures (400-800 °C). When the starting from biomass with high moisture content, requirement for water removal makes the process even more energy intensive as additional heat is needed.

A new method for preparation of carbonaceous materials via *hydrothermal carbonization* has recently been developed, in which carbonization of the carbon sources takes place in hot compressed water at moderate temperature (150-250 °C) under self-generated pressure. Therefore, the process can convert wet raw material into *hydrothermal carbon* (HTC) without the need for prior drying (Fiori et al., 2014). For the hydrothermal carbonization process, the formation of HTC derived from biomass can be described by the two routes. Firstly, for polymerized HTC, the main components in lignocellulosic biomass such as cellulose, hemicellulose and lignin are converted to HMF, furfural and phenolic derivatives in the hydrothermal condition. By keeping the hydrothermal condition for longer time, these derivatives are further converted to form HTC via polymerization and aromatization. Secondly, polyaromatic HTCs, the original structure of non-dissolved cellulose, hemicellulose and lignin, completely disrupted and goes through a heterogeneous pyrolysis and forms interconnected network structure of carbon via intramolecular rearrangement, condensation, and decarboxylation reaction (Baccile et al., 2009; Kang et al., 2012; Lei et al., 2016). This process results in HTC that could be further functionalized to perform specific catalytic activity.

The process of hydrothermal carbonization is similar to that of biomass conversion to produce HMF, furfural, and other valuable products such as glucose, levulinic acid, and formic acid. The main difference is that the HTC production due to biomass requires much longer time from one to several hours (Libra et al., 2011). For this reason, biomass residues that have been extracted for the high value products could potentially be a very attractive carbon source for HTC production. Based on our previous studies, sufficient amount of residue (approximately 30% of the starting DRB) remained after subcritical extraction of DRB for phenolic compounds and amino acids (Wataniyakul et al., 2012; Watchararuji et al., 2008). However, the morphology of DRB residue obtained from subcritical extraction was indicated to be loose and irregular

surfaces caused by the cell rupture. It is different from morphology of HTCs derived from simple sugar including glucose, fructose, xylose, sucrose which showed the aggregation of spherical shaped particles (Titirici et al., 2008). Other than the difference in morphology, HTCs derived from various sources have been reported to require the different reaction times. Particularly, hydrothermal carbonization time of grape seed was investigated in ranges of 1-8 h, but that of sugar (i.e. glucose, fructose and xylose) was examined in ranges of 4-43 h (Fiori et al., 2014; Fraile et al., 2012; Guo et al., 2012; Titirici et al., 2008).

This study therefore aims to investigate the possibility of synthesizing a HTC from low-cost biomass such as DRB and from simple sugar (glucose), with a specific objective to understand the effects of hydrothermal conditions on the characteristics of DRB and glucose-based HTCs and use them as catalyst supports for biomass conversion. Provided with the fact that the steps of HTC formation follow the exact same paths of HMF production, it is of utmost importance therefore, to ensure that the catalyst must be derived from a HTC support that are stable enough that, by itself, does not decompose and form HMF.

1.2 Objectives

1.2.1 To study the effect of hydrothermal carbonization conditions: temperatures and times, on the stability of HTC derived from DRB and glucose.

1.2.2 To determine the suitable hydrothermal carbonization conditions for preparation of HTC derived from DRB and glucose.

1.2.3 To prepare sulfonated HTC catalysts derived from DRB and glucose for biomass conversion to HMF.

1.3 Scopes of work

As shown in **Figure 1.1**, DRB was used as a starting material for preparation of HTC-based acid catalyst, and the characteristics of the catalyst was compared with that prepared from glucose. The suitable hydrothermal conditions needed for HTC-based acid catalyst from both DRB and glucose were determined, which ensure the stability of the catalysts under the reaction conditions. The scopes of work with the DRB based

and the glucose based catalyst are shown in the diagram in **Figure 1.1 and 1.2**, respectively, and are detailed as follows:

1.3.1 Compare the sulfonated HTC-based catalysts derived from DRB and glucose.

1.3.1.1 Determine the suitable temperatures (180, 220, and 250 °C) and times (1, 3, and 8 h) for hydrothermal carbonization of DRB and glucose, based on carbon content.

The selected DRB and glucose derived HTC (HTCDRB and HTCG) were used to prepare sulfonated HTC-based catalyst (HTC-SO_3H) by sulfonation with sulfuric acid at 150 °C for 15 h.

1.3.1.2 Test the leaching of HMF and other biomass conversion products from the HTC-SO_3H from 1.3.1.1 under microwave irradiation at 200 °C for 5 min.

1.3.1.3 Test the catalytic activity of the HTC-SO_3H selected based on the result in 1.3.1.2 on cellulose hydrolysis with subcritical water at 180 °C for 5 min.

1.3.2 Improve the stability of sulfonated HTC-based catalyst derived from glucose.

1.3.2.1 Determine the suitable hydrothermal carbonizations of glucose: temperatures (180, 220, and 250 °C) and times (6, 12, 18 and 24 h), in order to prepare carbon catalyst support for biomass conversion to HMF. The selected HTCG was used as catalyst support to prepare HTCG-SO_3H by sulfonation with sulfuric acid at 150 °C for 15 h.

1.3.2.2 Test the catalytic activities of the HTCG-SO_3H from 1.3.2.1 on cellulose hydrolysis and fructose dehydration with subcritical water at 180 °C for 5 min.

1.3.2.3 Evaluate the stability on recyclability of HTCG-SO_3H from 1.3.2.1 for fructose dehydration with subcritical water at 180 °C for 5 min.

1.4 Expected benefits

1.4.1 Main results

1.4.1.1 This study can provide the suitable condition for utilization of biomass for the preparation of sulfonated HTC-based catalyst for HMF production from biomass.

1.4.1.2 The effect of hydrothermal carbonization condition on the stability of HTC derived from DRB and glucose can be used as guideline for catalyst preparation from other sources.

1.4.1.3 This study can provide the development of technology for production of value-added substances and materials including HMF and sulfonated HTC-based catalyst which can be derived from available agricultural by-products.

1.4.2 Overall benefits

1.4.2.1 The results of this study suggest ways in which available biomass in Thailand can be fully utilized.

1.4.2.2 The low-cost sulfonated HTC-based catalyst derived from biomass can potentially replace the commercial catalyst

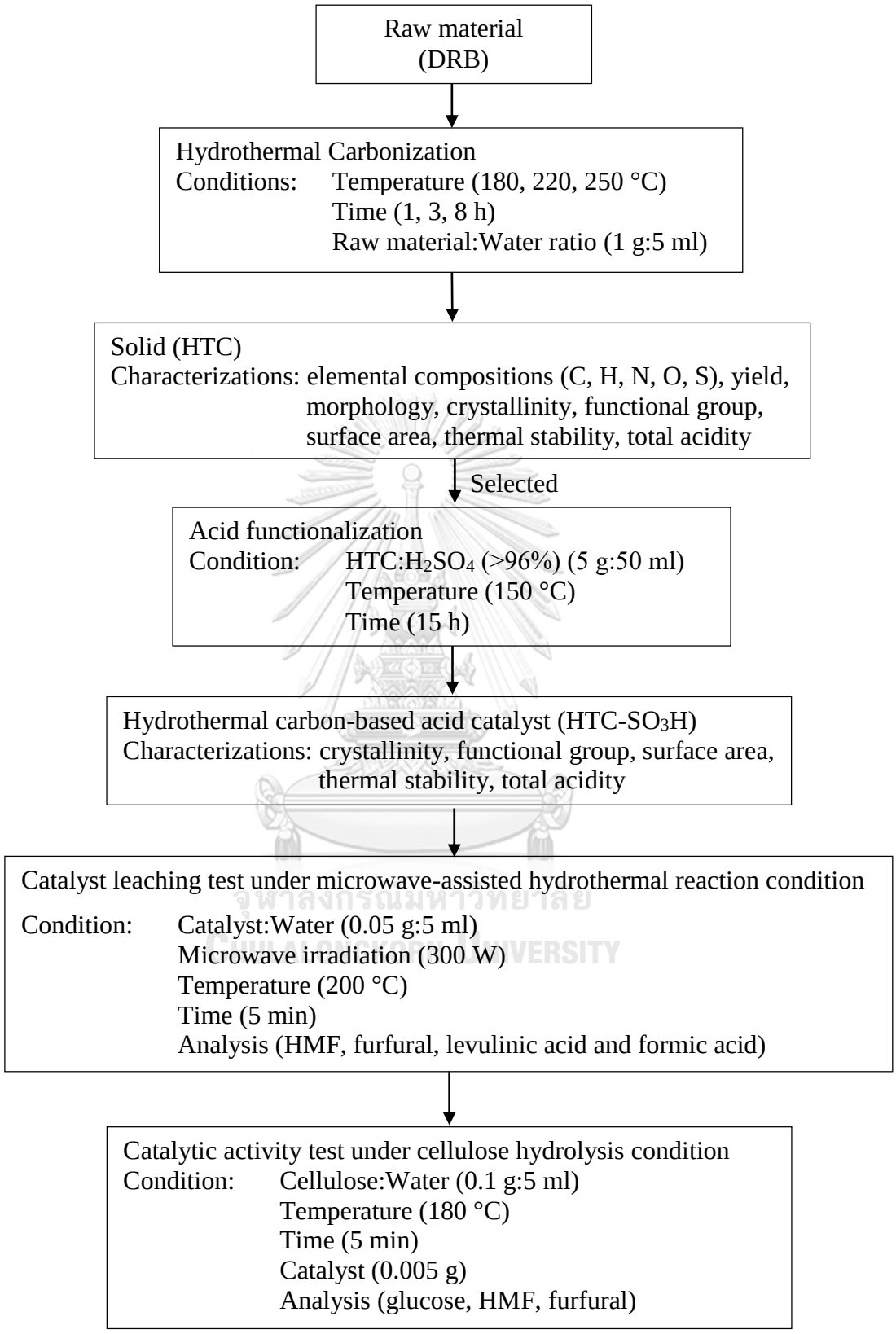

Figure 1.1: Working scope for DRB derived HTC-based catalyst

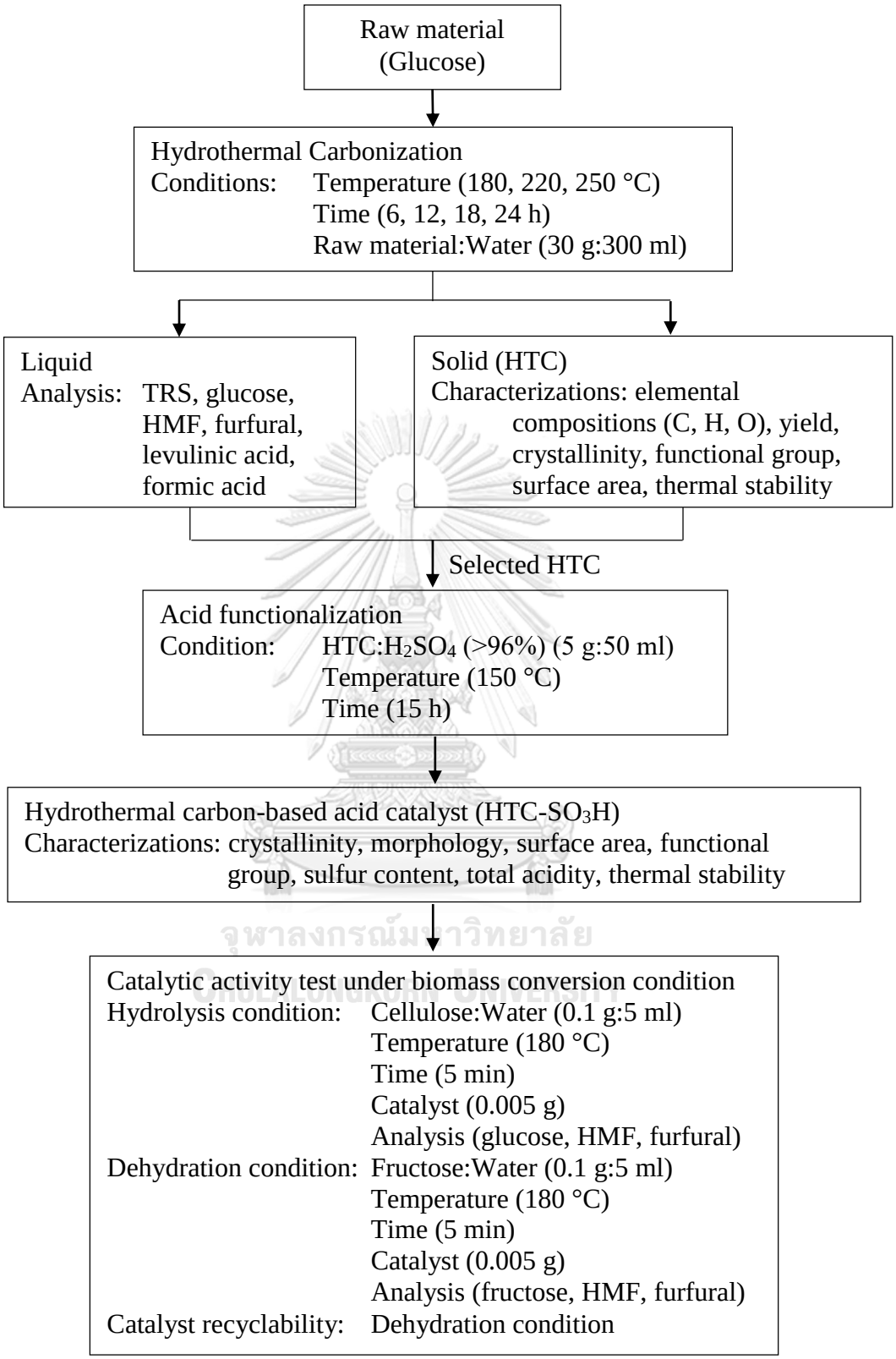

Figure 1.2: Working scope for glucose derived sulfonated HTC-based catalyst.

CHAPTER II
BACKGROUND AND LITERATURE REVIEWS

Current rising demand of energy for transportation and industries has driven interest in the development of new technology for the production of fuels from renewable feedstocks. Liquid fuels such as bio-ethanol, bio-butanol, biodiesels, as well as liquid alkanes have been studied worldwide to respond to the increasing energy requirements. Due to its low cost, biomass, including algal biomass (Yue et al., 2016), and lignocellulosic biomass such as that of agricultural residues (i.e., rice husks, corn cobs and corn stovers, and cassava waste) are important feedstocks for the production of the majority of the above liquid fuels (Daengprasert et al., 2011; Ding et al., 2016; Tian et al., 2016). In this chapter, the background is provided on biomass: biomass composition (i.e. cellulose, hemicellulose and lignin), and the composition and properties of defatted rice bran (DRB) which is a selected raw material for hydrothermal carbon (HTC) preparation in this study. The mechanism and reaction path way of biomass conversion for HMF production are reviewed along with the properties of the possible products from the process. In addition, the reviews on the hydrothermal process, the formation of HTC, the properties of sulfonated HTC catalyst and its application are also summarized.

2.1 Lignocellulosic biomass

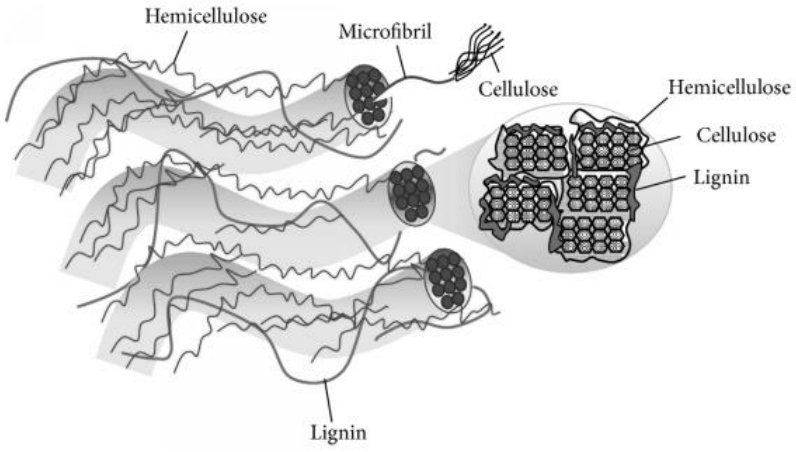

Figure 2.1: Composition of lignocellulosic biomass (Lee et al., 2014)

In most cases, biomass from agricultural residues which are generally referred to lignocellulosic biomass has been used as feedstocks for production of bioenergy. Lignocellulosic biomass is composed of three main organic components: cellulose, hemicellulose, and lignin bound together as shown in **Figure 2.1**. The ratios of these components vary depending on the types of the biomass raw materials as can be seen in **Table 2.1**.

Table 2.1: Composition of lignocellulose in several sources on dry basis (Sun and Cheng, 2002)

Lignocellulosic materials	Cellulose (wt.%)	Hemicellulose (wt.%)	Lignin (wt.%)
Hardwoods stems	40–55	24–40	18–25
Softwood stems	45–50	25–35	25–35
Nut shells	25–30	25–30	30–40
Grasses	25–40	35–50	10–30
Leaves	15–20	80–85	0
Paper	85–99	0	0–15
Corn cobs	45	35	15
Wheat straw	30	50	15
Sorted refuse	60	20	20
Switch grass	45	31.4	12

2.1.1 Cellulose

Cellulose is the main component of lignocellulosic biomass which may exist in two forms; the crystalline cellulose and amorphous cellulose. It is a complex of polysaccharides which consists of β-1,4-glycosidic bond linked with linear polymer of glucose units (**Figure 2.2**). It generally contains carbon (44.44 wt.%), hydrogen (6.17 wt.%), and oxygen (49.39 wt.%). The chemical formula of cellulose is $(C_6H_{10}O_5)_n$; where n, the degree of polymerization (DP), represents the number of glucose units, ranging from hundreds to thousands or even tens of thousands (Chen, 2014).

Utilization of cellulose from biomass sources as a feedstock for fuel productions starts with the separation of cellulose from the biomass origins. Cellulose is then converted to glucose via hydrolysis which can be carried out by various methods such as enzyme and alkali or acid hydrolysis (Wang et al., 2016). Alternatively, cellulose hydrolysis takes place in subcritical water at above 220 °C (Reza et al., 2014); in which β-1,4-glycosidic bonds are broken. In the past few years, different methods have been devised; for example, hydrolysis of microcrystalline cellulose using functionalized Bronsted acidic ionic liquids (Parveen et al., 2016) and hydrolysis of cellulose by sulfonated magnetic reduced graphene oxide (Yang et al., 2015). Biomass derived glucose can then be converted to bioethanol or biobutanol by means of fermentation (Dussán et al., 2014; Wang et al., 2016). Alternatively, via dehydration of glucose to produce furan compounds such as HMF and furfural, followed by further hydrogenation and dehydrogenation reactions, liquid alkanes can be produced (Chheda et al., 2007).

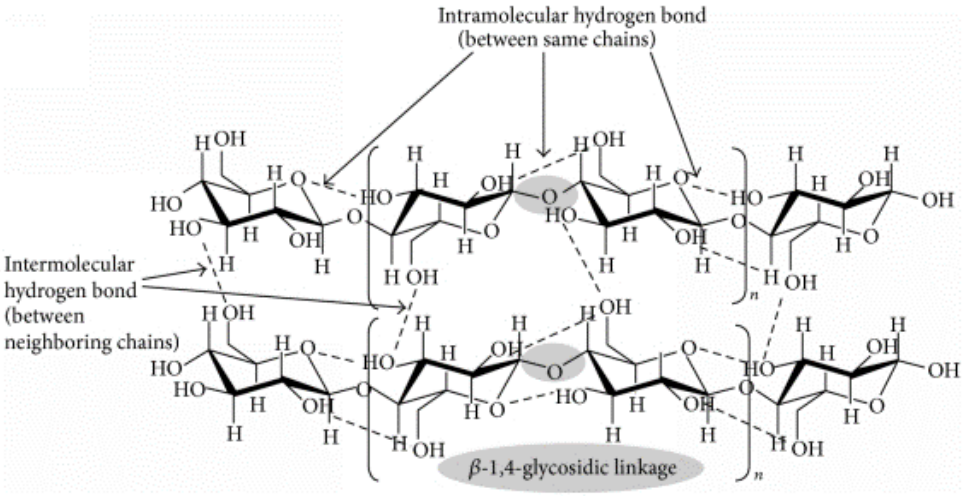

Figure 2.2: Chemical structure of cellulose (Lee et al., 2014)

2.1.2 Hemicellulose

Hemicellulose is polysaccharides (heteropolymers) such as arabinans, mannans, galactans, and others. Although it is composed of several sugars, the major sugar is xylose (85-90 wt.%) as the chemical structure shown in **Figure 2.3**. The rest consists

of the other five-carbon sugar, six-carbon sugar, mannuronic acid, and galacturonic acid. These components are linked by β-(1,4) bonds similar to cellulose but its degree of polymerization is lower than that of cellulose. Unlike cellulose which exists in two forms, hemicellulose only exists in a non-crystalline (amorphous) form. It is insoluble in water at low temperature; however, it is water soluble at high acidity. Decomposition of hemicellulose occurs at the temperatures above 180 °C, which is a lower decomposition temperature, compared with that of cellulose, thus, it can be hydrolyzed more easily than cellulose. Hemicellulose hydrolysis occurs as a result of the breakage of the β-(1,4) bonds to form sugars. Of these, the most abundant are glucose and xylose, which are important feed stocks for liquid fuel production.

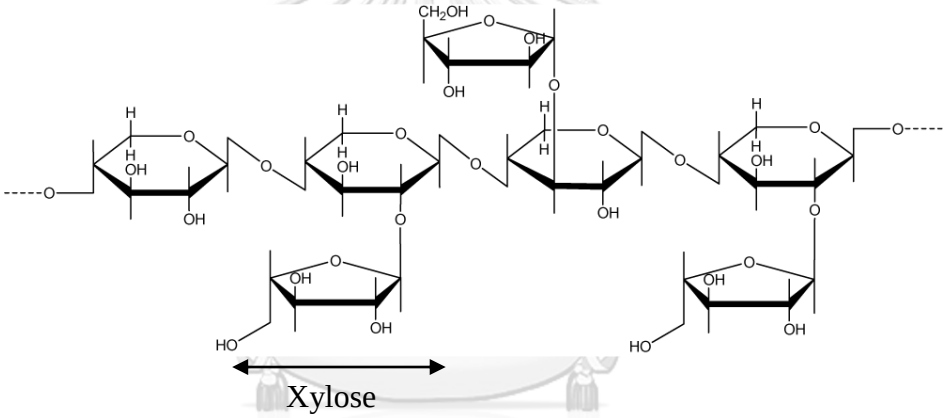

Figure 2.3: Chemical structure of xylose in hemicellulose (Bastawde, 1992)

2.1.3 Lignin

Lignin is a three-dimensional complex heteropolymer, which provides structural protection for plants and some algae from enzymatic digestion by microorganism. As shown in **Figure 2.4**, the three basic monomers in the structure of lignin are p-coumaryl alcohol (p-hydroxyphenyl), coniferyl alcohol (guaiacyl propanol), and sinapyl alcohol (syringl alcohol). Lignin is insoluble in water and non-polar solution, but it can considerably dissolve in polar solvent including alcohols, di-oxane, and acetone (Lee et al., 2014).

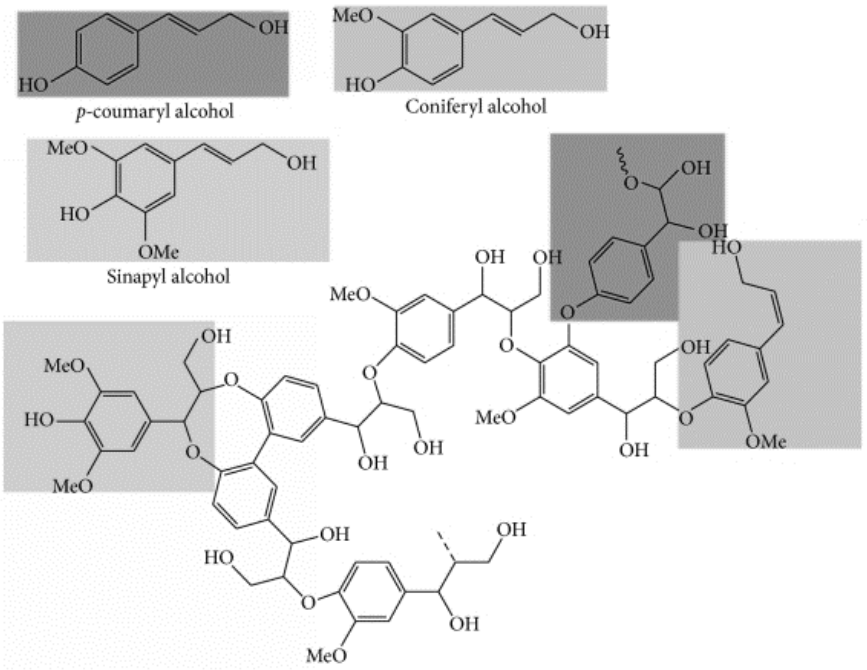

Figure 2.4: Chemical structures of lignin (p-coumaryl alcohol, coniferyl alcohol, and sinapyl alcohol) (Lee et al., 2014).

As lignin is a complex structure, it decomposes at higher temperature (260 ˚C) to phenolic compounds, which find uses in a number of processes. In addition, study by Konwar et al. (2014) has indicated that lignin is an important source of carbon, and that carbon fibers have been produced from lignin by thermal spinning (130-240 ˚C) following carbonization at 250 ˚C for 1 hour.

2.2 Defatted rice bran

Rice is one of the most important food crops in the world. In recent year, about 483.34 million metric tons of rice is produced annually worldwide. More than half of the production belongs of Asian countries including Chaina, India, Indonesia, Bangladish, Vietnam, and Thailand. Being No. 6 largest rice producer in the world in 2016, Thailand produced approximately 25.58 million metric tons of paddy and exported about 9.88 million metric tons of milled rice (Agricultural statistics of Thailand, 2016). Rice bran (RB) as a byproduct from rice milling contains valuable

products (i.e. vitamin E and gramma-oryzanol), which have beneficial effect to human health. Moreover, RB contains high oil content, which can be extracted to obtain high quality edible oil, having nutritional benefits such as gramma-oryzanol, tocotrienols and tocopherols which are effective in preventing disease and cancer (Bessa et al., 2017). After oil extraction, defatted rice bran (DRB) as a by-product of RBO processing is resulted and is generally used as low-cost animal feed. As shown in **Figure 2.5**, DRB is composed of 29.65 wt.% extractives, 25.63 wt.% lignin, 25.48 wt.% cellulose, 9.35 wt.% hemicellulose, and 9.89 wt.% ash, respectively.

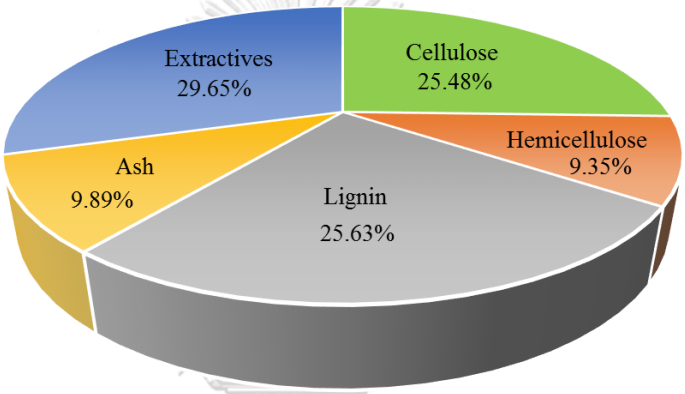

Figure 2.5: Compositions of DRB determined by National Renewable Energy Laboratory (NREL)

Each component of has a benefit; for example, Extractives in DRB include proteins and amino acids. They are beneficial to human health, and thus extraction of proteins and amino acid from DRB is therefore of considerable research interest (Sereewatthanawut et al., 2008; Sunphorka et al., 2012; Tang et al., 2002). Lignin in DRB has been used as feedstock to produce phenolic compounds which are important intermediates for a diversity of products, such as pharmaceuticals, dyes, and antioxidants (Sasaki and Goto, 2008; Wataniyakul et al., 2012). Cellulose and hemicellulose in DRB can be converted to sugars (i.e. glucose, xylose, and arabinose) and furan compounds (i.e. HMF and furfural), which are intermediates for liquid fuel production (Tsigie et al., 2012).

2.3 Biomass conversion to liquid alkanes

In recent years, production of fuels and chemicals from biomass has been a focus of research studies worldwide. Biomass conversion can be classified into three categories according to the process employed: thermo-chemical conversion, physico-chemical conversion, and biological conversion. Examples of thermo-chemical conversion processes include combustion, carbonization, and gasification. Those of physico-chemical processes include pressing and/or extraction. Biological conversion is devised by fermentative hydrolysis and anaerobic digestion. Moreover, biomass conversion may be classified based on the states (solid (char), liquid, and gas) of the product. Here, conversion lignocellulosic biomass into solid and liquid products is investigated, and the reviews of the processes are summarized as follows.

From **Figure 2.6**, it can be indicated that liquid alkanes are derived from two major components which are cellulose and hemicellulose. Dedsuksophon et al. (2010) explained that liquid fuel production from biomass consists of four steps including hydrolysis, dehydration, aldol-condensation and hydrogenation. In the first step, cellulose and hemicellulose are converted to monosaccharides (C_5 sugars such as glucose, fructose and hexose, and C_6 sugars such as xylose, pentose and arabinose) by using hydrolysis reaction. Then monosaccharides are converted to furan compounds such as HMF and furfural by dehydration reaction; C_5 sugars are converted to furfural, and C_6 sugars are converted to both of HMF and furfural. Subsequently, both HMF and furfural, as an intermediate of liquid alkanes (C_7-C_{15}) production, are converted to larger organic molecules by the C-C coupling between two smaller HMF and furfural compounds by aldol-condensation. However, HMF and furfural without α-H atom cannot undergo self-condensation. The carbonyl group in the HMF and furfural can react with carbonyl-containing molecules such as acetone and dihydroxyacetone. Then aldol condensation is carried out in polar solvents like water by using base-catalysts (e.g., NaOH, Mg–Al oxides). These aldol condensation reactions of HMF and furfural are shown in **Figures 2.7 and 2.8**, respectively.

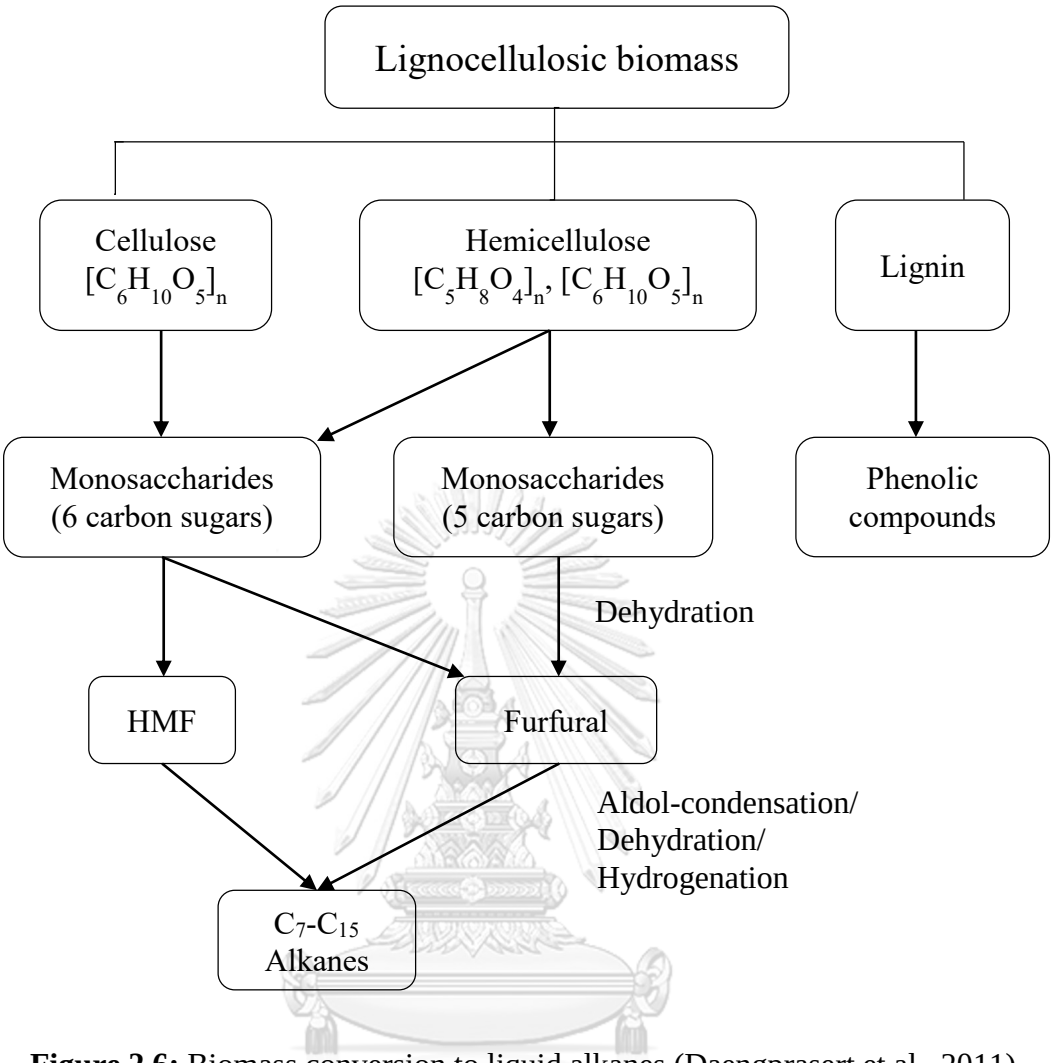

Figure 2.6: Biomass conversion to liquid alkanes (Daengprasert et al., 2011)

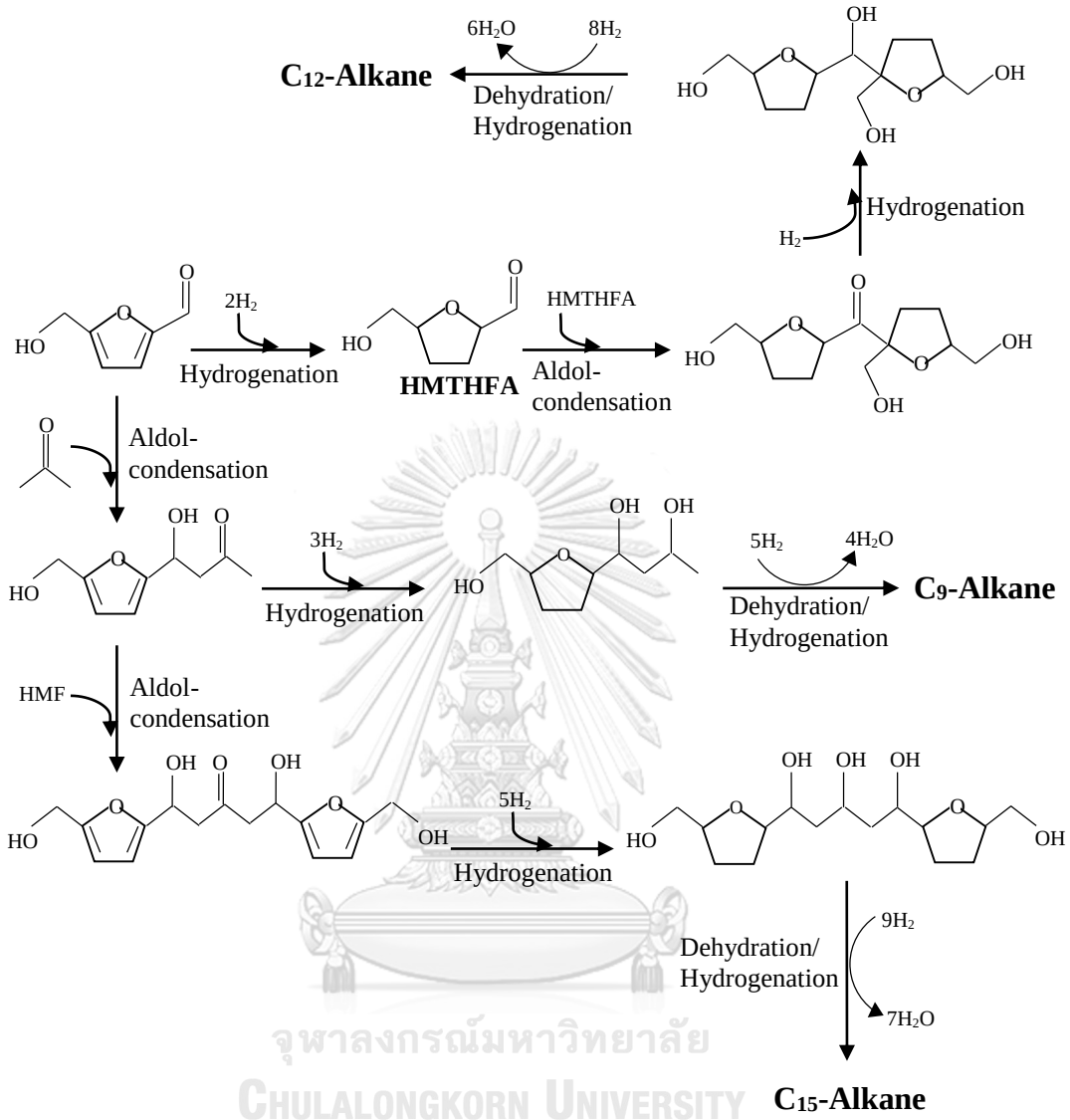

Figure 2.7: Reaction pathways for production of liquid alkanes via HMF (Serrano-Ruiz and Dumesic, 2011)

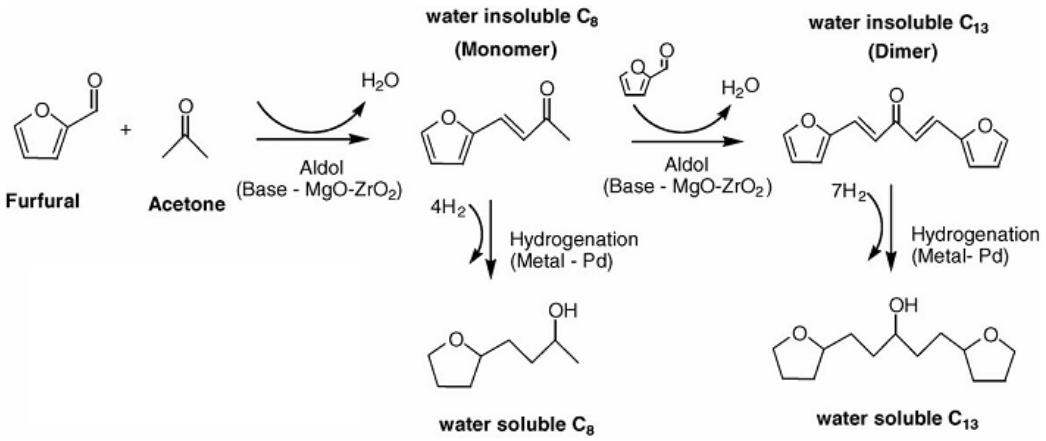

Figure 2.8: Reaction pathways for production of liquid alkanes via furfural (Serrano-Ruiz and Dumesic, 2011)

As previously mentioned, HMF and furfural are important intermediates for liquid alkanes production. These furans are also platform chemicals for various other useful polymers and fine chemicals. Detailed utilization of HMF and furfural are explained as follows.

2.3.1 5-Hydroxymethylfurfural (HMF)

Figure 2.9: Chemical structure of HMF
(Source: National Institute of Standards and Technology; http://webbook.nist.gov/cgi/cbook.cgi?Name=HMF&Units=SI)

5-(Hydroxymethyl) furfural, also known as Hydroxymethylfurfural (HMF), is an organic compound which consists of furan ring and contains functional groups of aldehyde and alcohol (**Figure 2.9**). It is yellow liquid or powder which is highly water-soluble and easily dissolved in methanol, ethanol, acetone, methyl isobutyl ketone, or

dimethylformamide (Zheng et al., 2016). Properties of HMF are shown in **Table 2.2,** HMF has a chemical formula of $C_6H_6O_3$, molar mass of 126.11 g/mol, density of 1.29 g/cm^3, melting point range of 30-34 °C and boiling point range of 114-116 °C.

Table 2.2: Properties of HMF

Properties of HMF	
Chemical formula	$C_6H_6O_3$
Molar mass	126.11 g/mol
Density	1.29 g/cm^3
Melting point	30 to 34 °C
Boiling point	114 to 116 °C

(Source: National Institute of Standards and Technology;
http://webbook.nist.gov/cgi/cbook.cgi?Name=HMF&Units=SI)

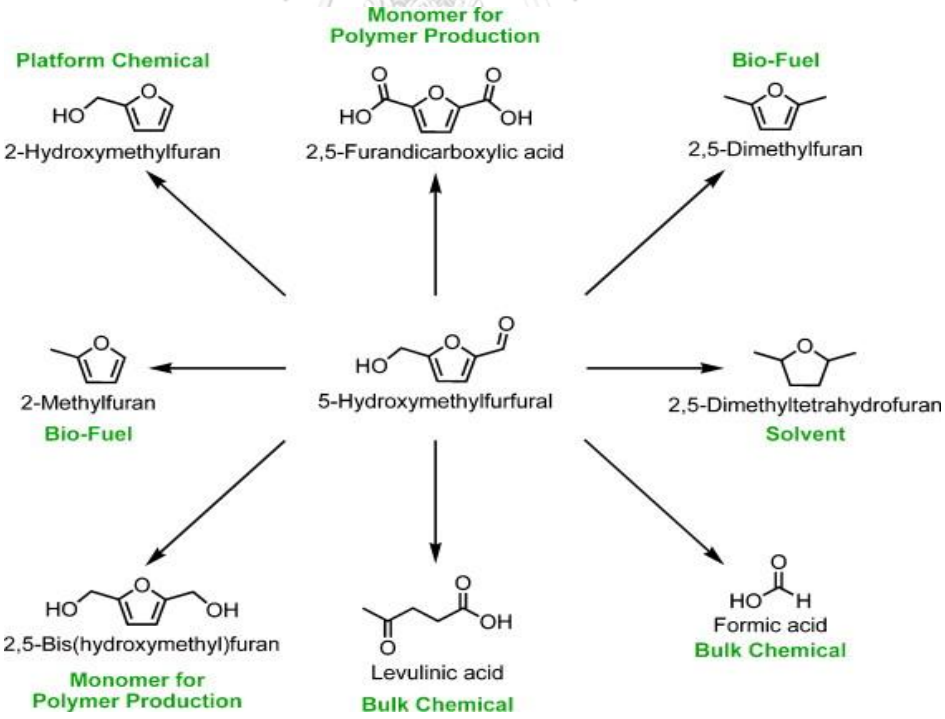

Figure 2.10: Chemicals obtained via HMF

(Source: Centre for Catalysis and Sustainable;
http://www.csc.kemi.dtu.dk/research/renewable-chemicals)

HMF, which has a price of 11,550 SGD per kilogram (Sigma Aldrich, online September 15, 2017), is a considerable high value chemical derived from cheap raw materials. It can be obtained from C_6 sugar, particularly fructose or glucose via isomerization to fructose, as well as directly from cellulose and hemicellulose via hydrolysis to glucose and hexoses. It is evident, by several utilizations of HMF reported, that not only as important platform chemicals for the production of fuels, but also for furan-based polymers, fine chemicals and pharmaceuticals (Wang et al., 2011). As shown in **Figure 2.10**, important chemicals (Levulinic acid, Formic acid, 2,5-Dimethyltetrahydrofuran, 2,5-Furandicarboxylic acid, 2-Methylfuran, 2-Hydroxymethylfuran, 2,5-Dimethylfuran and 2,5-Bis(hydroxymethyl)furan) can be obtained from HMF (Boisen et al., 2009).

2.3.2 Furfural

Figure 2.11: Chemical structure of furfural
(Source: National Institute of Standards and Technology;
http://webbook.nist.gov/cgi/cbook.cgi?Name=furfural&Units=SI)

Table 2.3: Properties of furfural

Properties of furfural	
Chemical formula	$C_5H_4O_2$
Molar mass	96.09 g/mol
Density	1.16 g/cm^3
Melting point	-37 °C
Boiling point	162 °C

(Source: National Institute of Standards and Technology;
http://webbook.nist.gov/cgi/cbook.cgi?Name=furfural&Units=SI)

Furfural, a chemical similar to HMF, consists of two important functional groups of an aromatic aldehyde (CHO) and a conjugated system (C=C-C=C) (**Figure 2.11**). It is a colorless oily liquid in the pure state, while quickly darkens to yellow color upon exposure to air. As properties of furfural are shown in **Table 2.3**, furfural has chemical formula of $C_5H_4O_2$, molar mass of 96.09 g/mol, density of 1.16 g/cm^3, melting point of -37 °C and boiling point of 162 °C.

In 2016, the furfural was produced approximately 250,000 metric tons (Machado et al., 2016), and its price has high value of 102.17 SGD per Liter (Sigma Aldrich, online September 15, 2017). Production of furfural can be achieved from C_5 and C_6 sugars such as glucose, fructose and xylose, or it can be directly produced from cellulose and hemicellulose and low-cost biomass raw material via hydrolysis to those sugars. Because of its several potential applications, as a solvent or a starting material for preparation of other organic solvents such as butanol, dihydropyran, pentanol and levulinic acid (**Figure 2.12**), furfural is a high value chemical.

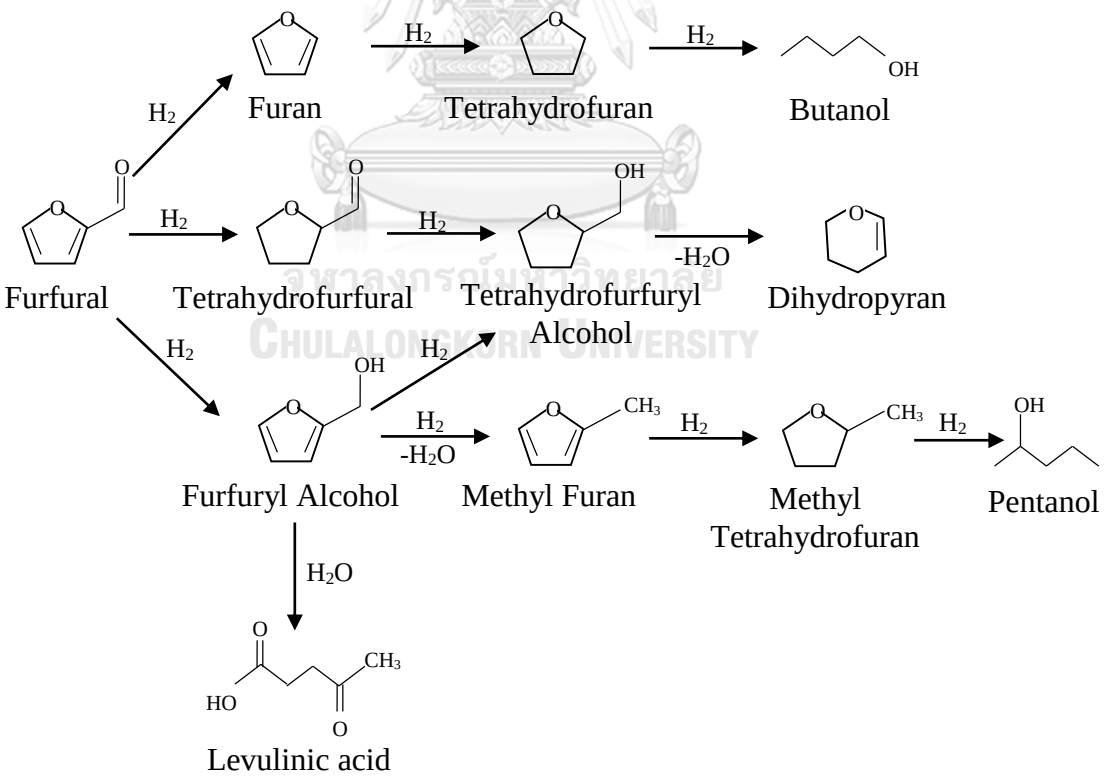

Figure 2.12: Chemicals obtained via furfural (O'Driscoll et al., 2017)

2.4 Production of HMF and furfural from lignocellulosic biomass

As can be seen from **Figure 2.6**, two steps to produce HMF and furfural from lignocellulosic biomass are hydrolysis and dehydration. Both of these reactions are commonly catalyzed by acid catalysts in hot compress water (HCW).

2.4.1 Hot compressed water

HCW (sub or supercritical water) is water near and above its critical point (T_c=647 K; P_c = 22.1 MPa). This technique presents a series of important advantages over the traditional hydrolysis techniques; it is faster and generally produces higher yields and minimizes formation of toxic products. Because the reaction medium is water, the wet biomass can be directly used as feedstock and the water contained in biomass can be removed in its liquid phase by a non-evaporative dewatering process under higher pressures (Wiboonsirikul et al., 2007). HCW serves as an excellent reaction medium due to the dielectric constant (ε, as a measure of its polarity) of water decreases at high temperature (**Figure 2.13**). The significant drops in the dielectric constant lead to a rapidly increase in solvent power. Besides, the ion product (hydronium and hydroxyl ions) of HCW increases with temperature; therefore, it can catalyze chemical reactions such as hydrolysis and degradation without any additional catalyst (Pourali et al., 2009).

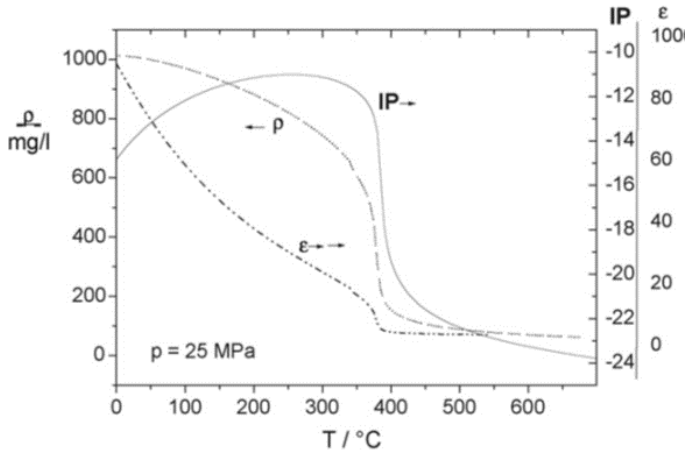

Figure 2.13: Selected properties of water at high temperature and high pressure (Kruse and Dinjus, 2007)

Table 2.4: Production of HMF and furfural from different raw materials by using HCW

Substrate	Study Conditions		Suitable condition	Y_{HMF}	$Y_{Furfural}$	References
	Temp. (°C)	Time (min)		(wt.%)	(wt.%)	
Sugarcane bagasse	200-300	3-20	270 °C, 10min	3.090	-	(Iryani et al., 2013)
Olive tree leaves	125-200	20	200 °C, 20min	3.169	-	(Herrero et al., 2012)
Flax straw	175-325	0-120	250 °C, 0min	-	5.000	(Harry et al., 2014)
Corn stover	160-200	4-8	200 °C, 4min	0.860	1.930	(Kim et al., 2016)
Switch grass	220-310	60	280 °C, 60min (HMF) 310 °C, 60min (furfural)	1.500	1.200	(Dhamdere et al., 2012)

Several research groups have investigated the production of water soluble furan compounds: HMF and furfural production via HCW process. With this technique, drying of raw materials, the process that often requiring large amount of energy, is not required (Watanabe et al., 2014). The HMF and furfural production from different raw materials by using HCW are summarized in **Table 2.4**. As can be seen in **Table 2.4**, the suitable conditions of HMF and furfural were high temperature (200-310 °C) and long time (10-60 min). It is noted that without use of catalyst, were used, the HMF and furfural yield from the HCW process, even at high temperature conditions, were still very low (approximately of 0.86-3.17 wt.%). Therefore, a catalyst is often needed to further enhance HMF and furfural yields in this process.

2.4.2 Catalyst for HMF and furfural production

It has been demonstrated that adding catalyst in HCW process could enhance the HMF and furfural yields (Chareonlimkun et al., 2010). As can be seen in **Figure 2.14**, the effect of TiO_2, ZrO_2 and mixed-oxide TiO_2–ZrO_2 as a catalyst in HCW was investigated based on HMF and furfural derived from biomass (i.e. sugarcane bagasse (BG), rice husk (RH) and corncob (CC)). It indicated that adding catalyst in the reaction can achieve product yields higher than that without catalyst (**Figure 2.14**). In addition, while increasing product yields, the catalysts also reduce energy requirement in the process. For BG conversion to HMF, the suitable HCW condition with catalyst was at the temperature of 250 °C for 5 min, which gave 8.60 wt.% HMF yield (**Figure 2.15**). While on the other hand, at the best condition of BG conversion with no catalyst at 270 °C for 10 min, lower HMF yield (3.09 wt.%) was resulted (**Table 2.4**).

In early researches, homogeneous mineral acids such as sulfuric acid, hydrochloric acid, phosphoric acid and acetic acid were used as acid catalysts in HCW to produce HMF and furfural (**Table 2.5**). **Table 2.5** showed that high production yield of HMF and furfural were achieved via homogeneous acid catalyzed reactions. However, homogeneous acids are typically associated with the problems of high toxicity, corrosion, catalyst waste, and difficulty of separation and recovery. Alternatively, heterogeneous acid catalysts overcome most disadvantages of homogeneous acid catalysts as they be more easily separated and recycled.

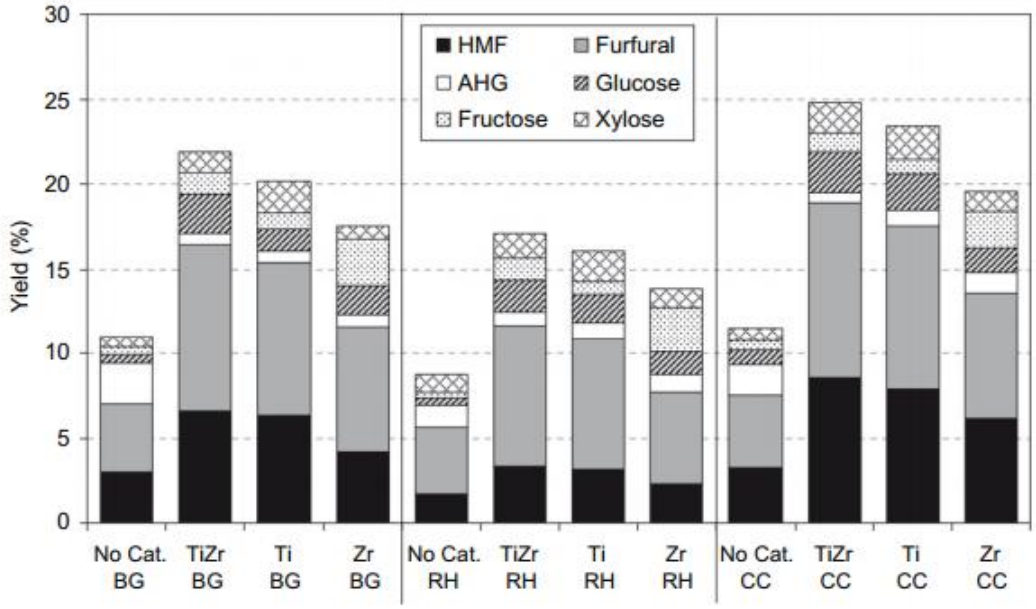

Figure 2.14: Yield of liquid products from the reaction of sugarcane bagasse (BG), rice husk (RH) and corncob (CC) (at 523 K and 5 min with and without the presence of catalysts) (Chareonlimkun et al., 2010a)

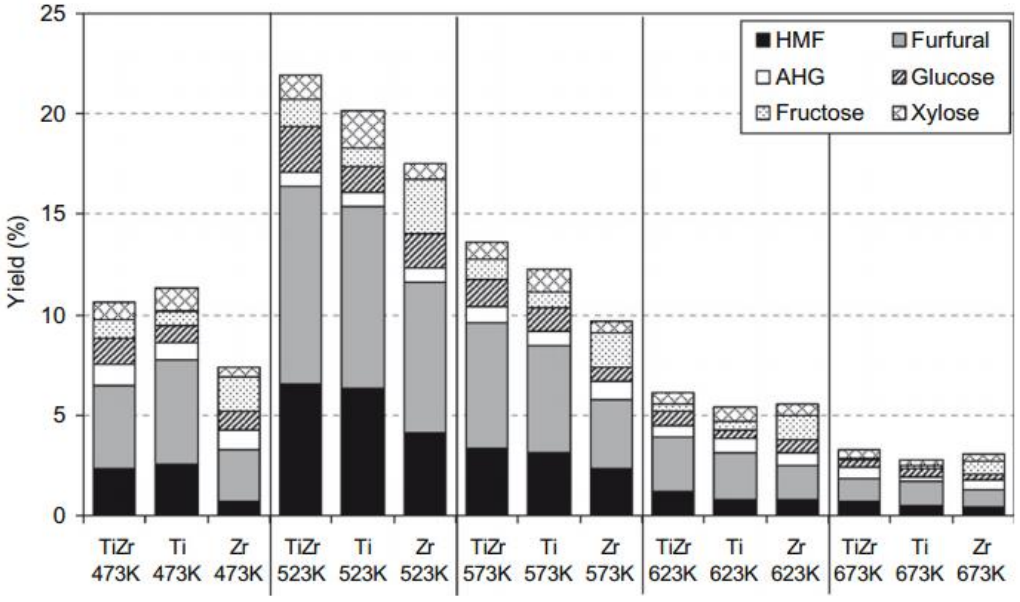

Figure 2.15: Effect of reaction temperature (473–673 K) on the yield of liquid products from the reaction of sugarcane bagasse in the presence of various catalysts at reaction time of 5 min (Chareonlimkun et al., 2010a)

Several types of heterogeneous acid catalysts have been used in HMF and furfural production process (**Table 2.6**). Chareonlimkun et al. (2010) synthesized several metal oxide catalysts including TiO_2 and ZrO_2 and used them to catalyze the conversion of sugars (C_5 and C_6 sugar) or raw biomass to furan compounds (i.e. HMF and furfural). They found that at 280 °C and short time, the TiO_2 and ZrO_2 promoted hydrolysis and dehydration of glucose, cellulose and lignocellulose to HMF and furfural (Chareonlimkun et al., 2010b). Moreover, the addition acidic group to metal oxides via acid functionalization (i.e. sulfonic acid ($–SO_3H$) functionalization to sulfonated solid acid catalyst) to enhance the catalytic performance on hydrolysis and dehydration reactions has also drawn considerable interest. For example, sulfonic acid functionalized mesoporous silica shells (MSHS–SO_3H) has been shown to have higher performance on xylose dehydration than mesoporous silica shells (MSHS) (Jeong et al., 2011). In addition to sulfonated metal based catalyst, sulfonated polymer-based catalyst such as Amberlyst has also been used to produce HMF and furfural from fructose. It was found in the study by Lansalot-Matras and Moreau (2003), as high as 80 wt.% yield of HMF was obtained within 24 hours, when the reaction was carried out in a mixture of 1-butyl 3-methyl imidazolium tetrafluoroborate and 1-butyl 3-methyl imidazolium hexafluorophosphate at 80 ℃. With this catalytic system, increased HMF yield and selectivity are favored under mild conditions (below 100 ℃) (Yang et al., 2011). Although sulfonated metal and polymer-based catalysts have good activities on biomass conversion, both are of non-decomposable (Mardhiah et al., 2017). The sulfonated carbon-based catalysts prepared from low-cost decomposable carbon sources such as sugar and lignocellulosic biomass have been developed to overcome this problem. These catalysts have been shown to have high activities on biomass conversion (Hara, 2010).

Table 2.5: Production of HMF and furfural from different raw materials in HCW with homogeneous acid catalyst

Substrate and Loading	Reaction Conditions	Catalyst and Loading	Y_{HMF}	$Y_{Furfural}$	References
Glucose	140 °C, 60 min	HCl	54 mol%	-	(Li et al., 2017)
Glucose	150 °C, 60 min	H_2SO_4	21 mol%	-	(Li et al., 2017)
Glucose	220 °C, 5 min	H_3PO_4	10 wt.%	-	(Daorattanachai et al., 2012)
Glucose	200 C, 3 min	H_2SO_4	2.4 mol%	2.25 mol%	(Qi et al., 2008)
Fructose	200 C, 5 min	H_2SO_4	47 mol%	0.19 mol%	(Qi et al., 2008)
Fructose ~ 1 wt.%	240 °C, 2 min	H_3PO_4	45.5 wt.%	2.8 wt.%	(Salak Asghari and Yoshida, 2006)
Fructose ~ 1 wt.%	240 °C, 2 min	H_2SO_4	27.8 wt.%	2.1 wt.%	(Salak Asghari and Yoshida, 2006)
Fructose ~ 1 wt.%	240 °C, 2 min	citric acid	12.6 wt.%	0.7 wt.%	(Salak Asghari and Yoshida, 2006)
Fructose	200 °C, 5 min	H_3PO_4	29 wt.%	-	(Daorattanachai et al., 2012)
Cellulose	230 °C, 5 min	H_3PO_4	8 wt.%	-	(Daorattanachai et al., 2012)
Olive stones	240 °C, 2.5 min	H_2SO_4	-	65wt.%	(Montané et al., 2002)

Table 2.6: Production of HMF and Furfural from different raw materials in HCW with solid acid catalyst

Raw materials	Condition	Catalyst	Y_{HMF} (wt.%)	$Y_{Furfural}$ (wt.%)	References
Fructose	200 °C, 5 min	TiO_2	38.1	5.07	(Qi et al., 2008)
	(Microwave)	ZrO_2	30.6	2.70	(Qi et al., 2008)
Glucose	200 °C, 3 min	TiO_2	7.68	0.51	(Qi et al., 2008)
	(Microwave)	ZrO_2	4.61	0.50	(Qi et al., 2008)
Xylose	140 °C, 240 min	SiO_2-Al_2O_3	-	28	(Bhaumik and Dhepe, 2016)
Xylose	200 °C, 35 min	sulfonated graphene	-	62	(Bhaumik and Dhepe, 2016)
Xylose	170 °C, 2 h	ZrP-HT-Am-C	-	52	(Cheng et al., 2013)
Xylose	190 °C, 1 h	MSHS–SO_3H	-	43.46	(Jeong et al., 2011)
Fructose	120 °C, 8 h	Amberlyst-15	15	-	(Son et al., 2012)
Cellulose	190 °C, 5 h	Amberlyst-15	14	-	(Lanzafame et al., 2012)
Corncob	300 °C, 5 min	TiO_2–ZrO_2	8.6	10.3	(Chareonlimkun et al., 2010a)

2.5 Sulfonated carbon-based catalyst

Recently, the development of sulfonated carbon-based acid catalyst is growing, aiming especially for the facile and economical preparation routes. This type of catalyst has been applied in several reactions including biodiesel production (i.e. esterification and transesterification) (Nata et al., 2017; Pileidis et al., 2014) as well as biomass conversion (i.e. hydrolysis and dehydration reactions) (Qi et al., 2014; Zhao et al., 2016) and reactive extraction of 1,3-Propanediol from glycerol (Boonoun et al., 2010).

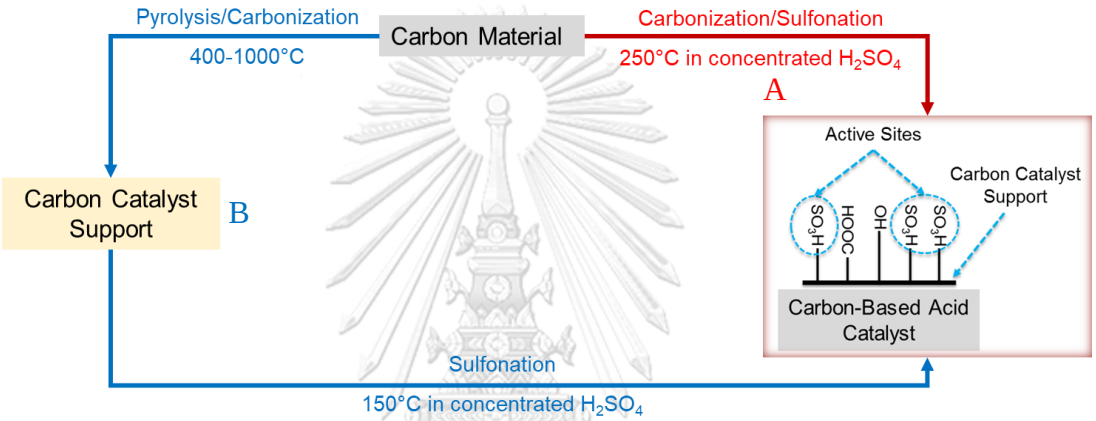

Figure 2.16: Preparation of sulfonated carbon-based catalyst: (A) via carbonization of sulfopolycyclic aromatic carbons and (B) sulfonation of carbonized inorganic/organic compounds

Typically, sulfonated carbon-based catalysts are prepared by pyrolysis/carbonization of carbonaceous materials at high temperatures, followed by (or together with) acid functionalization of the carbonized materials in concentrated acid such as sulfuric acid as shown in **Figure 2.16** (Boonnoun et al., 2010; Nakajima et al., 2007; L. H. Wang et al., 2015).

As shown in **Figure 2.16**, the process of the preparation of the sulfonated carbon-based catalyst, can follow either one of the two methods. Via method A, which is called the carbonization of sulfopolycyclic aromatic carbons, the catalyst is prepared by first mixing of carbon materials (polycyclic aromatic hydrocarbon such as naphthalene, anthracene, pitch, and tar) and concentrated sulfuric acid. The mixture is

then heated at high temperature (250 °C) for several hours. Although this method is simple and straight forward, the aromatic compounds used as starting materials are carcinogens, and boiling in concentrated sulfuric acid at high temperature is highly dangerous (Nakajima et al., 2007). On the other hand, via a safer method, method B, which is called the sulfonation of carbonized inorganic/organic compounds, the catalyst is prepared by two steps; (i) preparation of carbon catalyst support via pyrolysis/carbonization and (ii) sulfonation of carbon catalyst support via concentrated sulfuric acid at lower temperature (150 °C). Method B can be applied to existing abundant natural carbon sources (e.g., sugar, starch, cellulose, hemicellulose, lignin and lignocellulosic biomass). Starting with these carbon sources which have high moiture content however, the pyrolysis/carbonization requires high temperature (above 400 °C) to ensure water is completely removed, which leads to high operating cost (Dehkhoda et al., 2010; Fiori et al., 2014; Ormsby et al., 2012). Alternatively, the synthesis of the carbon catalyst support can be carried out via hydrothermal carbonization process. The resulting sulfonated carbon-based catalyst is called sulfonated hydrothermal carbon-based catalyst.

2.5.1 Sulfonated hydrothermal carbon-based catalyst

Sulfonated hydrothermal carbon-based catalyst is a new green catalyst that is developed in order to reduce cost and danger of preparation process. A synthesis of sulfonated hydrothermal carbon-based catalyst is divided into two steps which are preparation of carbon catalyst support via hydrothermal carbonization and further functionalization via sulfonation with concentrated sulfuric acid.

2.5.1.1 Hydrothermal carbonization

Hydrothermal carbonization is a new and green technology. It takes place in hot compressed water at subcritical temperature (temperature of water between the boiling point temperature (100 °C) and the critical temperature (374 °C)). To prepare carbon catalyst support via hydrothermal carbonization, carbonization takes place in water at relatively low temperatures (150-250 °C) under self-generated pressures. Therefore, the process can convert wet raw material into carbonaceous solid or hydrothermal carbon (HTC) without the need for prior drying (Fiori et al., 2014). This process is a suitable

technique for low-cost biomass with high moisture content. Generally, hydrothermal carbonization of biomass is operated at low temperature and long time from one to several hours (Funke and Ziegler, 2010). As shown in **Table 2.7**, a wide range of hydrothermal carbonization conditions have been employed with different raw materials. The results in various studies indicated that the hydrothermal carbonization temperature and time had effect on HTC yields. From glucose, HTC yields increased with temperature and time, nevertheless HTC could not be produced at temperature below 160 °C. From cellulose, lignin and rye straw on the other hand, HTC yields decreased with increased temperature and time (Falco et al., 2011; Sevilla and Fuertes, 2009a)

Table 2.7: Previous studies of hydrothermal carbonization condition

Raw material (RM)	Hydrothermal carbonization condition			Reference
	Temp. (°C)	Time (h)	RM: water (w/w)	
Glucose	180	4	2:5	(Guo et al., 2012)
Glucose	180	10	1:2	(Qi et al., 2015)
Glucose	180 and 195	8-43	9:50	(Fraile et al., 2012)
Glucose	220	1-8	3:10	(Fiori et al., 2014)
Glucose, Sucrose, Starch	170-240	0.5-15	1:1-1:3	(Sevilla and Fuertes, 2009a)
Glucose, cellulose, rye straw, alcell lignin	120-280	24	1:10	(Falco et al., 2011)
Glucose, xylose, maltose, sucrose, starch, furfural, amylopectin, HMF	180	24	1:9	(Titirici et al., 2008)
Cellulose	225-275	0-96	1:5	(Lu et al., 2013)
Eucalyptus bark	220-300	2-10	1:10	(Gao et al., 2016)
Grape seeds	180-250	1-8	3:10	(Fiori et al., 2014)
Corn stover	250	4	1:2	(Fuertes et al., 2010)
Corn stalk	200	3-44	2:65	(Lei et al., 2016)
Corn stalk	250	4	1:5	(Yan et al., 2014)
Corn stalk, Tamarix ramosissima	250	4	1:10	(Xiao et al., 2012)

2.5.1.1.1 Mechanism of hydrothermal carbon formation

The mechanism of HTC formation from sugar, cellulose, hemicellulose, lignin, and lignocellulosic biomass is reviewed here. The HTC formation from sugar was examined in the study by Kang et al. (2012), in which xylose was converted to furfural via dehydration, which was then converted to HTC via polymerization (Kang et al., 2012). The formation of HTC from other sugars such as glucose and fructose also have a similar mechanism as that of HTC formation from xylose (**Figure 2.17**). Titirici et al. (2012) proposed the HTC formation mechanism from glucose as shown in **Figure 2.18**, in which route A) was taken, and consisting of three steps. In the first step, glucose is converted to HMF via dehydration. Then the HMF is connected to form polyfuran (aromatic unit) via polymerization and aromatization in the second step. Finally in the third step, the polyfuran, containing oxygen functional group , is switched via condensation to carbon network (aromatic carbon), which is called hydrothermal carbon (HTC) (Titirici et al., 2012). The mechanism of HTC formation via route A also suggested that furan compounds (HMF is shown in glucose case) is an intermediate of HTC formation. Therefore, HTC can be produced from furan compounds (i.e. HMF and furfural) or raw materials which can be converted to furan compounds (i.e. sugar, cellulose, hemicellulose, and lignocellulosic biomass).

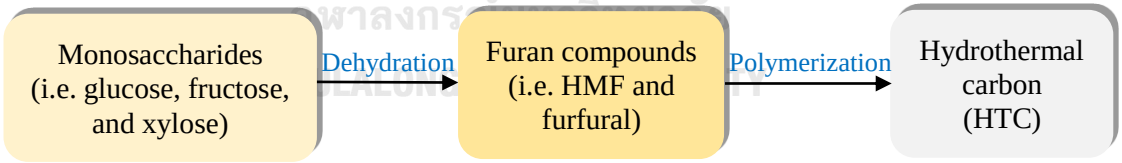

Figure 2.17: Mechanism of HTC formation from sugar (Kang et al., 2012)

Other than HTC formation from sugars, Titirici et al. (2012) also examined hydrothermal carbonization of cellulose as well as lignocellulosic biomass (i.e. rye straw). Their study suggested that unlike the formation of HTC from sugars (glucose, fructose, and xylose) which follow only route A of **Figure 2.18**, HTC could also be produced directly from cellulose via direct aromatization with melting, condensation and decarboxylation in one step to aromatic carbon (route B). In addition, due to similar

structures of cellulose and hemicelluloses, which are complex structures of monosaccharides, they also suggested that the HTC formation from both raw materials follow the same mechanism.

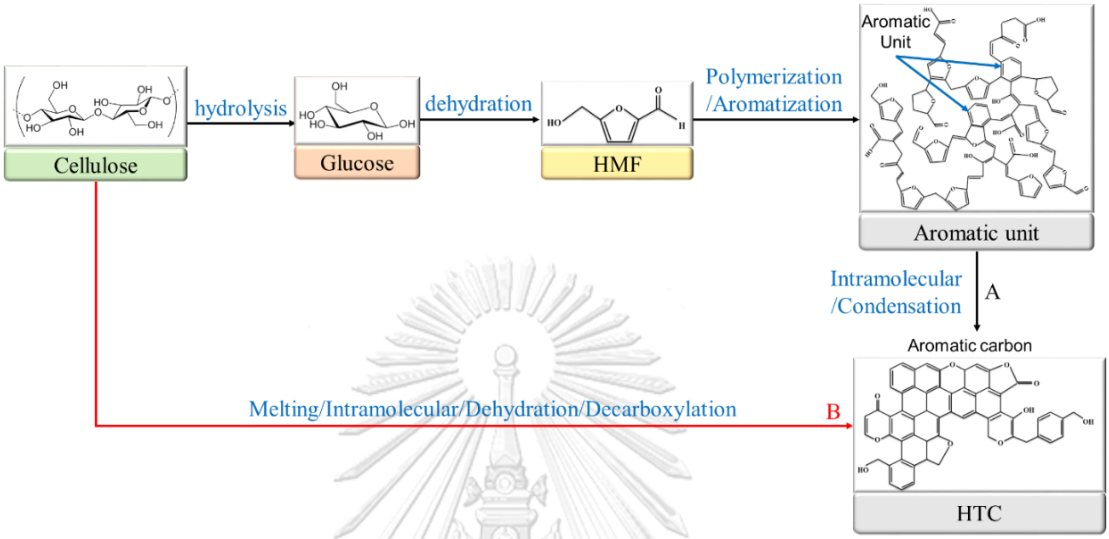

Figure 2.18: Mechanism of HTC formation via hydrothermal carbonization of cellulose: (A) via HMF and (B) direct aromatization (Titirici et al., 2012)

Beside sugars, cellulose and hemicellulose, HTC can also be derived from lignin. As shown in **Figure 2.19**, the mechanism of HTC formation from lignin also consists of two routes. Via Route A, lignin is hydrolyzed to phenolic compounds, which further form into HTC via polymerization/aromatization. Also, lignin derived HTC can be formed via direct aromatization (route B). Nevertheless, the hydrothermal carbonization is usually conducted at temperature lower than 300 °C, hence, it is difficult for most of lignin to form HTC through soluble phenolic compounds. Therefore, non-dissolved lignin is usually transformed to HTC via pyrolysis.

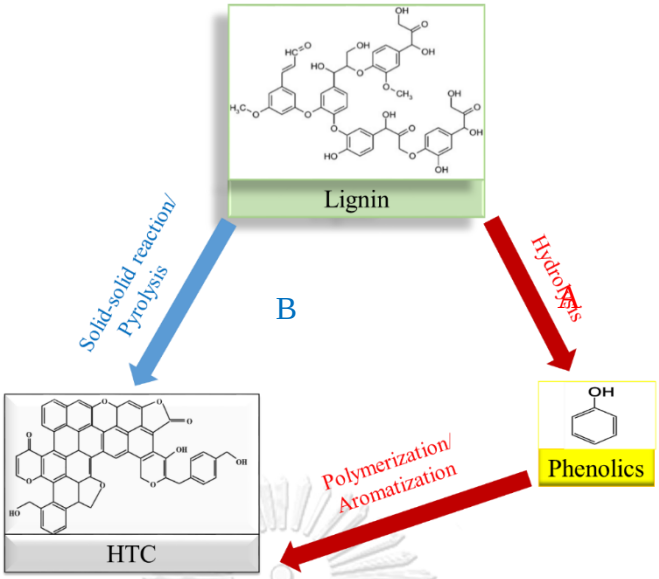

Figure 2.19: Mechanism of HTC formation via hydrothermal carbonization of lignin: (A) via phenolics and (B) direct aromatization (Kang et al., 2012)

For complex raw materials such as lignocellulosic biomass, although a number of studies have been carried out on the production of HTC from different lignocellulosic biomass (Eucalyptus bark, Corn stover, Grape seeds, Corn stalk, and Tamarix ramosissima), most of them focused on effect of hydrothermal carbonization conditions on the yields and the characteristics of the resulted HTCs. The investigation of HTC formation on the other hand is more challenging and only a few studies on this was found in literature. Lei et al. (2016) examined the formation mechanism of HTC prepared by hydrothermal carbonization of corn stalk as a lignocellulosic biomass by. They proposed two ways of HTC formation from lignocellulosic biomass as shown in **Figure 2.20**. By the first (route A), polymerized HTC is formed, in a similar manner with the HTC formation from sugars (route A in **Figure 2.18 and 2.19)**. Through the second route, polyaromatic HTC is formed directly from non-dissolved of fragments (cellulose, hemicellulose and lignin) via intramolecular rearrangement, dehydration, and decarboxylation reaction (Lei et al., 2016).

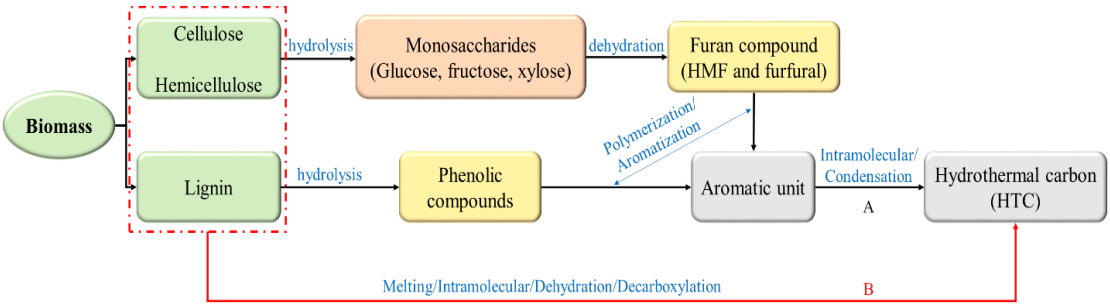

Figure 2.20: Mechanism of HTC formation via hydrothermal carbonization of biomass: (A) Polymerized HTC and (B) Polyaromatic HTC

As can be seen, HTC formation depends on components (i.e. cellulose, hemicellulose and lignin) of lignocellulosic biomass. Therefore, different lignocellulosic biomass components affect the characteristics of HTC. The HTCs derived from different starting carbon sources were shown as following.

2.5.1.1.2 Characteristics of hydrothermal carbon

Previously, the hydrothermal carbon has been synthesized by using various raw materials such as glucose, xylose, maltose, sucrose, amylopectin, starch, HMF, furfural, cellulose and biomass. The HTC derived from different carbon sources, seen by scanning electron microscope (SEM), showed different morphologies. As shown in **Figure 2.21**, The HTCs derived from sugars (glucose, fructose, xylose and sucrose) and furan compounds (HMF and furfural) were regular spherical shapes and smooth outer surfaces. A wide spherical particle sizes between 100 nm and 2 µm diameter were observed with difference of hydrothermal carbonization conditions (Titirici et al., 2012). For the effect of starting concentration of raw material, it was reported that the particle sizes of carbon spheres increased with increased concentration; as shown in **Figure 2.22**, a particle size of carbon spheres derived from glucose increased from 350 to 600 nm when the glucose concentration increased from 0.3 to 0.5 mol/L (Li et al., 2011). Increasing size of carbon spheres was also found when hydrothermal carbonization temperature and time were increased. When temperature was increased from 160 to 260 °C, the diameter of carbon spheres derived from glucose increased from 474 to 685 nm diameter, as can be seen in **Figure 2.23** (Falco et al., 2011). A

similar trend was observed with increasing hydrothermal carbonization time from 19 to 43 hours at the same temperature of 195 °C. The carbon spheres kept on growing, resulting in the increase of the diameter of carbon spheres from 300-400 nm to 1.5 µm (Fraile et al., 2012). In case of cellulose, as shown in **Figure 2.24**, at low temperature of 160 °C, the HTC was seen to take the form of fibers that are still intact and are arranged in a way the characteristics of cellulose were remained (**Figure 2.24**a). When carbonization temperature was increased to 220 °C, the spherical particles (**Figure 2.24**b), similar to glucose derived HTCs were formed. As the carbonization temperature was increased to 240 °C, HTCs of both spherical and irregular shapes were observed (**Figure 2.24**c), with the latter being the non-dissolved cellulose fragments. In case of biomass derived HTCs (**Figure 2.25)**, their morphologies were found to be similar to those of the cellulose derived HTCs. Although two morphologies were seen, the overall structure, however, seemed to remained similar to the structure of the original rye straw (Falco et al., 2011). Nevertheless, a microalgae residue derived HTC presented only one morphology of irregular particle (Fu et al., 2013). Therefore, it can be concluded that morphology of lignocellulosic derived HTCs depends on the type of raw materials.

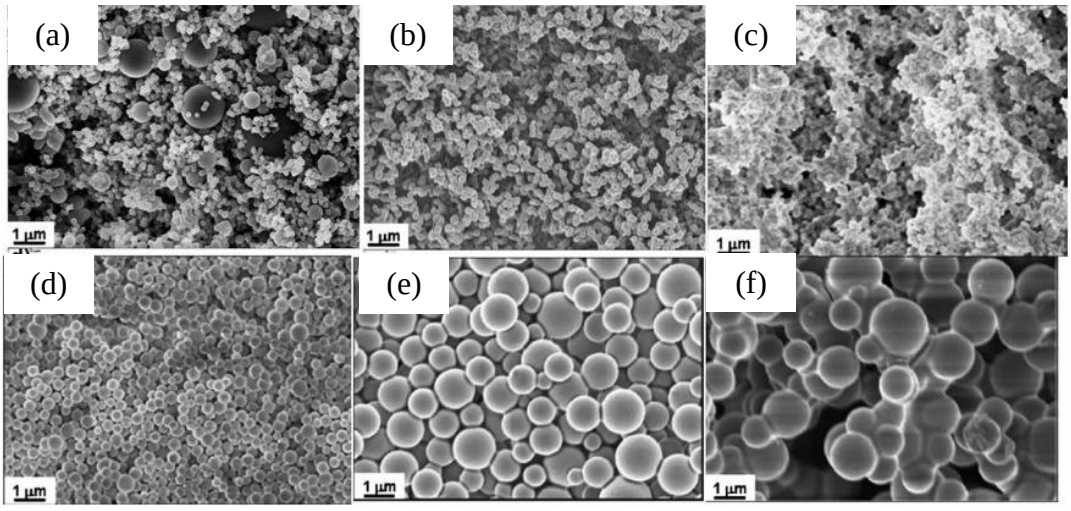

Figure 2.21: SEM images of HTCs obtained at 180 °C from: (a) glucose; (b) fructose; (c) hydroxymethyl furfural (HMF); (d) xylose; (e) furfural; and (f) sucrose (Titirici et al., 2012)

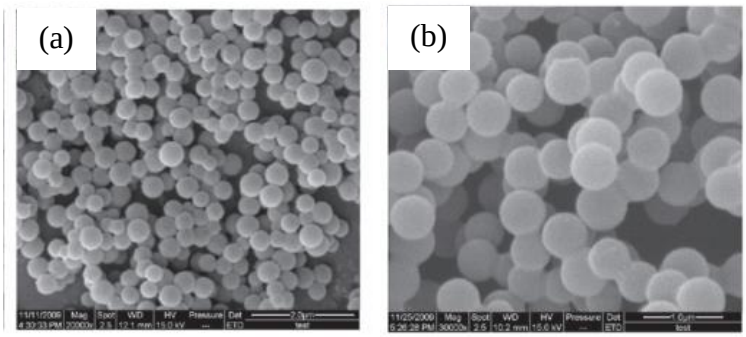

Figure 2.22: SEM images of glucose derived HTCs via hydrothermal carbonization temperature of 190 °C for 4 hours with starting glucose concentration of (a) 0.3 mol/L (b) 0.5 mol/L (Li et al., 2011)

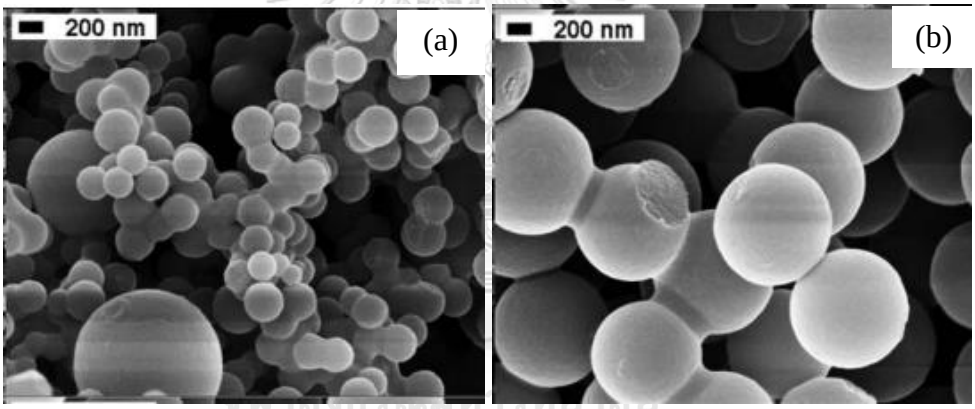

Figure 2.23: SEM images of glucose derived HTCs via hydrothermal carbonization at time of 24 hours and temperature of (a) 160 °C (b) 260 °C (Falco et al., 2011)

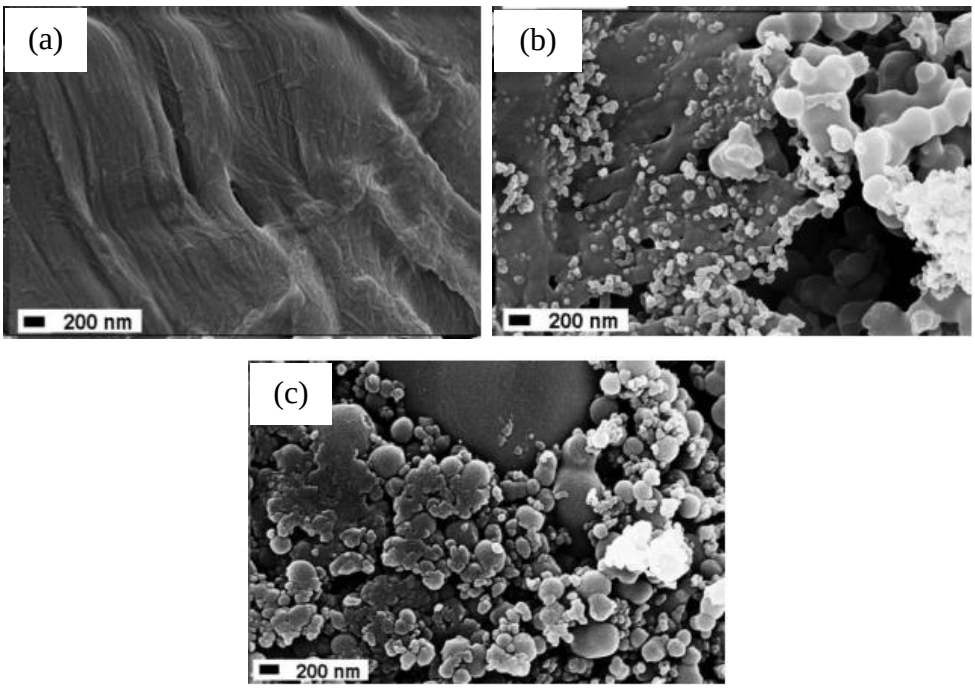

Figure 2.24: SEM images of cellulose derived HTCs via hydrothermal carbonization at time of 24 hours and temperature of (a) 160 °C, (b) 220 °C, and (c) 240 °C (Falco et al., 2011)

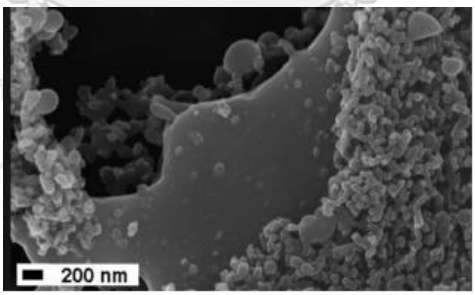

Figure 2.25: SEM images of rye straw derived HTCs via hydrothermal carbonization temperature of 240 °C for 24 hours (Falco et al., 2011)

Although the differences in HTC morphologies were observed, all HTCs have similar XRD pattern, of an are amorphous carbon with broad peak between 10 and 30 degrees. Furthermore, same three main elements (carbon (C), hydrogen (H), and oxygen (O)) were obtained in all HTCs. Generally, hydrothermal carbonization resulted

in decreasing of O and C contents due to dehydration and decarboxylation reaction (Röhrdanz et al., 2016). Carbon contents, on the other hand, were increased to approximately 60-70 wt.% carbon as a result of carbonization. HTCs were confirmed by Fourier transform infrared (FTIR) spectra (**Figure 2.26**), they were taken to be aromatic carbon. The stretching vibrations of aromatic C=C was presented by bands at 1600 cm^{-1}, whereas aromatic C-H out-of-plane bending vibrations was presented by bands at approximate range of 875-750 cm^{-1}. In addition, the bands at approximately 1710 cm^{-1} and those in the range between 3700-3000 cm^{-1} corresponded to stretching vibrations of aromatic C=O (carbonyl, ester, or carboxyl) and hydrogen bonded O-H (hydroxyl or carboxyl group), respectively, suggesting carboxylic acid group occurred as a result of hydrothermal carbonization process. The bands at approximately 1710 cm^{-1} corresponds to stretching vibrations of aromatic C=O (carbonyl, ester, or carboxyl). Based on the FTIR results, it was proposed that the structure of HTC takes the form of aromatic carbon, which is composed of hydroxyl groups and carboxylic groups as shown in **Figure 2.27** (Reza et al., 2016; Sevilla and Fuertes, 2009b).

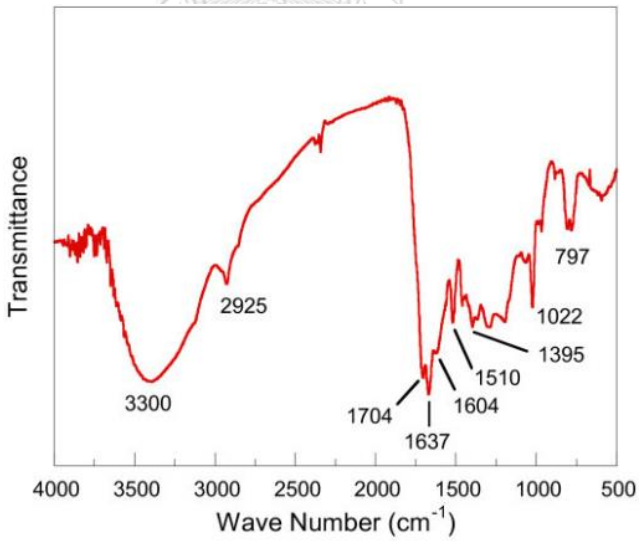

Figure 2.26: FTIR spectrum of HTC (Zhang et al., 2012)

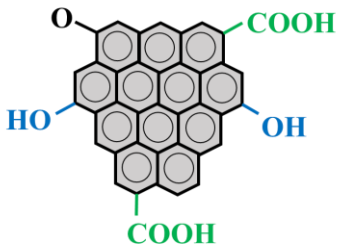

Figure 2.27: Structure of HTC

The structure of HTCs, as shown in **Figure 2.27**, leads to the potential applications of HTCs, as absorbents, energy storage or catalysts. For catalyst applications, the stability of catalyst should be concerned. The thermal stability of HTC can be measured by the loss of HTC mass when it is heated. Usually, the thermal stability of HTC depends on the carbon sources. When the sugar was used as starting raw material, three major weight loss regions was observed (**Figure 2.28**). The first region, small weight loss was found due to the water in HTC was removed by high temperature. The slight weight loss was found in the second region, possibly due to losing of functional groups on the surface of carbon such as hydroxyl group and carboxylic group. While the main structure of HTC was decomposed at temperature higher than 270 °C, which found in the last region of weight loss (Inada et al., 2017; Kim et al., 2015). For biomass derived HTC was shown in **Figure 2.29**, three major weight loss regions were also observed. The first weight loss region was similar to the loss of glucose derived HTC. While the loss of HTC mass, occurred in the second region, was explained that not only functional groups on carbon surface, but the main components of biomass (all hemicellulose as well as some cellulose and lignin) derived HTC were also decomposed. Lastly, the remaining cellulose and lignin were decomposed in the third region (Islam et al., 2015).

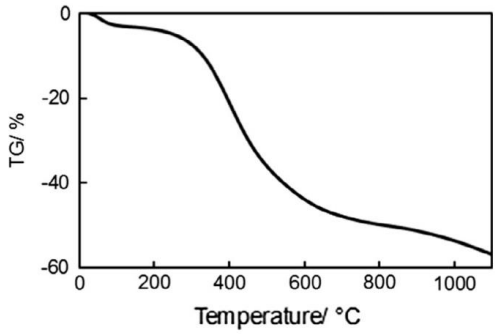

Figure 2.28: TG curve of glucose derived carbon spheres synthesized at 200 °C for 5 h. The measurement was carried out under N_2 gas flow at a heating rate of 7.5 °C/min. (Inada et al., 2017)

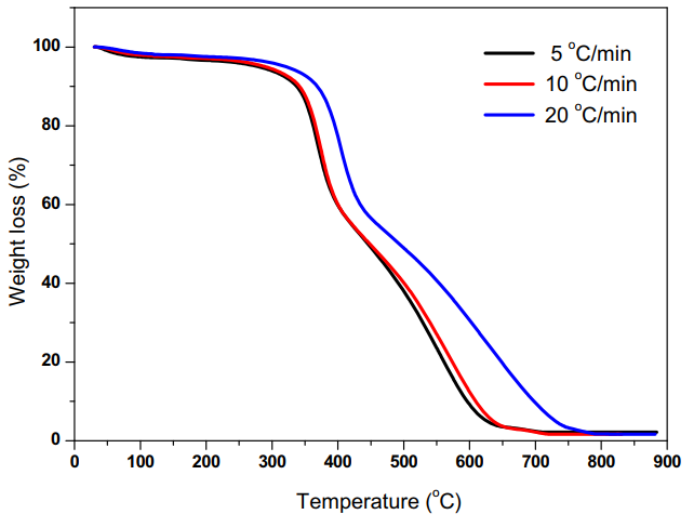

Figure 2.29: TG profile of Karanj fruit hulls derived HTC at different heating rates (Islam et al., 2015)

Previous research mostly reported that HTC is stable at the temperatures below 270 °C, therefore HTC can be used in the reactions carried out at the below this suggested temperature. Qi et al. (2014) examined the application of HTC as catalyst in hydrolysis reaction. They synthesized HTC from glucose, and used it as a catalyst in cellulose conversion to sugar at the reaction temperature of 130 °C and found that approximately 47 wt.% of total reducing sugar (TRS) yield was achieved. The achieved TRS yield however, is rather low (Qi et al., 2014). By increasing catalyst acidity, further improvement of the catalytic activity was possible. Since the HTC has only weak acidic

groups (-OH and –COOH), the strong acidic group such as sulfonic group (–SO_3H) should be functionalized in order to increase the acidity. Qi et al. (2014) improved the catalyst performance via functionalization of acidic groups on a glucose derived HTC (CM), by functionalization with sulfosalicylic acid and acrylic acid resulting in CM-SO_3H and CM-COOH, respectively. The results indicated carboxylic group was increased from 1.37 mmol/g in CM to 2.22 mmol/g in CM-COOH, while 0.12 mmol/g sulfonic acid group was present in CM-SO_3H. In addition, these catalysts were tested on the reactivity towards cellulose hydrolysis. The results on the total reducing sugar (TRS) products shown in **Figure 2.30** demonstrated that the catalytic activity of both CM-COOH and CM-SO_3H for cellulose hydrolysis was higher than that of CM. The highest TRS yield (59.4 wt.%) was obtained in the reaction catalyzed by CM-SO_3H. It was noted that sulfonic group had higher activity than the hydroxyl group and the carboxylic group. Therefore, sulfonic group functionalization is an important process to improve the catalytic activity of HTC.

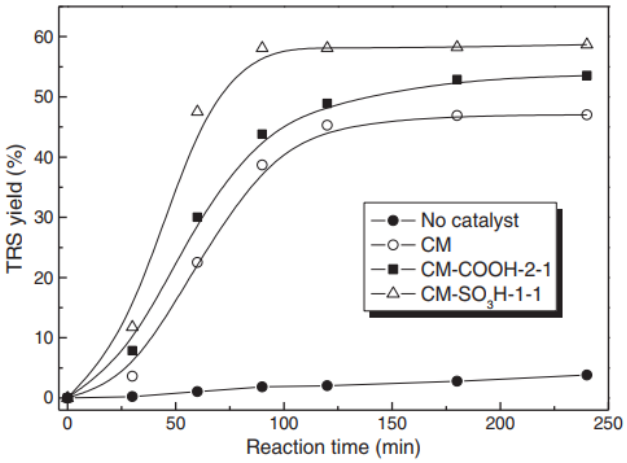

Figure 2.30: Hydrolysis of cellulose in an ionic liquid catalyzed by different carbonaceous materials from hydrothermal carbonization of glucose and different co-monomers. Catalyst CM represents carbonaceous material prepared by hydrothermal carbonization of glucose in the absence of additive, CM-SO3H and CM-COOH represent materials prepared by hydrothermal carbonization of glucose with SA and acrylic acid, respectively. Reaction conditions: cellulose (0.05 g), [BMIM][Cl] (1 g), catalyst (0.05 g), 130 °C (Qi et al., 2014).

2.5.1.2 Sulfonation of hydrothermal carbon

As the HTC is aromatic carbon, hence, the sulfonation of HTC occur by aromatic sulfonation, which is a reaction of sulfur trioxide (SO_3) and an organic molecule, in this case an aromatic carbon, to form sulfur-carbon bond. In general, sulfuric acid (H_2SO_4) and oleum ($SO_3 \cdot H_2SO_4$) are widely used as sulfonating reagent. In cases of oleum sulfonation, low cost of SO_3 is used. However, the process has a disadvantage of being an equilibrium reaction, which gives rise to large quantities of un-reacted sulfuric acid. Hence, the un-reacted sulfuric acid must be separated from the reaction mixture and subsequently eliminated. Alternatively, in absence of acid waste, sulfonation with sulfuric acid is advantageous. Because the water formed during reaction is removed by heating at higher boiling point, the reaction may therefore continue to completion (Foster, 1996).

2.5.1.2.1 Mechanism of hydrothermal carbon sulfonation with sulfuric acid

The mechanism of sulfuric acid sulfonation is described as consisting of the following four steps as shown in **Figure 2.31**. In the first, 2 H_2SO_4 molecules generate SO_3 molecule, positive ion of H_3O^+ and negative ion of HSO_4^-. In the second step, SO_3 molecule reacts with the aromatic hydrocarbon to form an arenium ion. Then the arenium ion gives a proton to HSO_4^- negative ion to form benzenesulfonate ion and H_2SO_4 by the third step. In the final step, benzenesulfonate ion accepts a proton from H_3O^+ positive ion to become benzenesulfonic acid. As a byproduct, water is produced in the process, and can be removed by heating at higher boiling temperature. Therefore, sulfonation process is generally operated at temperature between boiling point of water and sulfuric acid in order to remove water and maintain SO_3 molecule in concentrated H_2SO_4. There have been a number of research studies in which the sulfonation of HTC was investigated. Briefly, HTC and concentrated H_2SO_4 (>96 wt.%) were mixed with ratios between 1:10 and 1:60 (g HTC/ml H_2SO_4), and the mixture was then heated at temperature of 150-200 °C for 12-16 h under a nitrogen flow (Fraile et al., 2012; Kang et al., 2013; Liu et al., 2013; Roldán et al., 2015; Tran et al., 2016; K. Zhang et al., 2016). Although HTC sulfonation was operated at different conditions, however, the

characteristics of the resulted sulfonated solid catalyst, called sulfonated hydrothermal carbon-based catalyst or HTC-based catalyst (HTC-SO_3H), are similar.

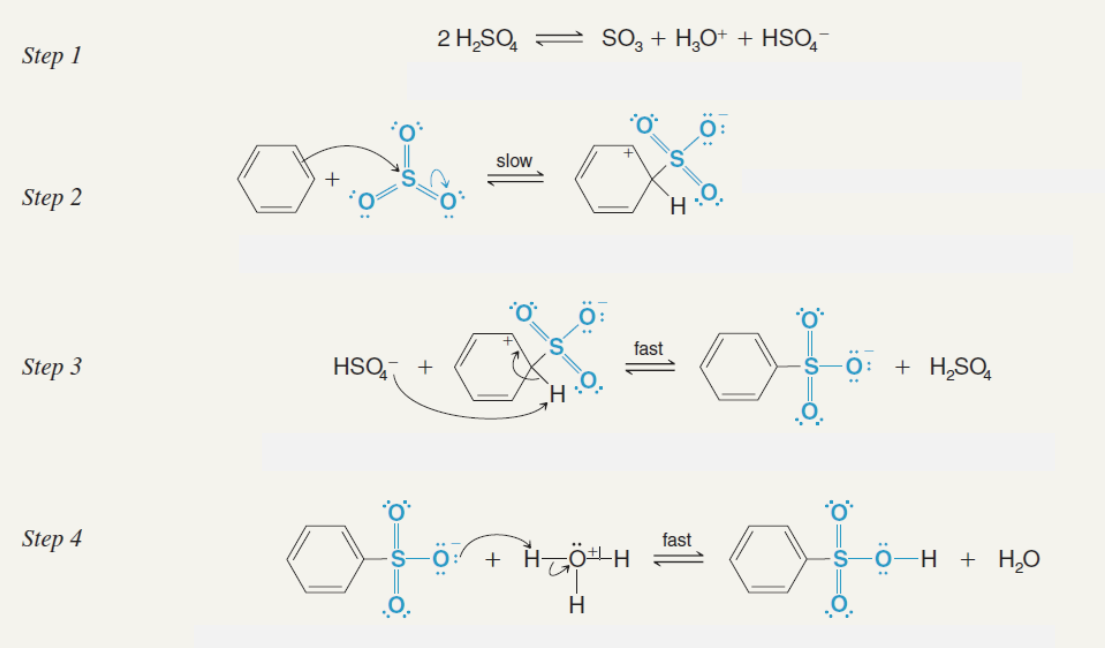

Figure 2.31: Mechanism of aromatic sulfonation via concentrated sulfuric acid (Shi, 2017)

2.5.1.2.2 Characteristics of sulfonated hydrothermal carbon-based catalyst

As for the first characteristics, the morphology the HTC-SO_3H may vary depending on the type of raw materials. The morphology of HTC-SO_3H seen under a scanning electron microscope (SEM) shows no major differences from that of the un-sulfonated HTC, except that agglomeration of spherical particles was observed. In cases of lignocellulosic biomass, the morphology was found to change after sulfonation. This might be due to the fact that sulfuric acid could act as a catalyst in the reaction, and could lead to additional dehydration-carbonization of the unreacted components in lignocellulosic biomass (Pileidis et al., 2014). Beside the morphologies, the N_2 adsorption isotherm characteristics of the carbon after sulfonation has also been examined (Liu et al., 2010). of sulfonated carbon catalyst. They demonstrated that

isotherm of sulfonated carbon catalyst (AC-SO_3H) was similar to that of the unsulfonated carbon (AC), which was of type IV isotherm with evident hysteresis loop in the relative pressure range of about 0.4-0.9 (**Figure 2.32**). Although the same type of isotherm was found in both carbon before and after sulfonation, after sulfonation however, the pore volume of the carbon decreases, suggesting that a small part of the pore space has been occupied by the grafted SO_3H groups (Liu et al., 2010). In addition to isotherm and pore volume, the surfaces area of sulfonated carbon-based catalyst was found to be a small, at approximately 1-15 m^2 g^{-1} (M. Wang et al., 2015)

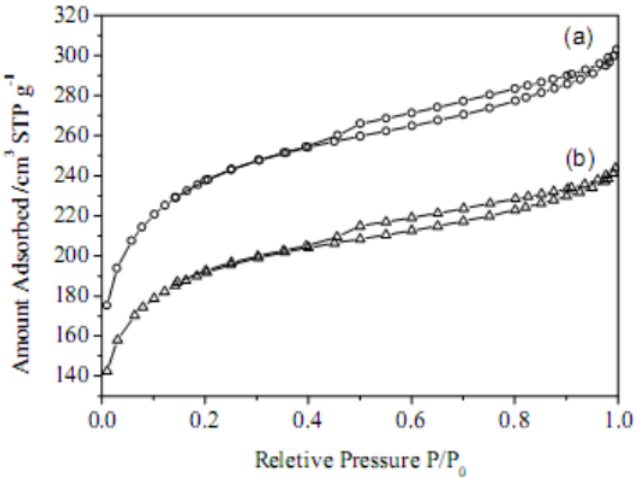

Figure 2.32: N_2 adsorption isotherms of (a) AC and (b) AC-SO_3H (Liu et al., 2010)

Having the X-ray diffraction (XRD) pattern with broad peaks between 10 and 30° (2θ), the HTC-SO_3H, similar to that of HTC, has an amorphous structure. In addition, some research work has reported that another diffraction peak (2θ=35°-50°) was also seen in HTC-SO_3H. This indicated that further carbonization occurred during sulfonation, resulting in HTC-SO_3H with larger carbon sheet than that of HTC (Okamura et al., 2006; Suganuma et al., 2008). The amorphous HTC-SO_3H consists of C, H, O and S, with S content increased after sulfonation. Approximately 5-6.4 wt.% of S was found after the sulfonation of glucose and cellulose derived HTC. While slightly lower S content (5 wt.%) was found in case of lignocellulosic biomass derived HTC, presumably due to the distribution of polar group and the presence of lignin in lignocellulosic biomass. Moreover, as confirmed by FTIR, S content obtained in HTC-

SO_3H represented sulfonic acid group. The sharp peak at 1025-1030 and 1160-1170 cm^{-1} are associated with symmetric O=S=O stretching vibrations and with sulfonic groups, respectively (Pileidis et al., 2014). In HTC-SO_3H catalyst, other functional groups in HTC remain. main. Thus, as shown in **Figure 2.33**, the HTC-SO_3H catalyst is composed of not only the hydroxyl and carboxylic acid groups, but it is also composed of sulfonic group.

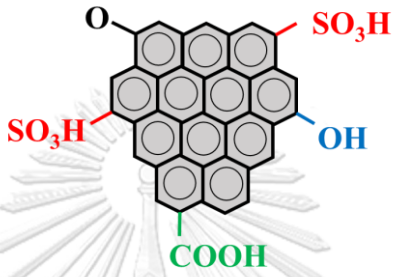

Figure 2.33: Structure of sulfonated HTC-based catalyst

Compared to HTC, thermal stability of HTC-SO_3H as analyzed by TGA is lower, since the sulfonic groups on the carbon surface is easily leached. Pileidis et al. (2014) reported that three major weight loss regions were observed in sulfonated glucose and cellulose derived HTC-SO_3H catalysts (**Figure 2.34**). The first region, 10% weight loss was found at temperature below 180 °C due to the decomposition of –SO_3H groups in the catalysts. While the loss of HTC-SO_3H mass in the second region (at temperature of 180-500 °C) represented the decomposition of –OH and –COOH groups. The loss of HTC-SO_3H mass in the last region (at temperature above 500 °C) is a result of the decomposition of the carbon structure (Pileidis et al., 2014; T. Zhang et al., 2016).

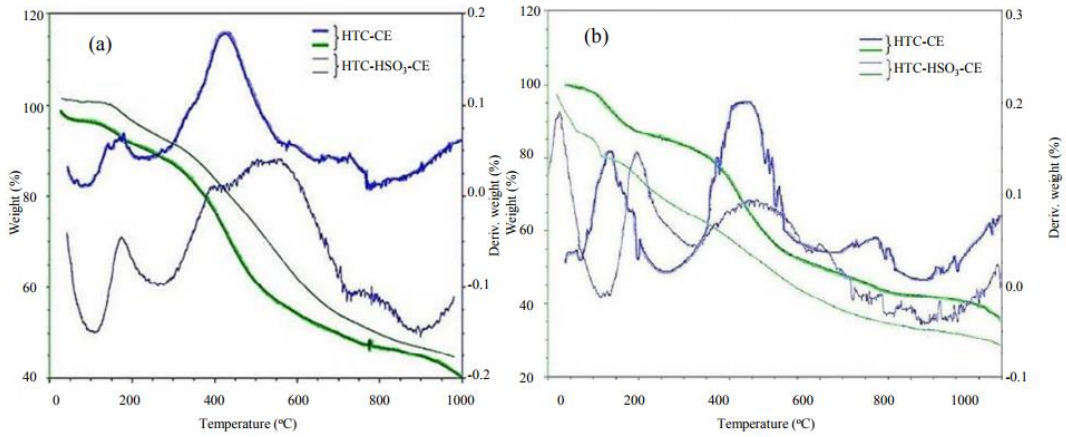

Figure 2.34: TGA results for cellulose (a) and glucose-derived (b) HTC: before sulphonation (bold) and after (normal) (Pileidis et al., 2014)

2.6 Application of sulfonated carbon-based catalyst

The sulfonated solid catalysts have been applied to several reactions. Commercial sulfonated solid acid catalyst such as Amberlyst has been used to produce biodiesel and high value chemical. The reactions catalyzed by Amberlyst usually achieve high product yields, however such catalyst has high cost. To replace high cost catalyst, the HTC-SO_3H catalysts have been developed from low-cost raw material. It is synthesized from simple sugar or lignocellulosic biomass with rather simple preparation. The HTC-SO_3H contains not only -SO_3H groups but also abundant –COOH and –OH groups. Therefore, HTC-SO_3H catalysts possess activities for biodiesel production and biomass conversion.

In case of biomass conversion to HMF via HTC-SO_3H catalyst, HTC-SO_3H catalysts derived from biomass have been proven to have high catalytic activity on HMF production (Kang et al., 2013). However, no study has reported the catalyst stability in term of conversion to products by itself. If not properly prepared and tested, the biomass derived HTC-SO_3H can by itself be leached to reaction mixture, because the HTC catalyst support is prepared the same pathway of biomass conversion. This research therefore aims to synthesize the biomass derived HTC-SO_3H as well as to test the stability of the catalyst for biomass conversion.

CHAPTER III
METERIALS AND METHODS

3.1 Materials and chemicals

Defatted rice bran was obtained from Thai Edible Oil Co., Ltd., Ayuthaya, Thailand. D-Glucose anhydrous was analytical grade and purchased from Ajax Finechem Pty Ltd (Thailand). Sulfuric acid was analytical grade and purchased from Fluka (Singapore). Cellulose powdered, HMF, furfural, levulinic acid, and formic acid were analytical grade and purchased from Wako Pure Chemical Company (Osaka, Japan). Fructose, ethanol and acetone were purchased from Wako Pure Chemical Company (Osaka, Japan). Chemicals used for chemical analyses: 3,5-dinitrosalicylic acid (DNS), potassium sodium (+) – tartrate tetrahydrate, sodium hydroxide, perchoric acid, acetic acid and methanol were also purchased from Wako Pure Chemical Company (Osaka, Japan). Water used in the experiments was deionized water.

3.2 Preparation of hydrothermal carbon-based acid catalyst from defatted rice bran

3.2.1 Preparation of hydrothermal carbon from defatted rice bran

The apparatus used for HTC preparation was shown in **Figure 3.1**, which consists of an 8.8 ml SUS-316 stainless steel closed batch reactor (AKICO Co., Japan), an electric heater, and a temperature controller. The hydrothermal carbonization was carried out in the reactor, into which 1 g of carbon materials (DRB or glucose) and 5 ml of deionized water were charged. The closed batch reactor containing water and the carbon source was heated with an electric heater to the desired temperature, 180-250 °C, and was controlled at a constant temperature by a controller connecting to it. This generally took approximately 15-25 min depending on the set point temperature. After a holding period of 1-8 h at the desired reaction temperature, the reactor was cooled to room temperature by submerging it into a water bath. The resulting solid HTC was separated from the liquid carbonization portion by a filter paper (Whatman no.1) and was then washed with deionized water until the pH of washed water was neutral. After

drying overnight at 110 °C, the resulted HTC was stored in a sealed plastic bag for further analysis. The DRB and glucose derived HTC were called HTCDRB and HTCG, respectively. The HTC yield was determined as the percentage of weight ratio (dry basis) of the produced HTC and raw materials (DRB or glucose).

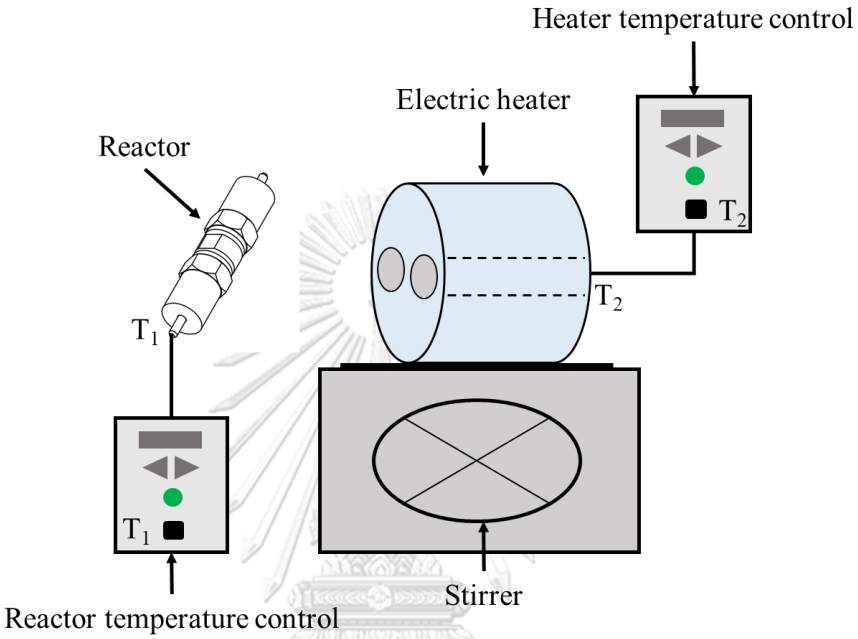

Figure 3.1: Schematic diagram of hydrothermal batch reactor (AKICO Co., Japan)

3.2.2 Preparation of sulfonated hydrothermal carbon-based catalyst from defatted rice bran

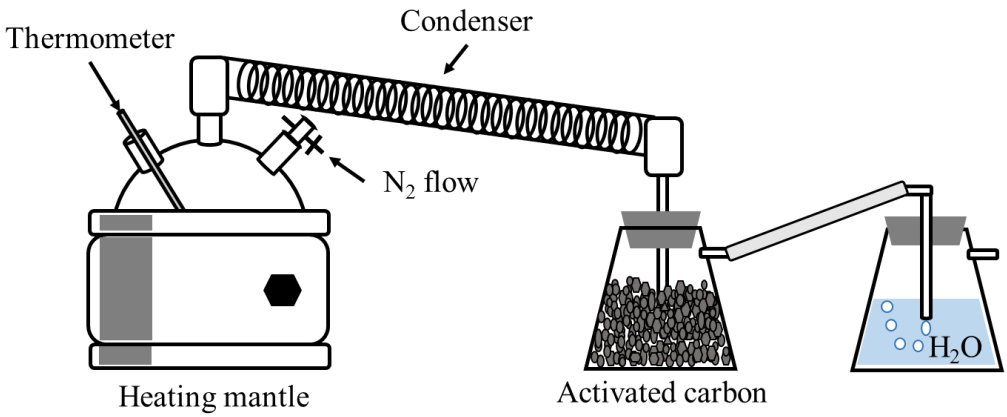

Figure 3.2: Apparatus setup of sulfonation of HTC

The sulfonation of HTC was set up following **Figure 3.2**. The HTC-based catalyst (HTC-SO_3H) was prepared by heating 5 g of HTC in 50 ml of concentrated H_2SO_4 (>96%) using a 3-neck round bottom flask at 150 °C for 15 h under N_2 flow (Yu et al., 2010). The condenser was connected to 3-neck round bottom flask to condense the acid vapor. A 1-liter flask containing the activated carbon was connected to condenser to trap the condensed acid, and a 1-liter flask containing the water was connected to trap remaining acid vapor. The obtained solid acid catalyst was washed with deionized water (1000 ml) before being separated with a vacuum filter. The solid was repeatedly washed with boiling distilled water until no change in water pH was observed. After drying overnight at 110 °C, the HTC-SO_3H catalyst was obtained. The DRB and glucose derived HTC-based catalysts are called HTCDRB-SO_3H and HTCG-SO_3H, respectively.

3.2.3 Characterizations of hydrothermal carbons and hydrothermal carbon-based acid catalyst from defatted rice bran

The elemental compositions (C, H, and N) of raw material and HTC samples derived from DRB and glucose were determined by a CHN analyzer (LECO CHN628 elemental analyzer). The sulphur content (S) of samples was determined by a TruSpec Sulphur (LECO Corporation, USA). The oxygen (O) was calculated by subtraction of C, H, N, and S contents from 100%. Furthermore, the surface morphologies of HTC were observed by Field Emission Scanning Electron Microscopy (FESEM) using a FEI Quanta 200 microscope (Eindhoven, Netherlands) operated at 2 kV.

The crystallinity analysis of HTC and HTC-SO_3H was examined by X-ray diffraction (XRD) performed using RINT 2100 diffractometer, RIGAGU. Each sample was scanned in the range of 2-60 degree. Fourier transform infrared (FTIR) spectra were obtained by using a Jasco FT-IR-4100 spectrometer to characterize the functional groups of the samples. Prior to each measurement, the sample was grounded into fine particles and mixed with KBr to prepare disks. The spectrum was recorded in wavenumber from 4000-500 cm^{-1} with resolution of 4 cm^{-1}. The thermal stability of each sample was determined by Thermogravimetric Analyzer (TGA) using a TG/DTA6200 Thermo-gravimetric analyzer. Non-isothermal combustion of HTCs was conducted in the furnace of the TGA system under a nitrogen gas atmosphere at flow

rate of 10 ml/min and heating rate of 10 °C/min from 45 °C to 500 °C. The sample weight was continuously recorded under the experimental conditions. The specific area, pore volume and pore size diameter of the samples were determined by N_2 physisorption technique using the Brunauer-Emmet-Teller (BET) method with a Belsorp-mini (BEL Japan, Tokyo, Japan); the samples were pretreated to remove moisture at 150 °C for 3 h prior to measurement. The total acidity and concentration of sulfonic (-SO_3H) groups of the samples were measured by neutralization titration method (Wu et al., 2010). The HTCDRB and HTCG were labeled as HTCDRBX-Y and HTCGX-Y, respectively, where X (X = 180, 220, 250 °C) was the hydrothermal carbonization temperature, Y (Y = 1, 3, 8 h) was the hydrothermal carbonization time. The HTCDRB-SO_3H and HTCG-SO_3H were labeled as HTCDRBX-Y-SO_3H and HTCGX-Y-SO_3H, respectively.

3.2.4 Catalyst leaching test under microwave-assisted hydrothermal reaction condition

Microwave heating, which offers the advantage of shorter required treatment times, accompanied by a consequent reduction in energy consumption, was used to evaluate the leaching of the synthesized HTC-SO_3H catalyst for biomass conversion. Microwave system from CEM Corp. (Matthews, NC, USA) (**Figure 3.3**) was used in our experiments. It consists of 100 ml closed polyetheretherketone (PEEK) vessels covered with special TFM sleeves, a power sensor, a temperature sensor, and a temperature controller of MARS 5^{TM}. In each batch of microwave treatment experiment, approximately 0.05 g of catalyst and 5 ml of deionized water were charged into a vessel. The vessel was then closed and placed in the microwave field. Microwave irradiation at 300 W was turned on until the temperature of the vessel content reached 200 °C (approximately 12 min) and was maintained at this temperature for the next 5 min. After allowing the system to cool down (taking approximately 20 min), the liquid and the solid catalyst were removed from the vessel and were separated using a filter paper. The solid residue was washed with 5 ml deionized water, while the liquid was assayed for the amount of HMF, furfural, levulinic acid, and formic acid.

The quantifications of HMF, furfural, levulinic acid, and formic acid in the liquid fraction were conducted using a high-performance liquid chromatography

(HPLC, JASCO International Co., Ltd., Japan), equipped with a Jasco PU980 pump, a Shodex SUGAR SH1011 (8.0mmID*300mm), a Sugai U-620 column heater, a Jasco AS-2055 plus automated sampler injector and a Jasco UV-970 detector. The column temperature was set at 60 °C and the injection volume was set at 10 µl, and perchoric acid ($HClO_4$) was used as an eluent at a flow rate of 0.5 ml/min. The amounts of the leached components from the catalyst were reported as percentage of the mass of the starting material (DRB or glucose derived HTC-SO_3H).

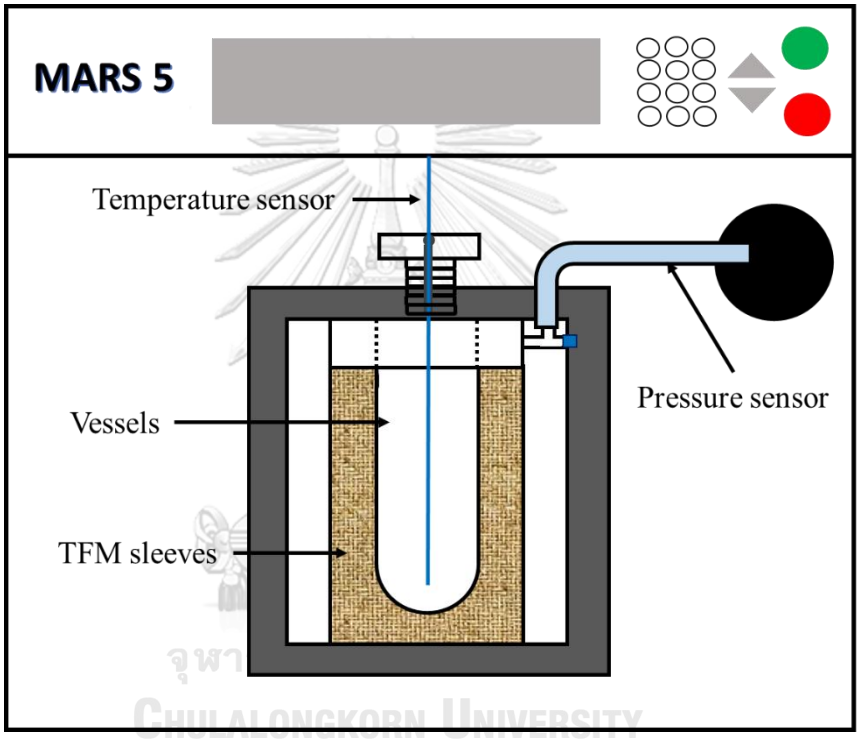

Figure 3.3: Microwave system from CEM Corp. (Matthews, NC, USA)

3.2.5 Catalytic activity test on cellulose hydrolysis

The HTC-SO_3H was tested on the cellulose hydrolysis. It is noted that the commercial grade sulfonated solid catalyst-Amberlyst 16 WET- was also tested for comparison. The Amberlyst 16 WET was purchased from Fluka Analytical (Sigma-Aldrich Chemie GmbH). The reaction was carried out in an 8.8 ml SUS-316 stainless steel closed batch reactor (Suan Luang Engineering Ltd., Part.) (**Figure 3.4**), into which 0.1 g of cellulose, 5 ml of deionized water, and 0.005 g of catalyst were charged. The

reactor was shaken and heated to the desired reaction temperature (180 °C) by an electric heater, connected to a temperature controller, as well as maintained at this temperature for 5 min. After the reaction, the reactor was quenched in a water bath at room temperature. Subsequent to the removal and the separation of the solid and the liquid reaction products by filtration through a Whatman No. 1 filter paper, the liquid products were determined for the amounts of glucose, HMF and furfural.

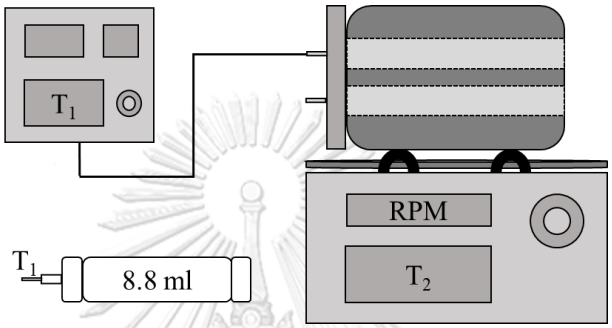

Figure 3.4: Batch reactor (Suan Luang Engineering Ltd., Thailand)

The quantification and identification of glucose in the liquid products was conducted using an HPLC equipped with an evaporative light scattering detector (ELSD) detector with a Rezex RPM Monosaccharide Pb+2 (7.8mmID*300) column. The column temperature was set at 60 °C. Injection volume was set at 5 µl and water was used as the eluent at a flow rate of 0.6 ml/min. The retention time of glucose was 13.3 min. The HPLC analyses for the amounts of HMF and furfural were carried out using a Varian C18 (4.6mmID*250) column at 25 °C, with 90% (1% aq. Acetic acid):10% methanol used as the eluent. The eluent flow rate was 1 ml/min, and the injection volume was set at 5 µl. The concentration of HMF and furfural were analysed based on UV absorbance at 285 nm. The retention times of HMF and furfural were 6.6 min and 9.0 min, respectively. The yields of the reaction products - glucose, HMF and furfural- were calculated as mass percentages of the products to the mass of the starting cellulose.

3.3 Stability improvement of hydrothermal carbon-based acid catalyst from glucose

3.3.1 Preparation of hydrothermal carbon from glucose

In this experiment, HTC derived from glucose was synthesized by hydrothermal process at the longer reaction time compared with the previous experiment in order to improve the stability of material. The experimental procedure was described as following. HTCG was prepared by hydrothermally carbonizing glucose in a 520 ml SUS-316 stainless steel closed batch reactor (OM LABTECH Co., Japan) (**Figure 3.5**). 30 g of glucose and 300 ml of de-ionized water were charged into the reactor. The mixture was stirred and heated with an electric heater to a desired temperature (180-250 °C), which took approximately 15-35 min heating time. At the desired temperature, carbonization reaction was allowed to proceed for a holding period of 6-24 h, after which the reactor was cooled to room temperature by an electric fan. The solid HTCG and liquid fraction of the reaction were then removed from reactor and were separated by means of vacuum filtration. The liquid fraction was analyzed to determine the amount of glucose and HMF, as well as total reducing sugar (TRS). The solid HTCG was washed with three solvents in the following sequence: de-ionized water, ethanol, and followed by acetone, in order to remove polar chemicals such as levulinic acid and formic acid produced during the reaction. For each washing step, HTCG was mixed with 500 ml of solvent and the mixture was sonicated for 1 h. The HTCG was then separated from the solvent by vacuum filtration, and was dried at 60 °C for 24 h. The resulting HTCG was stored in a desiccator for subsequent use. The HTCG yield was determined as the percentage of weight ratio (dry basis) of the produced HTCG and raw material (glucose).

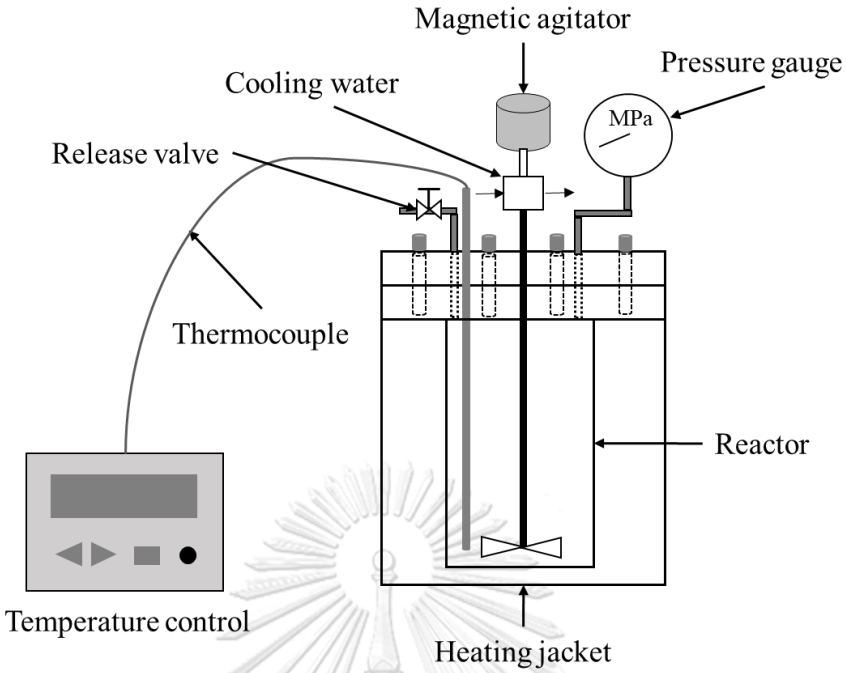

Figure 3.5: Batch reactor (OM LABTECH Co., Japan)

3.3.2 Preparation of sulfonated hydrothermal carbon-based catalyst from glucose

The HTCG-SO_3H was prepared by sulfonation following the method described by Okamura et al. (2006). The apparatus setup of sulfonation was shown in **Figure 3.6**. Briefly, 5 g of HTCG was heated in 50 ml of concentrated H_2SO_4 (>96%) at 150 °C for 15 h under N_2 flow in a 3-neck round bottom flask. The condenser was connected to 3-neck round bottom flask to condense the acid vapor. A 300 ml round bottom flask in ice bath was connected to condenser to keep the condensed acid. A 500 ml round bottom flask containing the water was connected to 300 ml round bottom to trap remaining acid vapor. The resulting solid acid catalyst was then washed with 1000 ml of distilled water, and was further washed with boiling distilled water until no pH change in the wash water was observed. The resulting solid catalyst was subsequently washed with 500 ml of ethanol and then with 300 ml of acetone. After drying overnight at 60 °C, the HTCG-SO_3H catalyst was obtained.

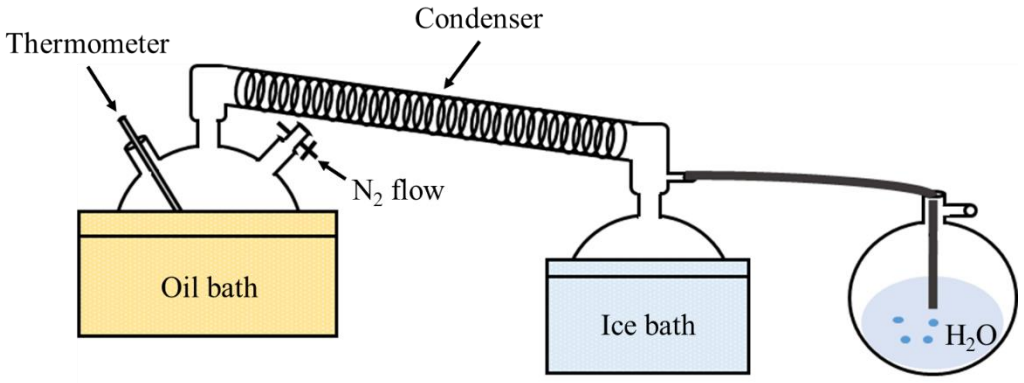

Figure 3.6: Apparatus setup of sulfonation of glucose derived HTC

3.3.3 Characterizations of hydrothermal carbon and hydrothermal carbon-based acid catalyst from glucose

The elemental analysis (C, H, and N) of HTCG and HTCG-SO_3H samples was carried out using elemental analyzer (J-Science Lab Micro Corder JM10), and the sulfur content was carried out using elemental analyzer (J-Science Lab Micro Corder JMSU10). The oxygen content was calculated by subtraction of C, H, N, and S from 100%. The crystallinity analysis of the samples was examined using the automatic X-ray diffractometer (XRD; RINT 2100, Rigaku) with Miniflex Guidance software. Each sample was scanned in the range of 3-90 degree. The surface morphologies of samples were acquired with Field Emission Scanning Electron Microscopy (FESEM, JSM-7610F) operated at 2.0 kV. Functional groups of samples were determined by FTIR spectra using Jasco FT-IR-4100 spectrometer (JASCO International Co., Japan). Prior to measurement, the sample was grounded into fine particles and mixed with KBr to prepare disks. Each sample was investigated in the wavenumber range of 4000-500 cm^{-1} with resolution of 4 cm^{-1}. The thermogravimetric analysis was conducted to determine the thermal stabilities of the samples using a thermogravimetric analyzer (TGA; TG/DTA6200, SII EXSTAR 6000, Hitachi High-Technologies Corporation, Japan). Non-isothermal combustion of all samples was conducted in the furnace of the TGA system under a nitrogen gas atmosphere at a flow rate of 10 ml/min and a heating rate of 10 °C/min from the starting temperature of 45 °C to 500 °C. The sample weight loss was continuously recorded under the experimental conditions. The specific area, pore

volume and pore size diameter of all HTC and HTC-SO_3H were determined by N_2 physisorption technique using the Brunauer-Emmet-Teller (BET) method with a Belsorp-mini (BEL Japan, Tokyo, Japan); the samples were pre-treated to remove moisture at 150 °C for 3 h prior to measurement. The total acidity of the samples was analyzed by temperature-programmed desorption (TPD) with ammonia (Y. Wang et al., 2015). The HTCG was labeled as HTCGX-Y, where X (X = 180, 220, 250 °C) represented the hydrothermal carbonization temperature and Y (Y = 6, 12, 18, 24 h) represented the hydrothermal carbonization time. The HTCG-SO_3H was labeled as HTCGX-Y-SO_3H.

3.3.4 Analysis of liquid fraction obtained via hydrothermal carbonization of glucose

The TRS obtained in the liquid fraction of hydrothermal carbonization of glucose was analyzed by a dinitrosalicylic (DNS) colorimetric method, using D-glucose as a standard (Miller, 1959). Into each 1 ml of the sample, 2 ml of de-ionized water and 3 ml of DNS reagent were mixed. The mixture was then heated in boiling water for 5 min until the red-brown color was developed. The mixture was then cooled to room temperature in a water bath. The absorbance was measured with a spectrophotometer (JASCO V-660 UV-VIS Spectrophotometer, JASCO International Co., Japan) at 540 nm. The amount of TRS was determined using standard calibration curve and % TRS was calculated based on the weight of the starting glucose.

The quantification of glucose and HMF components obtained in liquid fraction were conducted using a high performance liquid chromatography (HPLC, JASCO International Co., Ltd., Japan) which consisted of Jasco RI-2031 plus detector, Jasco UV-970 detector, Jasco PU980 pump system, Sugai U-620 column heater and Jasco AS-2055 plus automated sampler injector equipped with Shodex SUGAR SH1011 (8.0mmID×300mm) column. The column temperature was set at 60 °C and the injection volume was set at 10 μl, and perchloric acid ($HClO_4$) was used as an eluent at a flow rate of 0.5 ml/min. Glucose and HMF were detected by the refractive index (RI) detector and the UV detector at 220 nm, respectively. The concentrations of glucose (retention time = 16.2 min) and HMF (retention time = 39 min) were calculated using external calibration curves attained from standard solutions of known concentrations.

The analyses of HMF and glucose allowed the determination of HMF content, defined as weight percentage of HMF to the starting glucose, and the glucose conversion, which was the percentage of the mass difference between the starting glucose and the glucose remained in the liquid product, over the mass of the starting glucose.

3.3.5 Catalytic activity test of hydrothermal carbon-based acid catalyst from glucose

Both of synthesized HTCG and HTCG-SO_3H were tested on the cellulose hydrolysis and fructose dehydration. It is noted that the commercial grade sulfonated solid catalyst-amberlyst 16 wet (Fluka Analytical, Sigma-Aldrich Chemie GmbH), and graphene oxide (GO) prepared by modified Hummer's method (Allahbakhsh et al., 2014) were also tested for comparison. The reaction was carried out in an 8.8 ml SUS-316 stainless steel closed batch reactor (Suan Luang Engineering Ltd., Thailand) (**Figure 3.4**), into which 0.1 g of raw material (cellulose or fructose), 5 ml of deionized water, and 0.005 g of catalyst (5 wt.% of raw material) were charged. The reactor was shaken and heated to the desired reaction temperature (180 °C) by an electric heater, with a temperature controller connected to it. After the reaction, the reactor was quenched in a water bath at room temperature to stop the reaction. With additional amount of 5 ml of de-ionized water, the solid and liquid reaction products were completely removed from the reactor, and were separated from each other by Whatman filter paper no 1. The amounts of glucose, fructose, HMF and furfural in the liquid product were determined by HPLC.

The quantification and identification of glucose and fructose in the liquid products were conducted using an HPLC equipped with an evaporative light scattering detector (ELSD) detector with a Rezex RPM Monosaccharide Pb+2 (7.8mmID*300) column at 60 °C. Injection volume was set at 5 μl and water was used as the eluent at a flow rate of 0.6 ml/min. The retention times of glucose and fructose were 13.3 and 19.0 min, respectively. The analysis for the amount of HMF and furfural were carried out using a Varian C18 (4.6mmID*250) column at 25 °C, with 90% (1% aq. Acetic acid):10% methanol used as the eluent. The eluent flow rate was 1 ml/min, and the injection volume was set at 10 μl. The concentration of HMF and furfural were analyzed based on UV absorbance at 285 nm. The retention times of HMF and furfural were 6.6

and 9.0 min, respectively. The yields of the reaction products: glucose, HMF and furfural, were calculated as mass percentages of mass of products to the mass of the starting material (cellulose or fructose). The conversion of fructose was defined as the percentage of the mass difference of the starting fructose and the fructose remained in the liquid product over the mass of the starting fructose.

3.3.6 Catalyst recyclability of hydrothermal carbon-based acid catalyst from glucose

The recyclability of HTCG-SO_3H was evaluated for fructose dehydration. After the first cycle, the catalyst was separated from the reaction medium by means of filtration and washed with the deionized water until no pH change in the wash water was observed. The recovered catalyst was then washed with 30 ml of ethanol and 10 ml of acetone, and dried overnight, and reused. These steps were repeated for the total of five cycles.

CHAPTER IV
RESULTS AND DISSCUSION

The initial step to investigate the suitability of the acid functionalized HTC catalysts from defatted rice bran and glucose for the application in biomass conversion is indeed the catalysts preparation. Firstly, the effects of hydrothermal carbonization conditions including hydrothermal temperature and time on characteristics, yield and thermal stability of HTC were determined. After the functionalization of the HTC with sulfuric acid, the characteristics of the DRB- and glucose-HTC derived catalysts were compared. The DRB- and glucose-HTC derived catalysts prepared at the suitable conditions were then selected for the further test on the catalyst stability under hydrolysis reaction condition, by the analysis of the components (biomass conversion products such as glucose and HMF) leached into the liquid fraction. The catalytic activity of the catalysts was also evaluated in the reaction of cellulose hydrolysis and fructose dehydration. Furthermore, in case of glucose-derived HTC catalyst, longer hydrothermal carbonization time was investigated to further improve the stability of the catalyst. In this chapter, the characterization results of HTCs and the HTC based catalysts, the tests on catalyst stability and the catalytic activity, as well as the recyclability of the catalysts are reported.

4.1 Preparation of hydrothermal carbon catalysts from defatted rice bran

4.1.1 Effect of hydrothermal condition on yields and characteristics of hydrothermal carbon from defatted rice bran

The effect of hydrothermal carbonizations including temperature and time on yields and characteristics of HTC derived from DRB were studied at 180-250 °C and 1-8 h, respectively. The yields and characteristics of HTCDRB were compared with that of HTCG. The HTC yields obtained by hydrothermal carbonization of DRB and glucose were shown in **Table 4.1** and **Table 4.2**, respectively. The yield of HTCDRB was found to decrease with increasing carbonization temperature. Similar trend was also observed in Hoekman' and Kim' research (Hoekman et al., 2011; Kim et al., 2015). For the effect of the carbonization time, the HTCDRB yield stayed relatively constant

as residence time increased from 1 to 3 h, but significantly decreased when the residence time increased from 3 to 8 h at all carbonization temperatures. The HTCDRB yield decreased with increasing temperature and time, probably due to the hydrolysis and the decomposition of the components such as cellulose, hemicellulose, and lignin in DRB. As the carbonization temperature increased, the heated water, typically under subcritical condition, enhanced the dissolution of organic components of the biomass, as well as increased the extent of biomass gasification, resulting in the drop in HTCDRB yield (Falco et al., 2011; Gao et al., 2016). The effects of hydrothermal carbonization temperature and time on the yield of HTCG, on the other hand, were found to be in the opposite direction. The yield of HTCG increased with the increase in both temperature and residence time. At low temperature of 180 °C in particular, significant increase in HTCG yield with increased residence time was observed.

Morphological structures of HTCDRB and HTCG, as shown in **Figure 4.1** and **Figure 4.2**, respectively, were completely different. The HTCDRB was found to have highly complex structures, while on the other hand, HTCG was spherical, and had smooth surfaces. As shown in **Figure 4.2**, the spherical particles were of various sizes between 0.5-10 μm, and appeared to agglomerate (Nata and Lee, 2010; Titirici et al., 2012). It was also evident that the size of the HTCG became larger as the hydrothermal carbonization temperature and time increased, possibly due to the growth of the individual particles as well as the increase in agglomeration of the particles over time.

The time dependence of the HTC yields (see **Table 4.1 and Table 4.2**) and the morphological structures of the HTCDRB and HTCG (**Figure 4.1 and Figure 4.2**) suggested that the HTC formation from DRB and glucose took different routes. Baccile et al. (2009) explained that starting with glucose solution, the HTC formation would involve dehydration of glucose to HMF, polymerization and aromatization of HMF to aromatic unit, and condensation of aromatic unit to aromatic HTC. While HTC formation from DRB might take the same route with an additional DRB hydrolysis step, HTCDRB could also be formed directly from DRB via melting, condensation, and decarboxylation. Apparent from the decrease in the HTC yield with time and the HTCDRB morphologies, it was suggested that the direct route of HTC formation would be more prominent when starting from complex biomass such as DRB.

Table 4.1: HTC yields and elemental compositions of carbonaceous materials before and after hydrothermal carbonization from defatted rice bran

Sample name	Elemental compositions (wt.%)					Atomic ratio			HTC yield
	C	H	O	N	S	H/C	O/C	Composition	(wt.%)
DRB	38.44	7.36	50.92	2.55	0.73	0.19	1.32	$CH_{0.191}O_{1.325}N_{0.066}S_{0.019}$	-
HTCDRB180-1	55.65	13.36	28.12	2.10	0.77	0.24	0.51	$CH_{0.240}O_{0.505}N_{0.038}S_{0.014}$	40.06
HTCDRB180-3	65.54	14.16	18.74	0.98	0.58	0.22	0.29	$CH_{0.216}O_{0.286}N_{0.015}S_{0.009}$	40.92
HTCDRB180-8	62.44	15.13	21.88	0.00	0.55	0.24	0.35	$CH_{0.242}O_{0.350}S_{0.009}$	29.95
HTCDRB220-1	69.67	13.61	15.30	0.88	0.54	0.20	0.22	$CH_{0.195}O_{0.220}N_{0.013}S_{0.008}$	38.40
HTCDRB220-3	73.44	15.28	10.75	0.00	0.53	0.21	0.15	$CH_{0.208}O_{0.146}S_{0.007}$	38.77
HTCDRB220-8	72.23	14.30	12.43	0.53	0.51	0.20	0.17	$CH_{0.198}O_{0.172}N_{0.007}S_{0.007}$	26.91
HTCDRB250-1	73.14	14.25	11.68	0.44	0.49	0.19	0.16	$CH_{0.195}O_{0.160}N_{0.006}S_{0.007}$	33.68
HTCDRB250-3	75.49	12.74	9.77	1.53	0.47	0.17	0.13	$CH_{0.169}O_{0.129}N_{0.020}S_{0.006}$	32.03
HTCDRB250-8	70.91	9.30	16.58	2.70	0.51	0.13	0.23	$CH_{0.131}O_{0.234}N_{0.038}S_{0.007}$	24.04

Table 4.2: HTC yields and elemental compositions of carbonaceous materials before and after hydrothermal carbonization from glucose

Sample name	Elemental compositions (wt.%)			Atomic ratio			HTC yield (wt.%)
	C	H	O	H/C	O/C	Composition	
Glucose	39.10	8.07	52.83	0.21	1.35	$CH_{0.206}O_{1.351}$	-
HTCG180-1	64.56	13.09	22.35	0.20	0.35	$CH_{0.203}O_{0.346}$	3.25
HTCG180-3	62.34	7.65	30.01	0.12	0.48	$CH_{0.123}O_{0.481}$	12.74
HTCG180-8	61.90	7.04	31.06	0.11	0.50	$CH_{0.124}O_{0.502}$	23.90
HTCG220-1	66.28	8.90	24.82	0.13	0.37	$CH_{0.134}O_{0.374}$	29.45
HTCG220-3	69.29	9.38	21.33	0.14	0.31	$CH_{0.135}O_{0.308}$	37.42
HTCG220-8	70.08	10.31	19.61	0.15	0.28	$CH_{0.147}O_{0.280}$	39.84
HTCG250-1	68.41	7.30	24.29	0.11	0.36	$CH_{0.107}O_{0.355}$	36.76
HTCG250-3	72.74	10.21	17.05	0.14	0.23	$CH_{0.140}O_{0.234}$	39.03
HTCG250-8	71.22	9.53	19.25	0.13	0.27	$CH_{0.134}O_{0.270}$	41.12

The elemental compositions of carbonaceous materials: DRB and glucose before and after hydrothermal carbonization were summarized in **Table 4.1 and Table 4.2**, respectively. It can be seen from these tables that, for DRB, the percentage of carbon considerably increased after hydrothermal carbonization. The percentage of carbon was also found to increase with increasing carbonization time from 1 to 3 h, but stayed relatively constant when carbonization time increased from 3 to 8 h at all temperatures. For glucose, similar trend was observed, particularly at temperature of 220 and 250 °C at 3-8 h. At the carbonization temperature of 180 °C, on the other hand, the percentages of carbon were relatively low (62-64 wt.%) and remained rather constant with increasing residence times, suggesting that the temperature of 180 °C might not be sufficient for carbonization of the carbon substrates. The hydrothermal carbonization condition that gave the highest carbon content for both DRB and glucose was 3 h and 250 °C, resulting in 75 wt.% and 72 wt.% carbon, respectively. Moreover, the H/C and O/C atomic ratios were also analyzed. For HTCDRB, an increase in the hydrothermal carbonization temperature from 180 to 250 °C caused a decrease in the H/C and O/C atomic ratios (see **Table 4.1**), suggesting an increase in the degree of condensation as temperature increased. The effect of temperature was much higher than that of the reaction time. For instance, at 220 °C, an increase in reaction time from 1 to 8 h did not lead to the decrease in those atomic ratios. For glucose, the ratio of O/C decreased at greater extent than the H/C ratio when the temperature increased from 180 to 220 °C (see **Table 4.2**), indicating that decarboxylation reactions were more relevant in the elemental transformation than dehydration. Particularly, the observed values of O/C below 0.4 indicated that dehydration was nearly completed and the decarboxylation became more prominent (Röhrdanz et al., 2016). Both HTCDRB and HTCG at the hydrothermal carbonization temperature of 220 and 250 °C had the O/C atomic ratios below 0.4 for all residence times. The carbon contents in all HTCDRB and HTCG, prepared at both temperatures, however were not significantly different. Therefore, the HTCs formed at the hydrothermal carbonization conditions of 220 °C for 1 and 3 h were selected for further use as an acid catalyst support for biomass conversion.

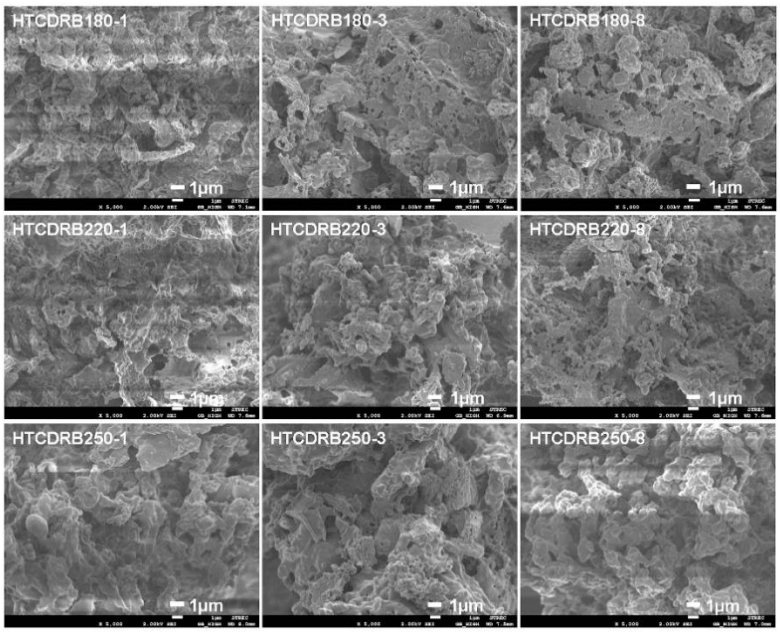

Figure 4.1: SEM images of DRB-derived carbons by hydrothermal carbonization at various temperatures and times

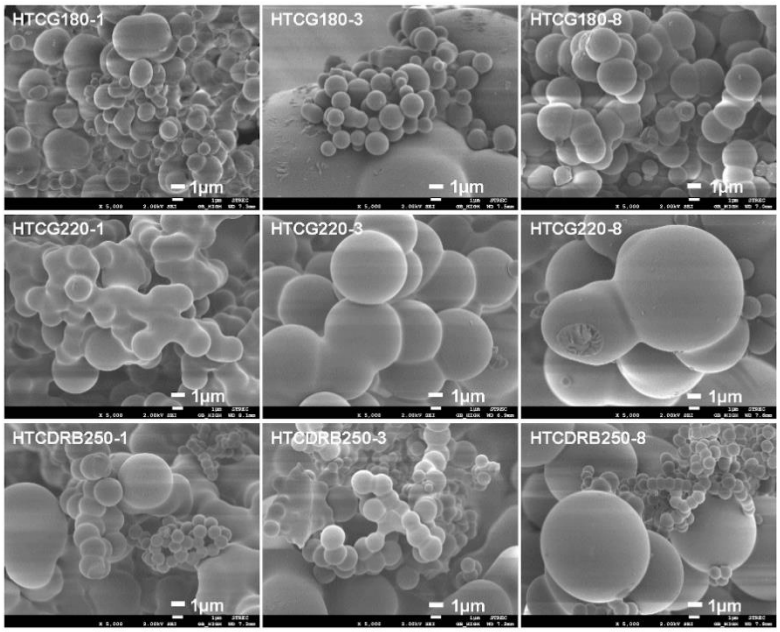

Figure 4.2: SEM images of glucose-derived carbons by hydrothermal carbonization at various temperatures and times

4.1.2 Characteristics of sulfonated hydrothermal carbon-based catalysts from defatted rice bran and glucose

From the previous results in section 4.1.1, HTCs formed at the hydrothermal carbonization conditions of 220 °C for 1 and 3 h were selected to be sulfonated with concentrated sulfuric acid at 150 °C for 15 h to prepare HTC-SO_3H. The characteristics of HTC and the corresponding HTC-SO_3H were compared base on XRD, FTIR and TGA measurements as shown in **Figures 4.3-4.5**. The XRD patterns of the selected HTCDRB showed amorphous carbon structure, suggesting that it was composed of aromatic carbon sheets oriented in a considerably random fashion at broad diffraction peak (2ɵ=10°-30°) (**Figure 4.3**(a)). After sulfonation, beside the broad diffraction peak (2ɵ=10°-30°), a diffraction peak (2ɵ=35°-50°) was also seen in HTCDRB-SO_3H (**Figure 4.3**(b)). The XRD results indicated that further carbonization occurred during sulfonation, resulting in HTCDRB-SO_3H with larger carbon sheet than that of HTCDRB (Okamura et al., 2006; Suganuma et al., 2008). It was noted that HTCG and HTCG- SO_3H had similar XRD patterns to those of HTCDRB and HTCDRB-SO_3H, respectively.

Table 4.3: Contents of sulphur, sulfonic group and total acidity of HTCDRB and HTCG (carbonization temperature of 220 °C for 1 and 3 h) and of sulfonated HTCDRB and HTCG based catalysts

Sample name	Sulphur (wt.%)	Sulfonic group (μmol g^{-1})	Total acidity (μmol g^{-1})
HTCDRB220-1	0.5	0.0	809
HTCDRB220-3	0.5	0.0	745
HTCG220-1	0.0	0.0	634
HTCG220-3	0.0	0.0	647
HTCDRB220-1-SO_3H	1.3	35.4	1,064
HTCDRB220-3-SO_3H	1.4	33.9	1,017
HTCG220-1-SO_3H	0.8	39.8	1,083
HTCG220-3-SO_3H	1.0	45.8	1,117

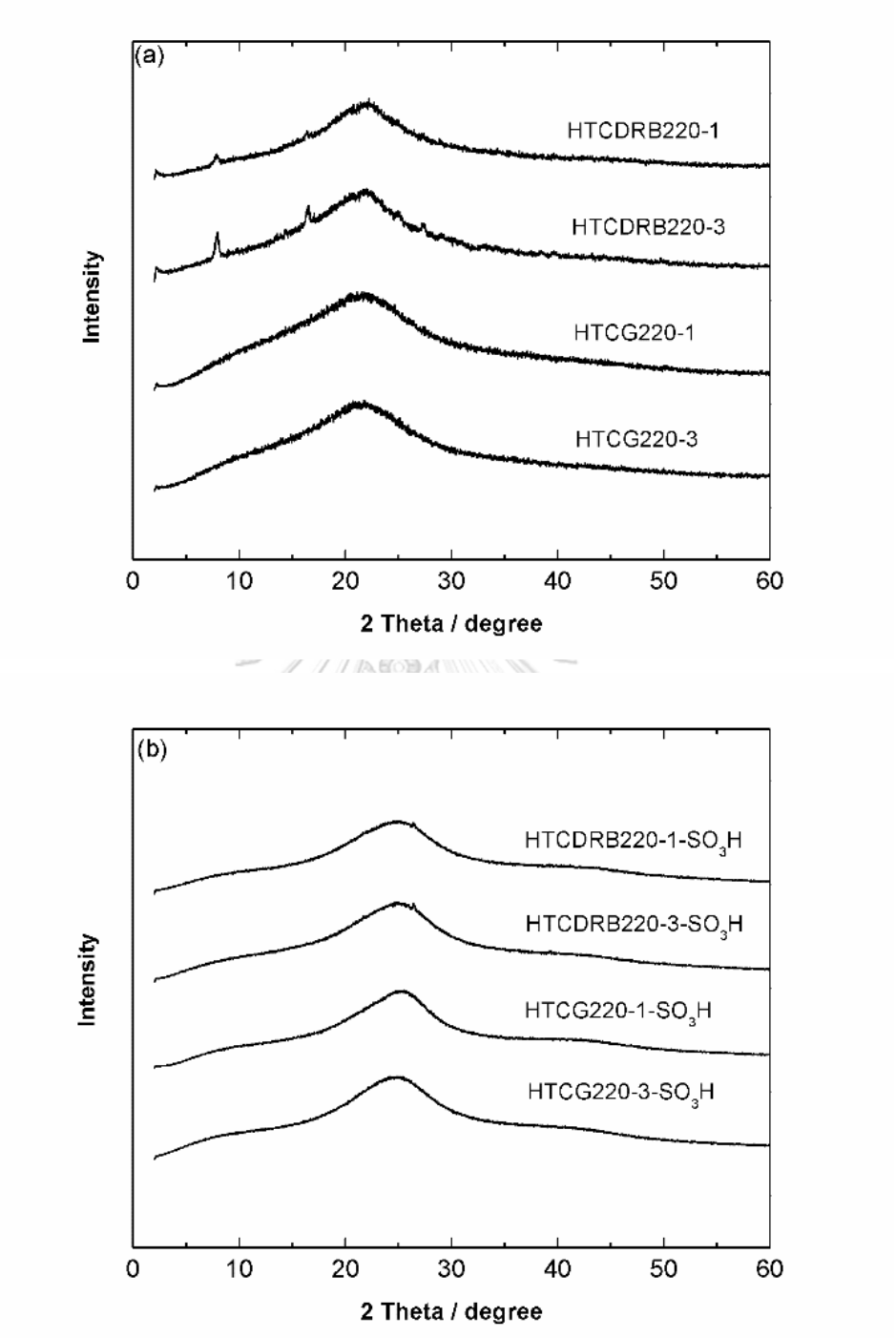

Figure 4.3: XRD patterns of (a) HTC and (b) HTC-SO_3H catalysts prepared from DRB and glucose. Hydrothermal carbonization temperature was 220 °C and times were 1 and 3 h

The FTIR spectra of HTC and the corresponding HTC-SO_3H were shown in **Figure 4.4**(a) and **Figure 4.4**(b), respectively. The results indicated that the functional groups of HTCDRB were similar to those of the HTCG. Similarly, the functional groups of HTCDRB-SO_3H and HTCG-SO_3H were also similar. The presence of aromatic components was evidenced by the aromatic C-H out-of-plane bending vibrations at bands in the 875-750 cm^{-1} region, and the C=C vibrations band approximately at 1600 cm^{-1}. Moreover, the presence of oxygen groups was suggested by the bands at 3700-3000 cm^{-1} (a wide band attributed to O-H stretching vibration in hydroxyl or carboxyl groups), 1710 cm^{-1} (C=O vibrations corresponding to carbonyl, quinone, ester or carboxyl), and 1000-1460 cm^{-1} (C-O stretching vibration in hydroxyl, ester or ether and O-H bending vibrations) (Fu et al., 2013; Sevilla and Fuertes, 2009). For HTC, the presence of a peak appearing at approximately 3000-2815 cm^{-1} was attributed to stretching vibrations of aliphatic C-H, indicating that carbonization might have not been completed. After sulfonation, the aliphatic group however no longer appeared, possibly because further carbonization occurred during sulfonation (Fraile et al., 2012). This was also confirmed by the presence of the XRD diffraction peak (2θ = 35°-50°) in HTC-SO_3H. In addition, the appearance of sulfonic groups, suggested by the bands at 1072 cm^{-1} ($-SO_3^{2-}$ stretching modes in $-SO_3H$ group) and 1265 cm^{-1} (symmetric O=S=O stretching vibrations of sulfonic groups), indicated that sulfonated HTC-based catalysts was successfully prepared (Nakhate and Yadav, 2016). This was also suggested by the increase in the contents of sulphur, sulfonic group as well as the total acidity, both in HTCDRB-SO_3H and HTCG-SO_3H catalysts, as can be seen in **Table 4.3**.

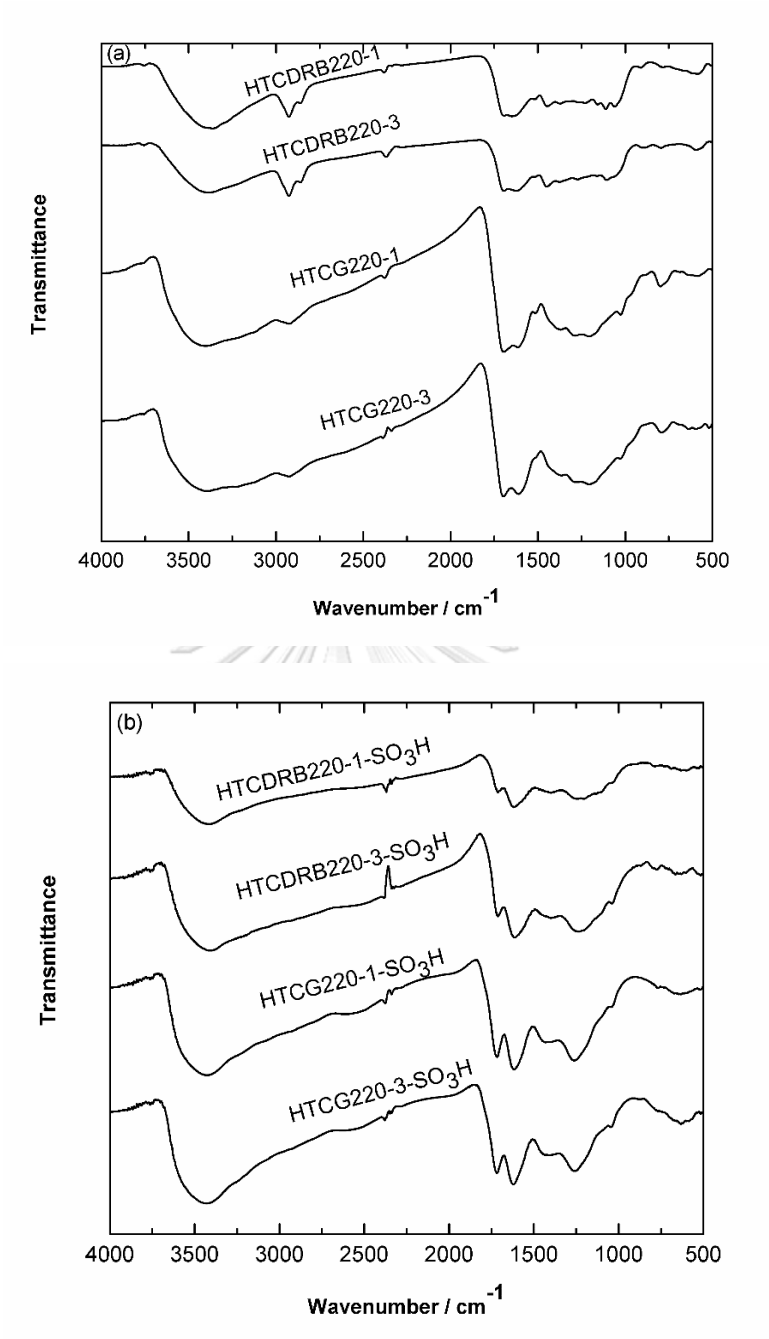

Figure 4.4: FTIR spectra of (a) HTC and (b) HTC-SO_3H catalysts prepared from DRB and glucose. Hydrothermal carbonization temperature was 220 °C and times were 1 and 3 h

The TGA patterns of the HTC and the corresponding HTC-SO_3H are shown in **Figure 4.5**. **Figure 4.5**(a) indicated that the HTCDRB had lower thermal stability than the HTCG, while on the other hand the thermal stability of the HTCDRB-SO_3H was slightly higher than HTCG-SO_3H (**Figure 4.5**(b)). The weight loss of HTCG and HTCG-SO_3H followed the same trend, while the weight loss characteristics of HTCDRB and HTCDRB-SO_3H appeared to be different. Three major weight loss regions were observed for HTCDRB. The first weight loss of about 2% occurred at the temperatures below 140 °C, which was attributed to the loss of water and free moisture adsorbed on the carbon surface. The second weight loss took place in the temperature range between 140 and 350 °C, attributing to the loss of HTCDRB structural components such as hemicellulose, cellulose and lignin. Corresponding to the decomposition temperature of hemicelluloses at 180 °C, and that of cellulose and lignin at 220 °C (Reza et al., 2014), the initial weight loss was related to hemicellulose loss that occurred sluggishly, followed by more rapid weight losses of cellulose and lignin, as well as the remaining hemicellulose toward the end of this interval. Lastly, the rapid weight loss at temperatures above 350 °C was attributed to the loss of the remaining char, caused by the decomposition of the remaining cellulose and lignin structure (Islam et al., 2015). For HTCDRB-SO_3H, three distinctive weight loss regions were found. The first rather rapid water loss occurred below 100 °C. The second weight loss occurred as the remaining moisture sluggishly evaporated at the temperature between 100 and 200 °C. The last weight loss occurring at above 200 °C, was observed upon the thermal decomposition of SO_3H (Kang et al., 2013; Malins et al., 2015). Based on the TGA results, HTCDRB-SO_3H and HTCG-SO_3H appeared to be stable at temperatures below 200 °C, and were suggested to be suitable for reactions below this temperature.

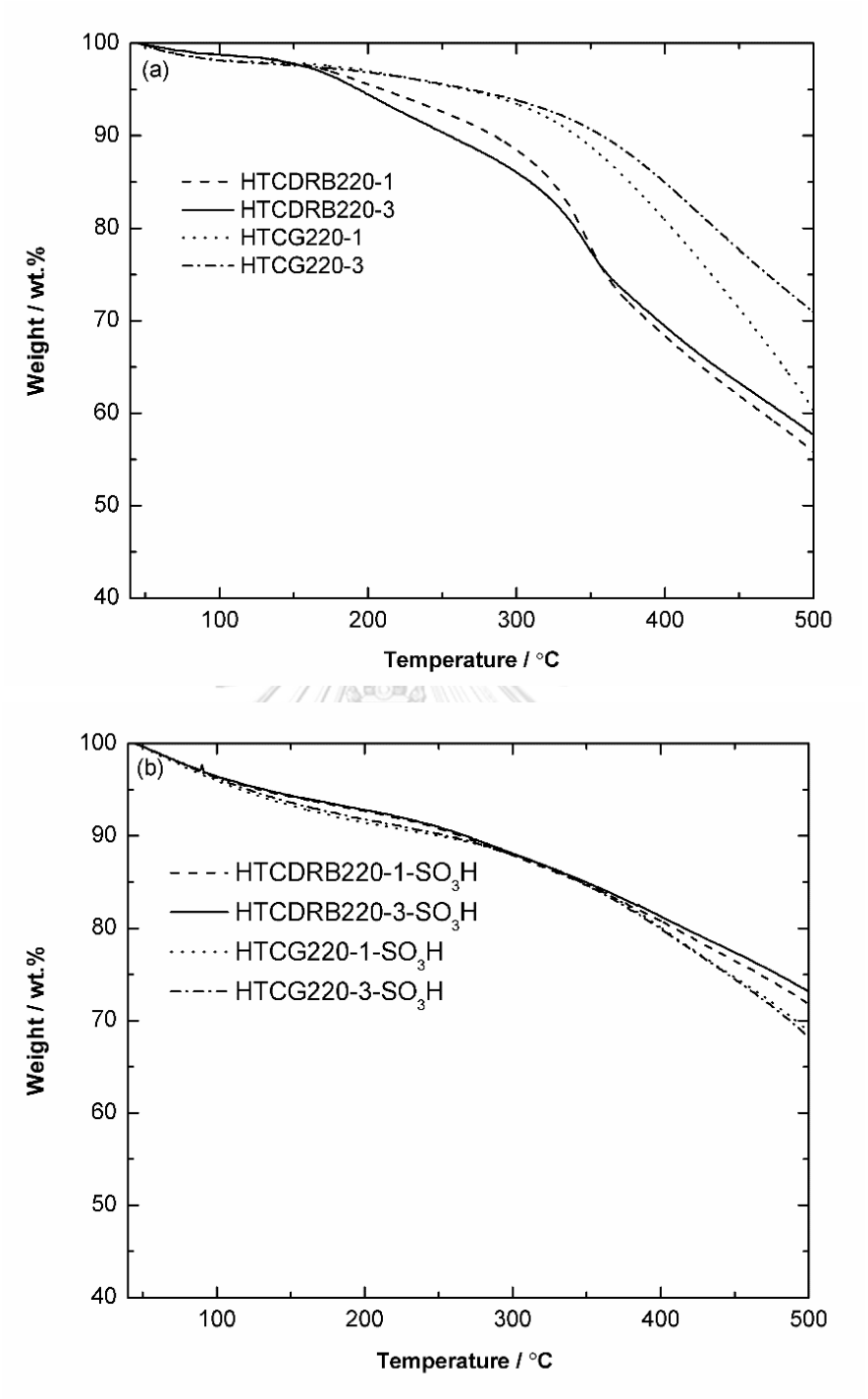

Figure 4.5: TGA patterns of (a) HTC and (b) HTC-SO_3H catalysts prepared from DRB and glucose. Hydrothermal carbonization temperature was 220 °C and times were 1 and 3 h

4.1.3 Catalyst leaching under hydrothermal reaction condition

Since the catalyst was prepared by sulfonation of hydrothermally carbonized for both, when it is applied to chemical reactions such as biomass conversion, it should be ensured that the prepared HTC-SO_3H catalyst itself does not undergo the conversion that would interfere with the reaction of interest. For this reason, under a specified biomass hydrolysis condition (200 °C and 5 min under microwave irradiation), the leaching of biomass conversion products from the catalyst into water was evaluated. The photographs of the liquid fractions obtained after the leaching experiments were shown in **Figure 4.6**. From this figure, the liquid fractions for the glucose derived HTC-SO_3H catalyst appeared to have red brown color, implying that large amounts of biomass conversion products (i.e. HMF, furfural, levulinic acid and formic acid) were leached out from the HTCG-SO_3H catalysts. It was noted from these results that even though the catalysts were washed repeatedly with boiling distilled water to remove chemical residues from the catalysts during their preparation, this washing process could not guarantee that the catalysts would not further undergo chemical reactions. The liquid fractions obtained by DRB derived HTC-SO_3H catalysts, on the other hand, were found to have light pale yellow color, thus implying that small amounts of biomass conversion products were leached from the catalysts. These liquid fractions were also analyzed via HPLC and the results were shown in **Figure 4.7**. As shown in **Figure 4.7**, the leaching of biomass conversion products from both the HTCDRB-SO_3H and HTCG-SO_3H catalysts decreased (or catalyst stability increased) with increasing carbonization time from 1 to 3 h. It could be implied from **Figure 4.7** that the stability of HTCDRB-SO_3H was higher than that of the HTCG-SO_3H catalyst prepared at the same carbonization condition, since the amounts of leached components (i.e. HMF, furfural, levulinic acid and formic acid) from the HTCDRB-SO_3H catalysts were considerably lower. The higher stability of HTCDRB-SO_3H could be attributed to the difference in the HTC formation mechanisms. Starting with glucose in an aqueous solution, HTCG was formed largely via glucose dehydration to HMF, which upon condensation, aromatized HTC structures were subsequently formed. While starting with DRB on the other hand, the HTCDRB was formed partly via biomass hydrolysis, followed by glucose dehydration, and condensation and aromatization, and partly by the direct condensation and aromatization of the biomass raw material. With the direct

route that was also undertaken, it would be expected therefore that, at the same carbonization condition, a more highly stable and aromatized HTC could be obtained from DRB. It was noted that at the hydrothermal carbonization temperature of 220 °C for 3 h (HTCDRB220-3-SO_3H), no HMF and furfural, and only relatively small amount of levulinic acid (1.75 wt.%) and formic acid (0.42 wt.%) were leached from that catalyst. This suggested that the HTCDRB220-3-SO_3H catalyst was relatively stable and could suitably be used to prepare a HTC-based catalyst for biomass conversion.

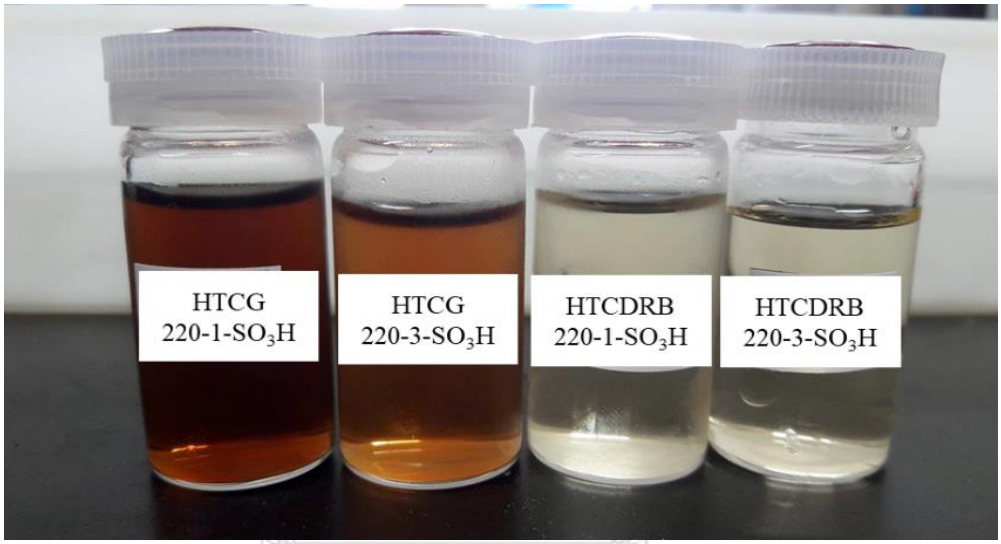

Figure 4.6: Liquid fractions from leaching experiments under microwave irradiation at temperature of 200 °C for 5 min

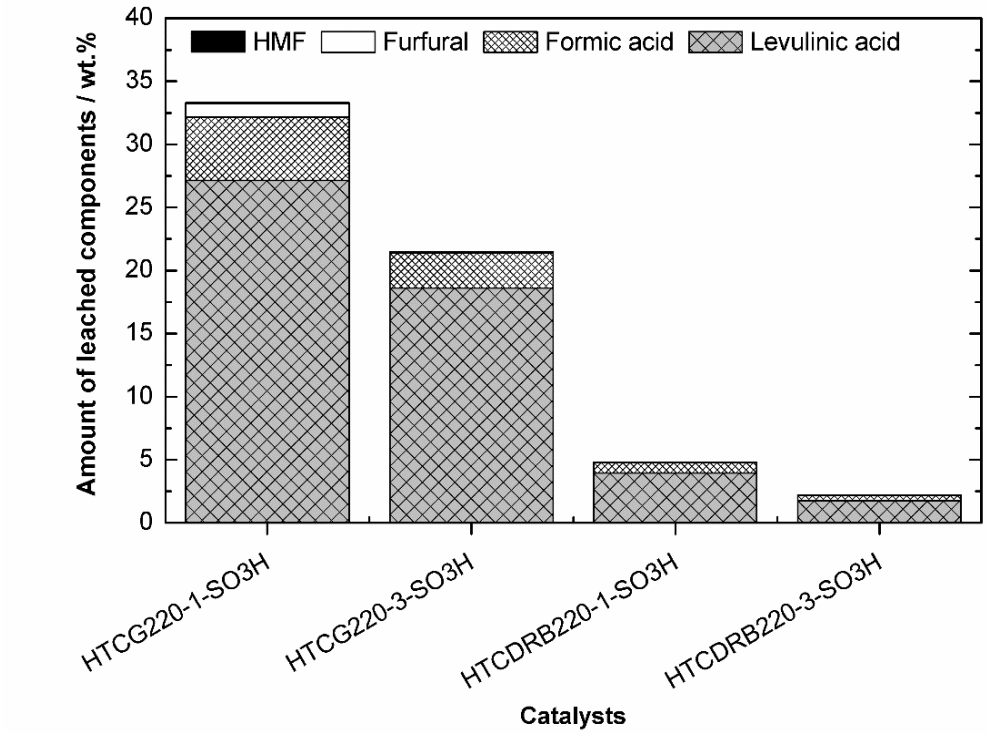

Figure 4.7: Amounts of HMF, furfural, levulinic acid, and formic acid in liquid fraction of HTC-SO_3H catalysts hydrolysis under microwave at temperature of 200 °C for 5 min

4.2 The stability improvement of hydrothermal carbon catalyst derived from glucose

From the previous results in section 4.1.3, the leaching analysis at the hydrothermal condition revealed that the stable HTCDRB catalyst could be prepared by hydrothermal carbonization at 220 °C for 3 h. However, hydrothermal glucose-derived catalyst was not stable at the same condition. The stability improvement of hydrothermal glucose-derived catalyst was therefore investigated at the longer hydrothermal carbonization time (6-24 h). The characteristics, stability, catalytic activity and recyclability of the prepared HTCG catalyst are reported in this section.

4.2.1 Effect of hydrothermal condition on yield and characteristics of hydrothermal carbon from glucose

In this section, the effect of hydrothermal temperature and time on yield and characteristics of HTC derived glucose was studied at 180-250 °C and 6-24 h, respectively. For the effect of carbonization temperature was similar trend previous results in section 4.1.1. As shown in **Table 4.4**, HTCG yield was found to increase with increasing temperature. Similar trends were also reported by Falco et al. (2011) that increasing hydrothermal carbonization temperature from 160 °C to 200 °C, the glucose derived HTC yield increased. For the effect of carbonization time, it was found in this work that at low carbonization temperature of 180 °C, HTCG yield increased from 6.91 wt.% to 28.53 wt.% as the carbonization time increased from 6 h to 24 h. At higher carbonization temperatures of 220 °C and 250 °C, the yield of HTC derived from hydrothermally carbonized glucose was insignificantly increased with increasing carbonization times. The morphological structures of HTCGs produced at various carbonization conditions as shown in **Figure 4.8** suggested that the glucose derived HTC particles were of spherical shape, with smooth surfaces, and having approximate size ≥0.25 μm. It was also revealed from these SEM images that the increase in carbonization times not only affected the growth of individual particles, but also the particle agglomeration. From BET measurement, the surface area, pore volume and pore size diameter of the HTCG samples were approximately 1.66-4.04 $m^2 g^{-1}$, 0.002-0.01 $cm^3 g^{-1}$, and 5.70-11.80 nm, respectively (**Table 4.5**).

Table 4.4: HTC yields and elemental compositions of carbonaceous materials before and after hydrothermal carbonization

Sample name	Elemental compositions (wt.%)			Atomic ratio			HTC yield (wt.%)
	C	H	O	H/C	O/C	Composition	
Glucose	39.68	7.07	53.15	0.18	1.34	$CH_{0.178}O_{1.340}$	-
HTCG180-6	63.62	3.97	32.29	0.06	0.51	$CH_{0.062}O_{0.508}$	6.91
HTCG180-12	63.77	3.94	32.24	0.06	0.51	$CH_{0.062}O_{0.506}$	17.96
HTCG180-18	64.29	3.98	31.60	0.06	0.50	$CH_{0.062}O_{0.492}$	24.32
HTCG180-24	64.69	3.98	31.21	0.06	0.48	$CH_{0.062}O_{0.482}$	28.53
HTCG220-6	65.82	4.03	30.02	0.06	0.46	$CH_{0.061}O_{0.456}$	29.58
HTCG220-12	66.79	4.13	28.95	0.06	0.43	$CH_{0.062}O_{0.433}$	31.65
HTCG220-18	66.49	4.18	29.21	0.06	0.44	$CH_{0.063}O_{0.439}$	31.98
HTCG220-24	66.90	4.25	28.73	0.06	0.43	$CH_{0.064}O_{0.429}$	32.63
HTCG250-6	68.11	3.99	27.74	0.06	0.41	$CH_{0.059}O_{0.407}$	32.53
HTCG250-12	69.09	4.14	26.63	0.06	0.39	$CH_{0.060}O_{0.385}$	31.87
HTCG250-18	68.75	3.98	27.15	0.06	0.40	$CH_{0.058}O_{0.395}$	33.12
HTCG250-24	69.06	3.85	26.98	0.06	0.39	$CH_{0.056}O_{0.391}$	33.38

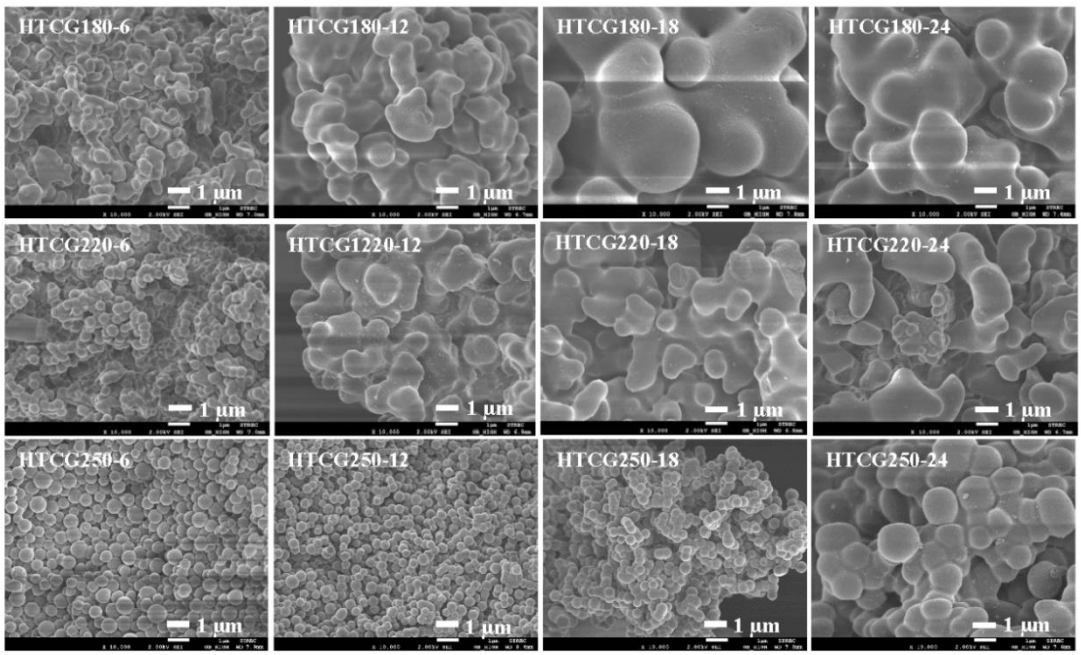

Figure 4.8: SEM images of HTCs prepared by hydrothermal carbonization of glucose at various temperatures and times.

Table 4.5: Surface area, pore volume, and pore size of hydrothermal carbon from glucose

Sample	BET surface area (m^2 g^{-1})	Pore volume (cm^3 g^{-1})	Pore size (nm)
HTCG180-6	1.720	0.002	5.691
HTCG180-12	2.399	0.005	9.322
HTCG180-18	1.759	0.004	8.178
HTCG180-24	1.802	0.004	7.892
HTCG220-6	2.001	0.006	11.311
HTCG220-12	3.421	0.009	10.526
HTCG220-18	1.982	0.005	10.538
HTCG220-24	2.713	0.006	9.967
HTCG250-6	3.245	0.009	11.799
HTCG250-12	1.656	0.004	10.766
HTCG250-18	4.039	0.010	10.246
HTCG250-24	3.844	0.009	10.558

The elemental analyses of glucose before and after hydrothermal carbonization were summarized in **Table 4.4**. The hydrothermal carbonization of glucose led to an increase in carbon content from 39.68 wt.% to 63.62-69.09 wt.%. In contrast, the amount of oxygen and hydrogen decreased in all HTC samples, suggesting dehydration as well as aromatization and condensation took place during hydrothermal carbonization. Moreover, the decrease of H/C ratio from 0.18 in glucose to 0.06 in HTC and of O/C ratio from 1.34 in glucose to 0.39-0.51 in HTC also confirmed that after hydrothermal carbonization, HTC had high level of aromaticity (Fang et al., 2015; Sevilla and Fuertes, 2009). It was also revealed from this study that the carbonization temperature showed greater impact on the product characteristics than the carbonization time. The percentage of carbon was slightly increased when the temperature of hydrothermal carbonization increased from 180 °C to 250 °C. As the temperature increased, the O/C ratio decreased but H/C ratio was nearly constant. This indicated that dehydration (water was removed from glucose) almost reached completion, while decarboxylation (production of carboxyl including carboxylic acid) became more prominent (Röhrdanz et al., 2016). The elemental data, therefore, suggested the mechanism of hydrothermal carbonization to involve glucose dehydration to HMF, the aromatization of HMF to aromatic unit, and finally the condensation of aromatic unit to aromatic carbon. Aromatic carbons or HTC samples, confirmed by crystallinity analyses, were amorphous carbon structures, with broad C diffraction peak (2θ = 15°-30°) (**Figure 4.9**). Similar results have been reported by Okamura et al. (2006).

As shown in **Figure 4.10**, the FTIR spectra of all HTC samples were similar to those of HTC from glucose in saline solution reported previously (Reza et al., 2016). The bands at approximate range of 875-750 cm^{-1} were assigned to aromatic C-H out-of-plane bending vibrations, whereas the bands at 1600 cm^{-1} corresponded to stretching vibrations of aromatic C=C. The existence of these bands suggested that aromatization took place during carbonization reaction. Moreover, the HTC samples were found to contain several bonds associated with acid functional groups. The bands at approximately 1710 cm^{-1} and those lied in the range between 3700-3000 cm^{-1} corresponded to stretching vibrations of aromatic C=O (carbonyl, ester, or carboxyl) and hydrogen bonded O-H (hydroxyl or carboxyl group), respectively, suggesting

carboxylic acid group occurred as a result of hydrothermal carbonization process (Sevilla and Fuertes, 2009).

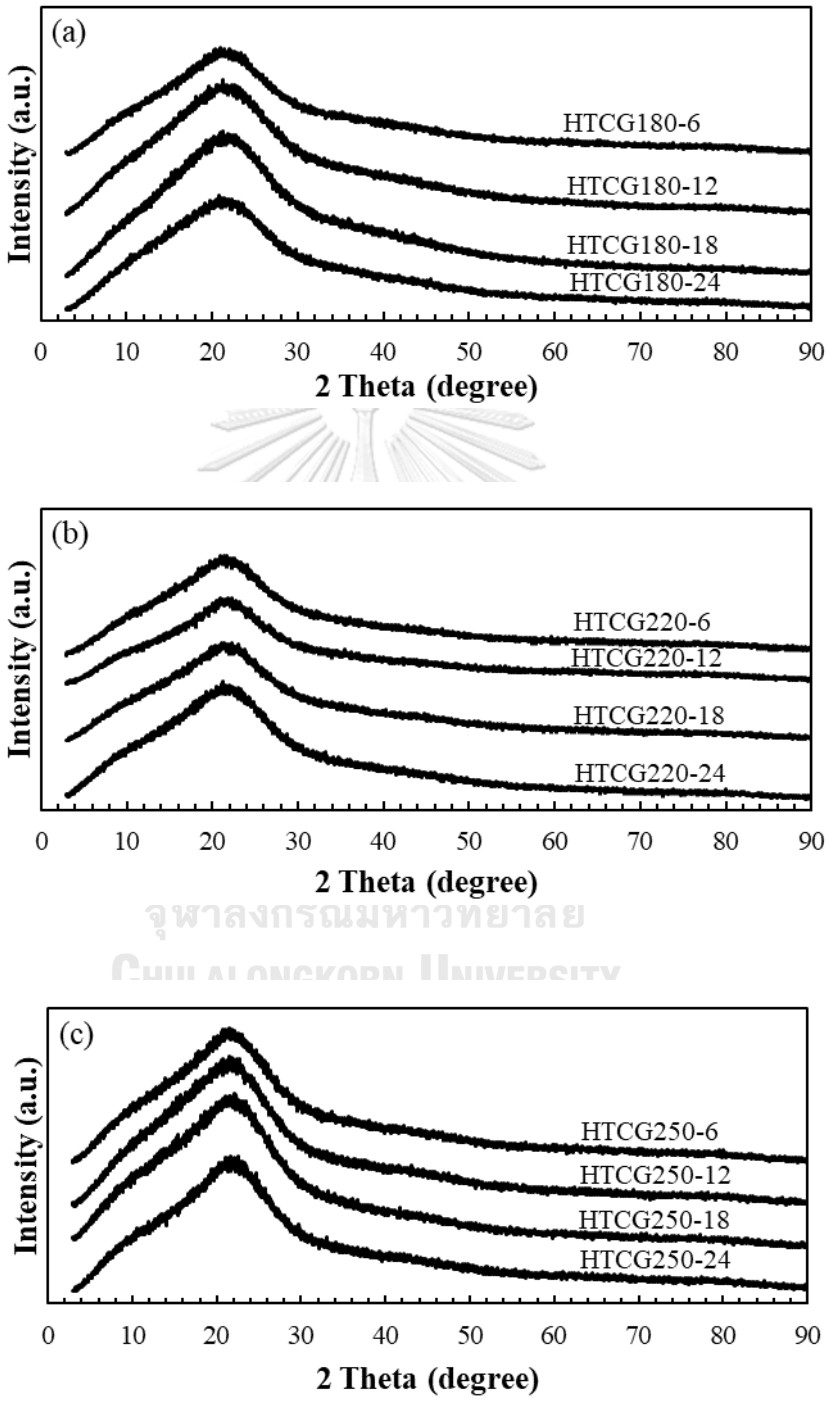

Figure 4.9: XRD patterns of HTCs prepared from glucose by hydrothermal carbonization temperature of (a) 180 °C, (b) 220 °C, and (c) 250 °C at various times

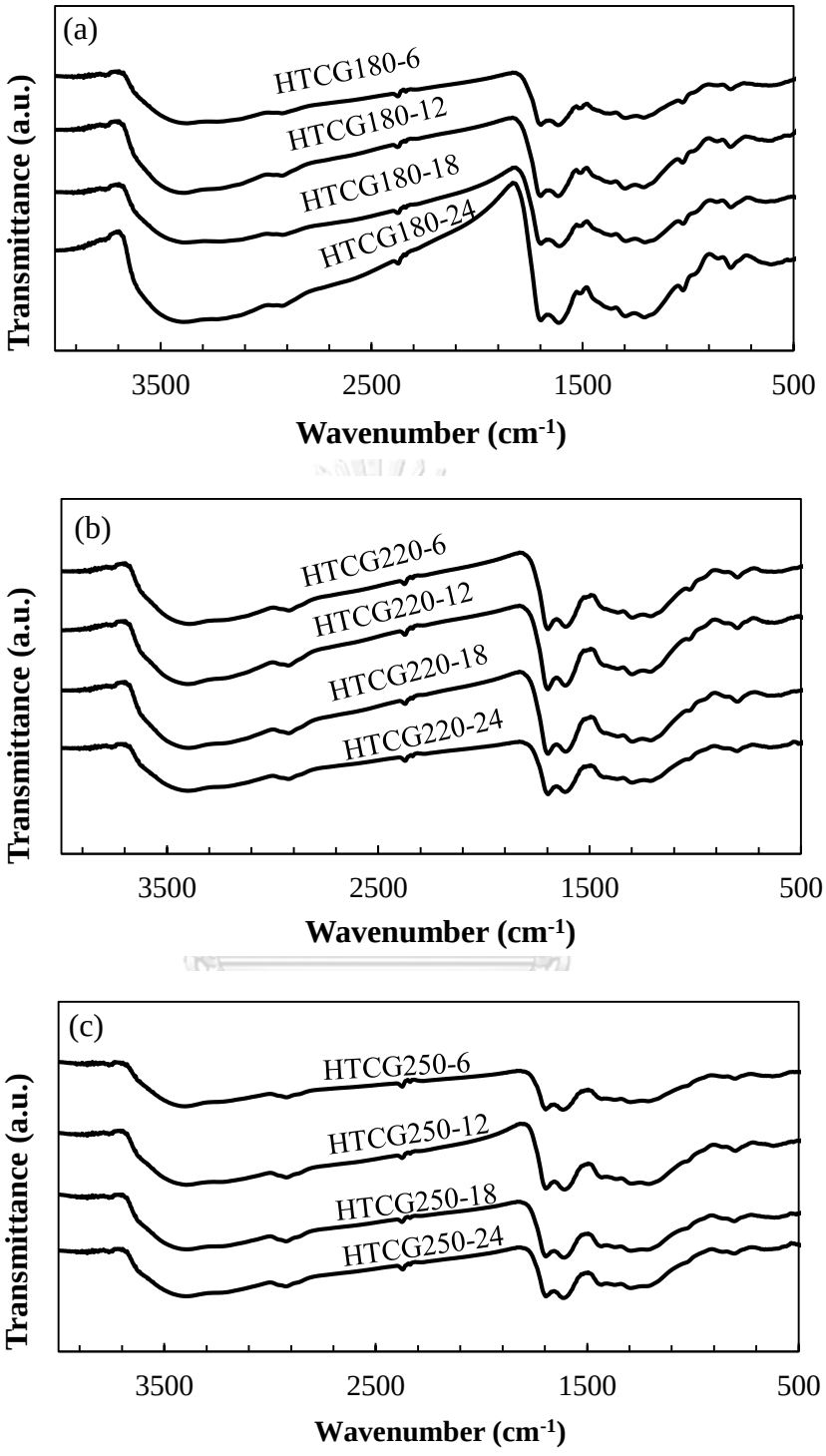

Figure 4.10: FTIR spectra of HTCs prepared from glucose by hydrothermal carbonization temperature of (a) 180 °C, (b) 220 °C, and (c) 250 °C at various times

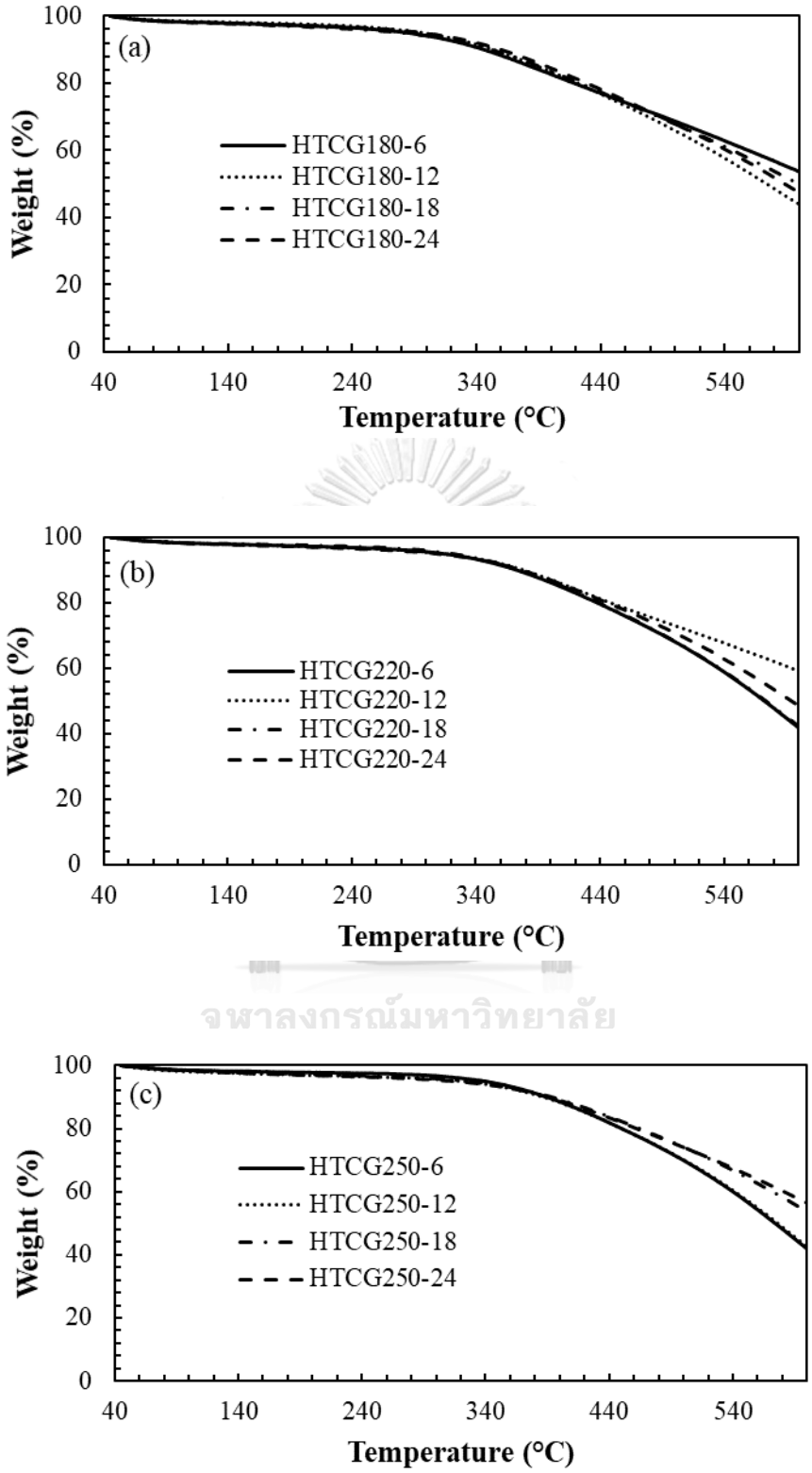

Figure 4.11: TGA patterns of HTCs prepared from glucose by hydrothermal carbonization temperature of (a) 180 °C, (b) 220 °C, and (c) 250 °C at various times

Similar trends on the TGA results were observed for all of HTC samples as shown in **Figure 4.11**. The HTC samples were found to be thermally stable at temperature below 300 °C, with insignificant weight loss (<6%) observed. The rapid weight loss at the temperature above 350 °C on the other hand, was possibly due to the decomposition of acids such as hydroxyl and carboxyl groups from the carbon structure. The recommended reaction temperatures would therefore be below 300 °C.

4.2.2 Analysis of liquid fractions obtained via hydrothermal carbonization of glucose

One way to confirm the stability of the HTCG-based acid catalyst is to ensure that complete carbonization was achieved during the preparation of HTCG. Specifically, the liquid fraction after carbonization must contain the minimum amount of sugar (glucose in this case) and furan compounds (i.e. HMF). The amounts of TRS, glucose and HMF in liquid fraction from reactions under various hydrothermal carbonization conditions were therefore analyzed. The results shown in **Figure 4.12** suggested that the highest TRS was found in the liquid fractions obtained at temperature of 180 °C after 6 h, and tended to decrease as the carbonization time increased from 6 h to 24 h. This implied that at 180 °C, the reducing sugar still continued to decompose to other chemicals (i.e. HMF) as the reaction time increased. While at higher hydrothermal carbonization temperature at 220 °C and 250 °C, the TRS in the liquid fractions stayed relatively constant for all hydrothermal carbonization times. The %TRS results corresponded to the glucose conversion, in which higher glucose conversion was found at longer carbonization time at 180 °C, and the complete conversion of glucose was observed at high temperatures: 220 °C and 250 °C.

It should be noted that the results of liquid fraction analysis were in good agreement with those of the HTCG yield. Specifically, at low carbonization temperature of 180 °C, the change in glucose conversion and HMF content with carbonization time was observed, which correspond to the increase in the HTC yield with increasing time. On the other hand, at higher temperatures of 220 °C and 250 °C, 100% glucose conversion had been reached after 6 h, and remained unchanged with carbonization time, which corresponded to results of relatively no HMF content in liquid fraction and those of relatively high and unchanged HTCG yields with time. It can be drawn from

the above results that the proper hydrothermal carbonization conditions required for the preparation of HTCG for biomass conversion should be above 220 °C and 6 h.

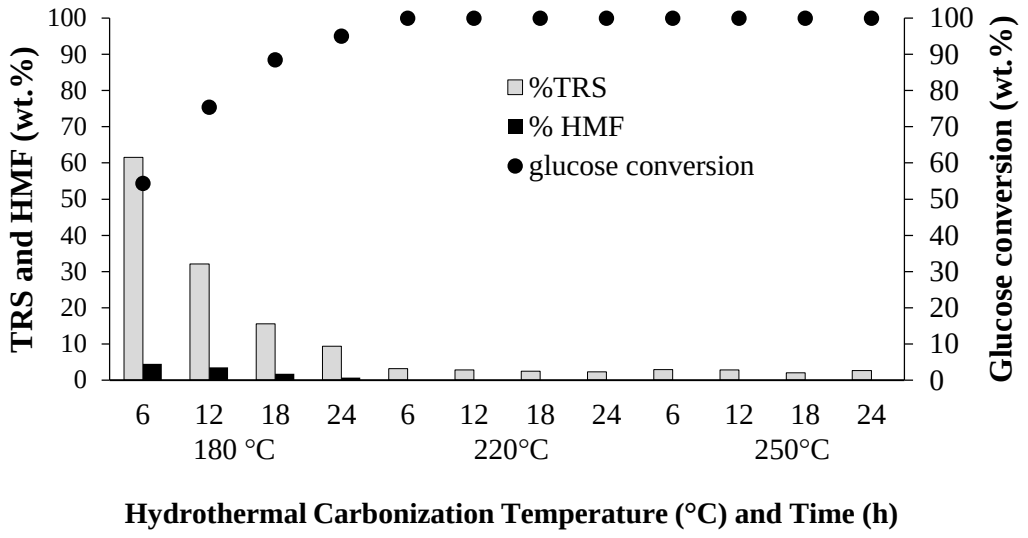

Figure 4.12: Glucose conversion, %TRS and HMF of liquid fractions obtained via hydrothermal carbonization of glucose at various temperatures and times.

4.2.3 Characteristics of sulfonated hydrothermal carbon-based catalyst from glucose

HTCG prepared at 220 °C for 6 h (HTCG220-6) was selected as a catalyst support, and was further sulfonated to obtain a HTCG220-6-SO_3H catalyst. Its catalytic activity toward the production of HMF from biomass was subsequently determined.

As shown in **Figure 4.13**, HTC220-6-SO_3H and HTC220-6 were found to have similar XRD patterns (**Figure 4.13(**a)). The broad C diffraction peak (2θ = 15-30º) can be attributed to the amorphous carbon structures. The XRD patterns of carbons before and after sulfonation showed no noticeable difference, suggesting that sulfonation process had no effect on carbon structure. On the other hand, according to the SEM images of HTCG220-6-SO_3H and HTCG220-6 in **Figure 4.13(**b), HTCG220-6-SO_3H clearly possess rougher surfaces, which possibly due to the surface coverage of the HTCG220-6 with sulfuric acid. The surface area of the HTCG220-6-SO_3H was also found to be higher than that of the HTCG220-6 (**Table 4.6**). In addition, the adsorption-

desorption isotherm of HTC220-6-SO_3H (**Figure 4.14)** indicated that HTCG220-6-SO_3H is of type IV isotherms with evident hysteresis loops in the relative pressure range of about 0.79-0.97. In addition, the decrease in the pore volume and the pore size from 0.006 cm^3 g^{-1} and 11.311 nm in HTCG220-6 to 0.005 cm^3 g^{-1} and 4.274 nm in HTCG220-6-SO_3H, respectively, implied the presence of sulfuric acid within the pores. Furthermore, as a result of sulfonation, the acidity and the sulfur content of HTCG220-6-SO_3H increased to 7.944 (from 6.620) mmol g^{-1} and to 0.709 (from 0) mmol g^{-1}, respectively (**Table 4.6**).

Table 4.6: Surface area, pore volume, pore size, total acidity, and sulfur content of HTCG220-6 and HTCG220-6-SO_3H

Samples	HTCG220-6	HTCG220-6-SO_3H
BET surface area (m^2 g^{-1})	2.001	7.394
pore volume (cm^3 g^{-1})	0.006	0.005
Pore size (nm)	11.311	4.274
Total acidity (mmol g^{-1})	6.620	7.944
Sulfur content (mmol g^{-1})	-	0.709

The FTIR spectrums of HTC220-6 and HTC220-6-SO_3H (**Figure 4.13**(c)) clearly indicated the presence of SO_3H group in the latter, confirmed by the stretching vibration bands of O=S=O and $–SO_3^{2-}$ at 1167 and 1027 cm^{-1}, respectively. Based on FTIR result, the hydrothermal glucose based acid catalyst prepared in this study (HTC220-6-SO_3H) is similar to the carbon-based catalyst prepared from microalgae residue (Fu et al., 2013).

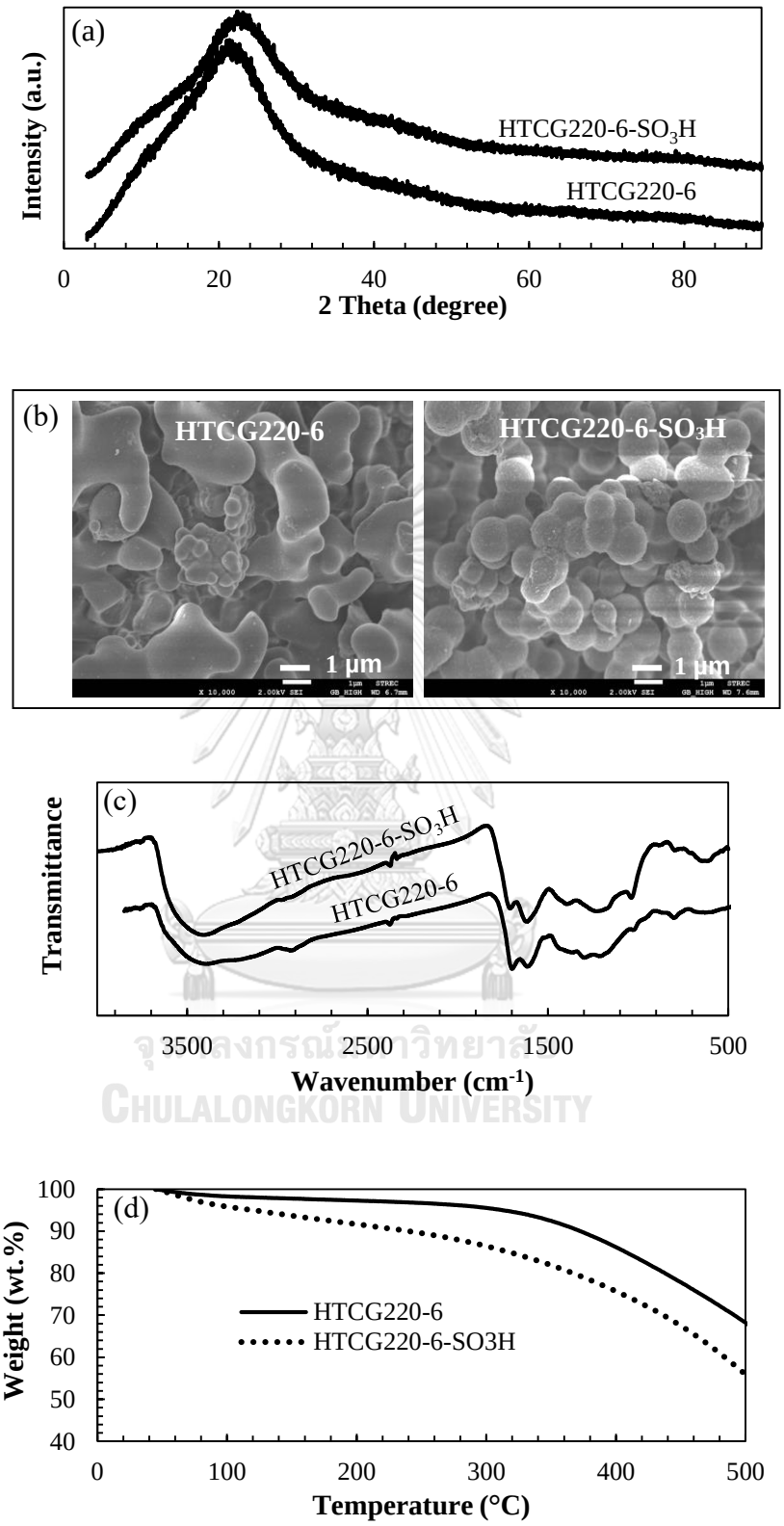

Figure 4.13: Characteristics: (a) XRD patterns, (b) SEM images, (c) FTIR spectra, and (d) TGA patterns of HTCG220-6 and HTCG220-6-SO_3H.

Moreover, the TGA result (**Figure 4.13(**d)) demonstrated that the thermal stability of HTCG220-6-SO_3H was lower than that of HTCG220-6, possibly due to the decomposition of SO_3H group. In addition, thermal stability of HTCG220-6-SO_3H was found to be similar to that of the HTC-based catalyst derived from D-xylose (HTCD-SO_3H) reported by Kang et al. (2013), except for the slight water loss observed below 100 °C, observed in HTCD-SO_3H but not in HTCG220-6-SO_3H. This difference was possibly explained by the fact that the HTCG220-6-SO_3H was more completely dried after the washing step with water, ethanol and acetone. Nevertheless, the decomposition characteristics of both catalysts were identical, from which rapid decomposition started to occur at 250 °C. Therefore, temperatures below 250 °C were suggested to be suitable for reaction condition.

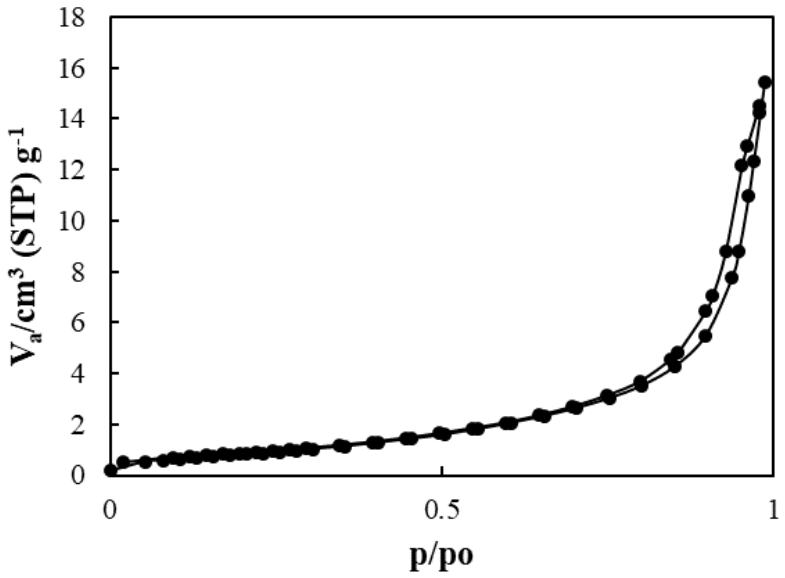

Figure 4.14: Adsorption/Desorption isotherm of HTCG220-6-SO_3H

4.3 Catalytic activity

The HTCDRB220-3-SO_3H and HTCG220-6-SO_3H, which were proved to be stable for biomass conversion to HMF, were tested toward cellulose hydrolysis to monosaccharides in subcritical water at 180 °C for 5 min with 0.005 g catalyst loading. The percent product yields of glucose, HMF, and furfural were measured, and the results were compared with non-catalytic condition and with different type of solid acid catalysts including HTCDRB220-3, HTCG220-6, Amberlyst 16 wet and GO at the same operating conditions. The results shown in **Figure 4.15** revealed that HTCDRB220-3-SO_3H, HTCG220-6-SO_3H, GO and Amberlyst 16 WET had catalytic activities over cellulose hydrolysis. Among of catalyst used, HTCDRB220-3-SO_3H exhibited the highest cellulose hydrolysis activities, as suggested by the highest glucose yield of (49.62±4.59 wt.%). The glucose yield from the reaction catalyzed by HTCDRB220-3-SO_3H was higher than that catalyzed by HTCDRB220-3 (3.38±1.87 wt.%), due to the higher acidity (as shown in **Table 4.3**). For glucose-derived catalyst, similar activities as DRB-derived catalyst were observed. The glucose yield from the reaction catalyzed by HTCG220-6-SO_3H (43.63±1.62 wt.%) was higher than that catalyzed by HTCG220-6 (6.99±0.11 wt.%). This clearly indicated the importance of SO_3H addition on the catalytic activity toward hydrolysis reaction. However, the results with HTCG220-6-SO_3H showed relatively similar glucose yield with the reactions in the presence of GO and Amberlyst 16 Wet (41.71±3.16 wt.% and 45.17±0.35 wt.%, respectively). The yields of hydrolysis byproduct including HMF and furfural were also found to be similar for GO and Amberlyst 16 Wet catalysts. This indicated that both HTCDRB220-3-SO_3H and HTCG220-6-SO_3H exhibited similar activity for sugar dehydration to GO and Amberlyst 16 Wet. To confirm the catalytic activity of HTC-based catalyst for dehydration, the HTCG220-6-SO_3H catalysts was also tested in fructose dehydration (**Figure 4.16**).

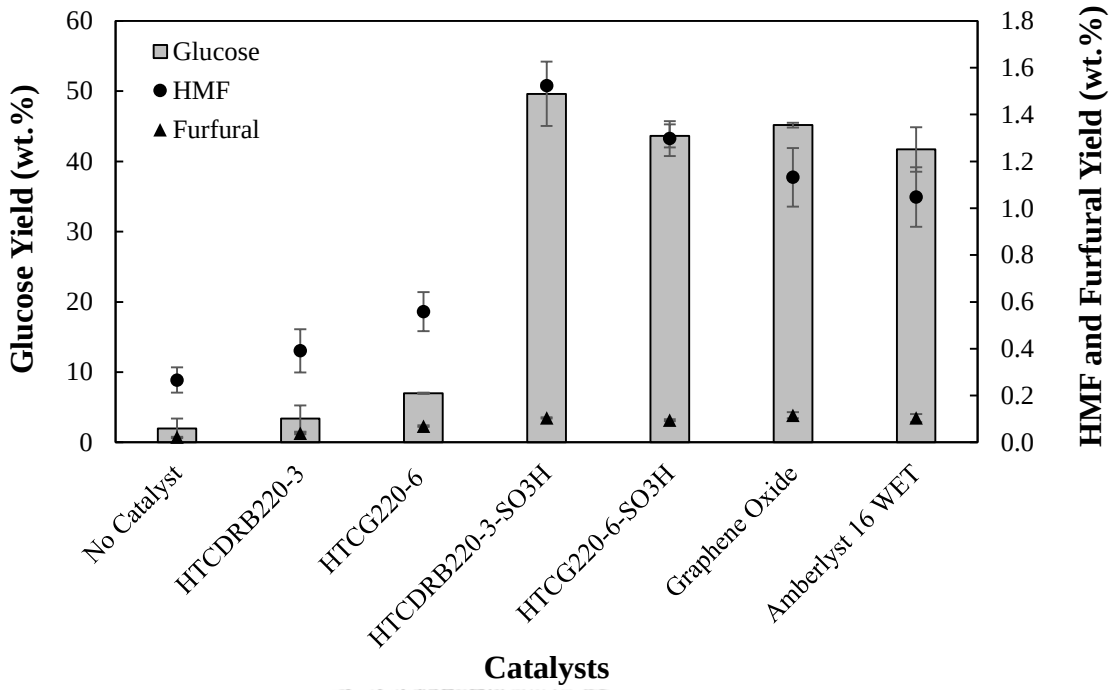

Figure 4.15: Glucose, HMF, and furfural yields in liquid products of cellulose hydrolysis in subcritical water at 180 °C and 5 min and 5 wt.% catalyst loading, catalyzed by different catalysts.

For catalytic activity test in fructose dehydration, the operating conditions at 180 °C for 5 min with 5 wt.% catalyst loading was used. The results shown in **Figure 4.16** revealed that the lowest fructose conversion (56.19±2.86 wt.%) was observed in the non-catalytic condition. Among the catalysts used, HTCG220-6-SO_3H exhibited the highest fructose dehydration activities, as suggested by the highest fructose conversion of 87.56±0.37 wt.% and the correspondingly highest HMF and furfural yields of 20.29±1.09 wt.% and 0.97±0.05 wt.%, respectively. Moreover, without sulfonation, HTCG220-6 was found to have reasonable catalytic activity for fructose dehydration, and gave comparable HMF and furfural yields with GO and Amberlyst 16 Wet. It can be implied from the above and previous results that sulfonation process can improve the catalytic activities for cellulose hydrolysis and fructose dehydration. Importantly, this high acidity catalyst showed comparable activity with other high-cost acid catalysts (e.g., GO and Amberlyst catalysts); hence, it can potentially be used to replace these catalysts for some specific applications.

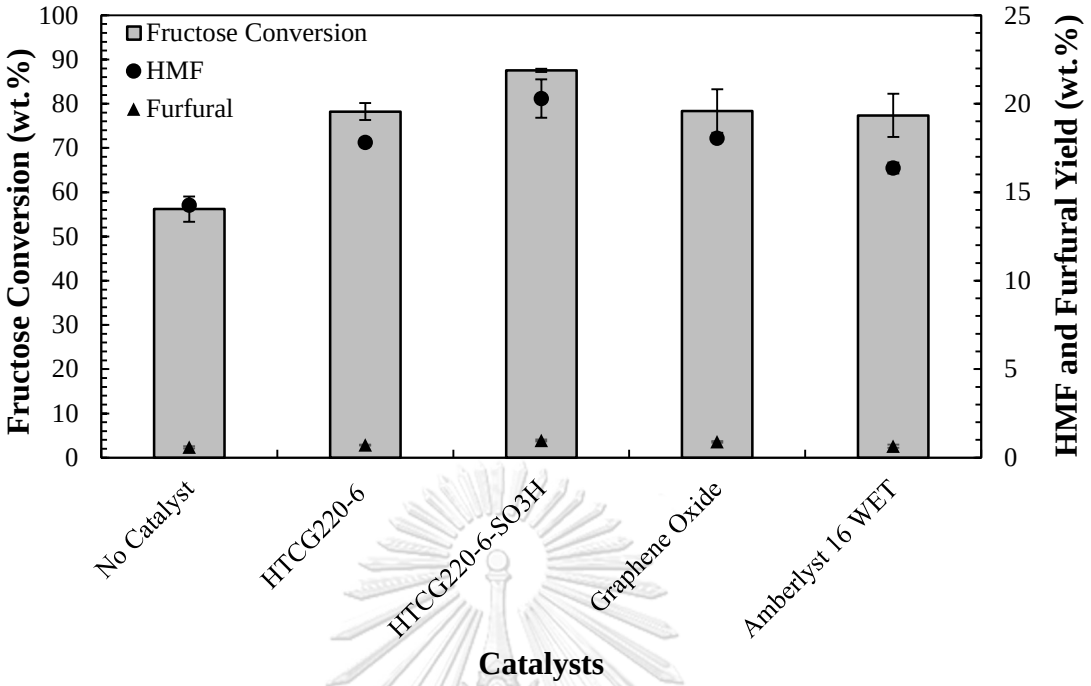

Figure 4.16: Fructose conversion, HMF and furfural yields in liquid product of fructose dehydration in subcritical water at 180 °C and 5 min and 5 wt.% catalyst loading, catalyzed by different catalysts.

4.4 Catalyst recyclability

The recyclability of HTCG220-6-SO_3H was conducted for fructose dehydration at the same reaction condition used previously (in subcritical water at 180 °C for 5 min with 5 wt.% catalyst loading). As shown in **Figure 4.17**, fructose conversion decreased from 87.56±0.37 wt.% to 54.58±4.09 wt.%, after 5 cycles. The most rapid decrease in reactivity was observed in the second and the third reaction cycles, possibly due to leaching of acid groups from the catalyst. Similarly, the HMF yields decreased from 19.62±0.14 wt.% to 14.11±0.06 wt.% after 5 cycles, while no difference was observed in furfural yields, possibly due to a very small amount of furfural in all reactions. It is worth noting that the fructose conversion and HMF yield in the second run were comparable to those obtained with fructose dehydration catalyzed by HTCG220, previously seen in- **Figure 4.16**. This result implies that leaching of -SO_3 group from the catalyst occurred during the reaction. Similarly, fructose conversion and HMF yield

obtained from the third reaction run onwards remained relatively unchanged, and are similar to those obtained with a non-catalytic reaction. This result suggested that it was possible that no acidity was no longer found on the catalyst after the third cycle. It could also be implied from these results that the -OH and -COOH might have been leached also after 3 reaction cycles. It is noted that acid leaching is the major and typical concern for sulfonated catalysts. Thus, in the future development of the catalyst, improvement of the recyclability of the catalyst would be one of the most important issues.

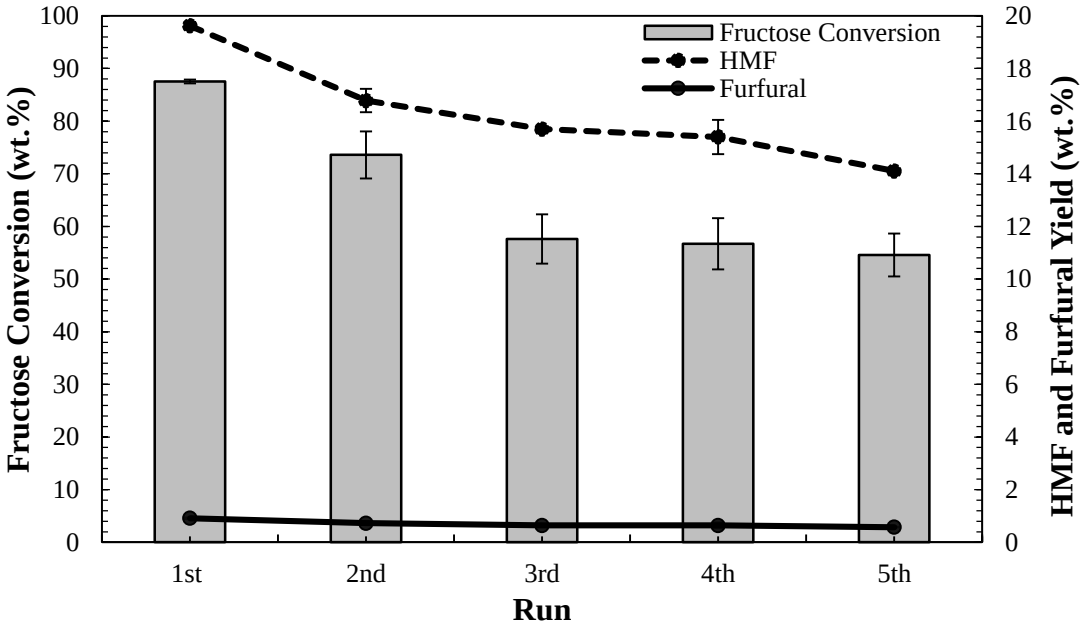

Figure 4.17: Fructose conversion, HMF and furfural yields in liquid product of fructose dehydration in subcritical water at 180 °C and 5 min and 5 wt.% catalyst loading, catalyzed by recycled catalyst

CHAPTER V
CONCLUSIONS AND RECOMMENDATION

5.1 Conclusions

To synthesize HTC-SO_3H catalysts from DRB and glucose for biomass conversion, HTCDRB and HTCG were prepared by hydrothermal carbonization. The chemical characteristics of the HTCDRB were similar to that of HTCG. While the yield and the morphological structures suggested the different formation of carbon. The HTCs were further functionalized with sulfuric acid to prepare a HTCDRB-SO_3H and HTCG-SO_3H catalysts. Both catalysts showed similar crystallinity structures, functional groups and thermal stability. In term of catalyst stability for biomass conversion to HMF, however, the leaching of catalysts to HMF was tested under biomass conversion condition without raw material. From this result, it was found that the HTCDRB-SO_3H was more stable more than HTCG-SO_3H. For the HTCDRB-SO_3H, hydrothermal carbonization at 220 °C and 3 h was suitable for the preparation of HTCDRB support for the HTCDRB220-3-SO_3H catalyst. On the other hand, the preparation of HTCG-SO_3H required the stability improvement before the catalyst can be used in biomass conversion to HMF.

Improvement of HTCG-SO_3H stability was therefore examined by extending hydrothermal carbonization time to prepare the stable HTCG as a catalyst support. The HTCG samples prepared at all conditions showed similar crystallinity structures, functional groups and thermal stability. While the liquid fractions of hydrothermal carbonization indicated the hydrothermal carbonization condition for the preparation of a stable HTCG support would be at temperature of 220 °C or above, and for at least 6 h. The HTCG from prepared from the suitable condition, HTCG220-6, was further sulfonated with sulfuric acid to prepare a HTCG220-6-SO_3H. The HTCG220-6-SO_3H characteristics demonstrated that it was stable and had high acidity which is suitable for use in biomass conversion to HMF.

The activities of catalysts prepared at suitable condition (HTCDRB220-3-SO_3H and HTCG220-6-SO_3H) were compared with a commercial -Amberlyst 16 Wet- and graphene oxide (GO). Both HTCDRB220-3-SO_3H and HTCG220-6-SO_3H exhibited the catalytic activities for biomass conversion on cellulose hydrolysis and fructose dehydration. However, the test on catalyst recyclability in fructose dehydration suggested that the synthesis of the hydrothermal carbon-based acid catalyst requires further improvement for the long term use of the catalyst.

5.2 Recommendations

From this research, the suitable hydrothermal conditions were determined to prepare DRB and glucose derived HTC-SO_3H catalysts for biomass conversion to HMF. These catalysts were proved to have activity on biomass conversion including hydrolysis and dehydration reaction, but the yield of HMF obtained in the liquid product was still relatively low, can potentially be improved. Moreover, the acid groups on the HTC support were found to leach after the catalyst use in the reaction, suggesting that recyclability of the catalyst should also be improved. There are two recommendations to complete our research.

(i) From the recyclability and stability study, the functionalization process for both DRB and glucose derived HTC-based acid catalyst should be developed to minimize the acid leaching of sulfonated catalyst. The minimization of acid leaching of sulfonated catalyst was reviewed in section 5.2.1.

(ii) From the catalytic activities study, the activity of catalyst should be developed to increase HMF yield. The enhancement of HMF yield was reviewed in section 5.2.2

5.2.1 Acid leaching of catalyst improvement

The study of catalyst reusability (**Figure 4.17**), tested with fructose dehydration indicated the catalyst reactivity rapidly dropped in the second and third reaction cycles. The drop of catalyst reactivity due to leaching of acid groups implied that the acid site

of catalyst was not stable. Further improvement on the functionalization process could be the solution of this problem.

Several researches were conducted to prepare hydrothermal carbon-based acid catalysts and to test the stability of the catalysts based on their reusability. Similar to this research, two-step catalyst preparation was examined by Zhao et al. (2016), in which glucose derived carbon catalyst support was prepared by hydrothermal carbonization at temperature of 180 °C for 10 h in first step. Then carbon (CS) was functionalized with sulfuric acid solution at temperature of 180 °C for 4 h. Compared with the method applied in this study, stirring of carbon and sulfuric solution was employed by Zhao's method prior to the functionalization. The CS catalyst was tested on fructose conversion, and the results showed a slight decrease in fructose conversion after the first run. The conversion then stayed relatively high at 96.2% after the fifth run. In addition, the stability of $–SO_3H$ groups was tested by leaching of $–SO_3H$ from carbon structure. CS catalyst was dissolved in DMSO and heated then at 140 °C and stirred for 2 h before use in the fructose dehydration. The reaction catalyzed by such catalyst having undergone such treatment achieved similar fructose conversion and HMF yield with the reaction catalyzed by the original CS catalyst, indicating the high stability of $–SO_3H$. Moreover, similar morphology of the catalysts were observed before and after the reaction (Zhao et al., 2016).

In addition to the two step of catalyst preparation, the hydrothermal carbon-based acid catalyst can be synthesized by a one step process. Glucose derived carbon functionalized with sulfonic group (CM-SO_3H) was synthesized by mixing glucose solution and sulfosalicylic acid and was then heated at 180 °C for 4 h. The resulting CM-SO_3H catalyst was then tested for the catalytic activity and recyclability on cellulose hydrolysis. It was demonstrated that the reaction catalyzed with such catalyst achieved 57.4% TRS yield, and the yield remained relatively unchanged after the fifth cycles. Furthermore, CM-SO_3H used after fifth run were not differences in the SO_3H groups and the total acid sites, compared with fresh CM-SO_3H. It indicated that CM-SO_3H catalyst had high stability of functional group in the catalyst (Qi et al., 2014).

As mentioned, CS catalyst and CM-SO_3H catalysts are the improved acid functionalized catalysts, whose -SO_3H acid group leaching of hydrothermal carbon-

based acid catalyst was improved. These synthesis methods should be considered and functionalized acid catalyst could be further investigated in the future study.

5.2.2 Enhancement of HMF yield improvement

HMF in this research was produced using a hydrothermal method in which water was used as a solvent. Since using water as a solvent is nonselective. The reaction in water achieved low yields of HMF, due to the relatively easy formation of by-products such as levulinic acid and formic acid. To improve HMF and furfural yields therefore, the solvothermal reaction might be employed. Because of the controllability of their properties and productivities, ionic liquids or organic solvents might be used. Generally, acetone and DMSO is of particular interest as solvents for such process because higher yield of HMF can be obtained with lesser by-products. Tuercke et al. (2009) demonstrated that dehydration of fructose, carried out using DMSO as a co-solvent and methyl isobutyl ketone/2-butanol as the extraction agent, achieved a higher fructose conversion (up to 98%) and higher HMF selectivity of 85%. As seen from Tuerche et al. (2009)'s study, in addition to co-solvent, the extraction agent was also employed for the efficient isolation of the desired product. Because HMF is not easily extracted from the aqueous phase, the use of organic solvent as the extraction solvent can solve this problem. Organic solvents such as MIBK (methyl isobutyl ketone), acetone, ethyl acetate, DCM (Dichloromethane), diethyl ether, and THF (Tetrahydrofuran) have been reported to be efficient extraction solvents. They may avoid by-product formation, resulting in improvement of HMF production (Rosatella et al., 2011). The further study should further be conducted to examine the ability of co-solvents or extraction solvents to help improve HMF yield and selectivity.

In addition to employing the solvothermal process, pretreatment of biomass prior to the reaction can enhance HMF production. For the production of HMF and furfural, the biomass with high content of cellulose and hemicellulose would be preferable. Lignin, on the other hand, is a complex structure, that acts as the protection of the plant tissue. It would therefore prevent the biomass from decomposing easily, thus hydrolysis and reaction of the biomass would require higher operating conditions. In addition, the decomposed products of lignin (phenolic compounds) are, often times, the undesirable product, particularly for hydrolysis of biomass to obtain monomer

sugars which will be used further in HMF production. In order to solve this problem, lignocellulosic biomass can undergo a pretreatment step that leads to the breakdown the macroscopic rigidity of biomass, disrupting and removing the cross-linked matrix of lignin. The HTC-SO_3H in this study was proved that have activity on hydrolysis reaction. Therefore, these catalysts can be further used for pretreatment of biomass to increase HMF yield.

REFERENCES

Adebiyi, A. P., Adebiyi, A. O., Hasegawa, Y., Ogawa, T. Muramoto, K. (2009). Isolation and characterization of protein fractions from deoiled rice bran. *European Food Research and Technology, 228*(3), 391-401.

Allahbakhsh, A., Sharif, F., Mazinani, S. Kalaee, M. (2014). Synthesis and characterization of Graphene Oxide in suspension and powder forms by chemical exfoliation method. *International Journal of Nano Dimension, 5*(1), 11.

Antonetti, C., Galletti, A. M. R., Fulignati, S. Licursi, D. (2017). Amberlyst A-70: A surprisingly active catalyst for the MW-assisted dehydration of fructose and inulin to HMF in water. *Catalysis Communications, 97*, 146-150.

Baccile, N., Laurent, G., Babonneau, F., Fayon, F., Titirici, M.-M. Antonietti, M. (2009). Structural characterization of hydrothermal carbon spheres by advanced solid-state MAS 13C NMR investigations. *The Journal of Physical Chemistry C, 113*(22), 9644-9654.

Bakar, R. A., Yahya, R. Gan, S. N. (2016). Production of high purity amorphous silica from rice husk. *Procedia Chemistry, 19*, 189-195.

Bandyopadhyay, K., Chakraborty, C. Barman, A. K. (2012). Effect of microwave and enzymatic treatment on the recovery of protein from Indian defatted rice bran meal. *Journal of oleo science, 61*(10), 525-529.

Bastawde, K. (1992). Xylan structure, microbial xylanases, and their mode of action. *World Journal of Microbiology and Biotechnology, 8*(4), 353-368.

Bessa, L. C., Ferreira, M. C., Rodrigues, C. E., Batista, E. A. Meirelles, A. J. (2017). Simulation and process design of continuous countercurrent ethanolic extraction of rice bran oil. *Journal of Food Engineering, 202*, 99-113.

Bhaumik, P. Dhepe, P. L. (2016). Solid acid catalyzed synthesis of furans from carbohydrates. *Catalysis Reviews, 58*(1), 36-112.

Binod, P., Sindhu, R., Singhania, R. R., Vikram, S., Devi, L., Nagalakshmi, S., Kurien, N., Sukumaran, R. K. Pandey, A. (2010). Bioethanol production from rice straw: an overview. *Bioresource technology, 101*(13), 4767-4774.

Boisen, A., Christensen, T., Fu, W., Gorbanev, Y., Hansen, T., Jensen, J., Klitgaard, S., Pedersen, S., Riisager, A. Ståhlberg, T. (2009). Process integration for the conversion of glucose to 2, 5-furandicarboxylic acid. *Chemical engineering research and design, 87*(9), 1318-1327.

Boonnoun, P., Muangnapoh, C., Prasitchoke, P., Tantayakom, V. Shotipruk, A. (2010). Reactive Extraction of 1, 3-Propanediol from Model Mixture of Fermentation Broth Using Novel Carbon Based Catalyst. *Journal of Sustainable Energy & Environment, 1*(1), 1-4.

Boonoun, P., Laosiripojana, N., Muangnapoh, C., Jongsomjit, B., Panpranot, J., Mekasuwandumrong, O. Shotipruk, A. (2010). Application of sulfonated carbon-based catalyst for reactive extraction of 1, 3-propanediol from model fermentation mixture. *Industrial & Engineering Chemistry Research, 49*(24), 12352-12357.

Cabús Llauradó, M. C. (2007). Catalytic non-oxidative dehydrogenation and reactivity of biobased fatty acid derivatives.

Centre for Catalysis and Sustainable. Renewable Chemicals. [Cited 2017 5 December]; Available from: h*ttp://www.csc.kemi.dtu.dk/research/renewable-chemicals*.

Chandra, R., Takeuchi, H. Hasegawa, T. (2012). Hydrothermal pretreatment of rice straw biomass: a potential and promising method for enhanced methane production. *Applied Energy, 94*, 129-140.

Chareonlimkun, A., Champreda, V., Shotipruk, A. Laosiripojana, N. (2010a). Catalytic conversion of sugarcane bagasse, rice husk and corncob in the presence of TiO 2, ZrO 2 and mixed-oxide TiO 2–ZrO 2 under hot compressed water (HCW) condition. *Bioresource technology, 101*(11), 4179-4186.

Chareonlimkun, A., Champreda, V., Shotipruk, A. Laosiripojana, N. (2010b). Reactions of C 5 and C 6-sugars, cellulose, and lignocellulose under hot compressed water (HCW) in the presence of heterogeneous acid catalysts. *Fuel, 89*(10), 2873-2880.

Chen, H. (2014). *Biotechnology of Lignocellulose: Theory and Practice*: Springer.

Cheng, L., Guo, X., Song, C., Yu, G., Cui, Y., Xue, N., Peng, L., Guo, X. Ding, W. (2013). High performance mesoporous zirconium phosphate for dehydration of xylose to furfural in aqueous-phase. *RSC Advances, 3*(45), 23228-23235.

Chheda, J. N., Román-Leshkov, Y. Dumesic, J. A. (2007). Production of 5-hydroxymethylfurfural and furfural by dehydration of biomass-derived mono- and poly-saccharides. *Green Chemistry, 9*(4), 342-350.

Chiou, T.-Y., Neoh, T. L., Kobayashi, T. Adachi, S. (2012). Extraction of defatted rice bran with subcritical aqueous acetone. *Bioscience, biotechnology, and biochemistry, 76*(8), 1535-1539.

Chittapalo, T. Noomhorm, A. (2009). Ultrasonic assisted alkali extraction of protein from defatted rice bran and properties of the protein concentrates. *International journal of food science & technology, 44*(9), 1843-1849.

Cui, S., Yu, S., Lin, B., Shen, X., Zhang, X. Gu, D. Preparation of amine-modified SiO2 aerogel from rice husk ash for CO2 adsorption. *Journal of Porous Materials, 24*(2), 455-461.

Daengprasert, W., Boonnoun, P., Laosiripojana, N., Goto, M. Shotipruk, A. (2011). Application of sulfonated carbon-based catalyst for solvothermal conversion of cassava waste to hydroxymethylfurfural and furfural. *Industrial & Engineering Chemistry Research, 50*(13), 7903-7910.

Daorattanachai, P., Namuangruk, S., Viriya-empikul, N., Laosiripojana, N. Faungnawakij, K. (2012). 5-Hydroxymethylfurfural production from sugars and cellulose in acid-and base-catalyzed conditions under hot compressed water. *Journal of Industrial and Engineering Chemistry, 18*(6), 1893-1901.

Dehkhoda, A. M., West, A. H. Ellis, N. (2010). Biochar based solid acid catalyst for biodiesel production. *Applied Catalysis A: General, 382*(2), 197-204.

Devi, R. R. Arumughan, C. (2007). Antiradical efficacy of phytochemical extracts from defatted rice bran. *Food and chemical toxicology, 45*(10), 2014-2021.

Dhamdere, R. T., Srinivas, K. King, J. W. (2012). *Carbochemicals Production from Switchgrass using Carbonated Subcritical Water at High Temperatures.* Paper presented at the 10th International Symposium on Supercritical Fluids, San Francisco.

Ding, J.-C., Xu, G.-C., Han, R.-Z. Ni, Y. (2016). Biobutanol production from corn stover hydrolysate pretreated with recycled ionic liquid by Clostridium saccharobutylicum DSM 13864. *Bioresource technology, 199*, 228-234.

Dussán, K. J., Silva, D. D., Moraes, E. J., Arruda, P. V. Felipe, M. G. (2014). Dilute-acid hydrolysis of cellulose to glucose from sugarcane bagasse. *CHEMICAL ENGINEERING, 38*, 433-438.

Falco, C., Baccile, N. Titirici, M.-M. (2011). Morphological and structural differences between glucose, cellulose and lignocellulosic biomass derived hydrothermal carbons. *Green Chemistry, 13*(11), 3273-3281.

Fang, J., Gao, B., Chen, J. Zimmerman, A. R. (2015). Hydrochars derived from plant biomass under various conditions: Characterization and potential applications and impacts. *Chemical Engineering Journal, 267*, 253-259.

Fiori, L., Bassoa, D., Castelloa, D. Baratierib, M. (2014). Hydrothermal carbonization of biomass: design of a batch reactor and preliminary experimental results. *CHEMICAL ENGINEERING, 37*, 55-60.

Foster, N. C. (1996). Sulfonation and sulfation processes. *Soap and Detergents: A Theoretical and Practical Review. Spitz, L.(Ed). AOCS Press, Champaign, Illinois*.

Fraile, J. M., García-Bordejé, E. Roldán, L. (2012). Deactivation of sulfonated hydrothermal carbons in the presence of alcohols: Evidences for sulfonic esters formation. *Journal of Catalysis, 289*, 73-79.

Fu, X., Li, D., Chen, J., Zhang, Y., Huang, W., Zhu, Y., Yang, J. Zhang, C. (2013). A microalgae residue based carbon solid acid catalyst for biodiesel production. *Bioresource technology, 146*, 767-770.

Fuertes, A., Arbestain, M. C., Sevilla, M., Maciá-Agulló, J. A., Fiol, S., López, R., Smernik, R., Aitkenhead, W., Arce, F. Macìas, F. (2010). Chemical and structural properties of carbonaceous products obtained by pyrolysis and hydrothermal carbonisation of corn stover. *Soil Research, 48*(7), 618-626.

Funke, A. Ziegler, F. (2010). Hydrothermal carbonization of biomass: a summary and discussion of chemical mechanisms for process engineering. *Biofuels Bioproducts and Biorefining*, (4), 160-177.

Gabbott, P. (2008). *Principles and applications of thermal analysis*: John Wiley & Sons.

Gao, P., Zhou, Y., Meng, F., Zhang, Y., Liu, Z., Zhang, W. Xue, G. (2016). Preparation and characterization of hydrochar from waste eucalyptus bark by hydrothermal carbonization. *Energy, 97*, 238-245.

Gao, S., Liang, X., Wang, W., Cheng, W. Yang, J. (2007). High efficient acetalization of carbonyl compounds with diols catalyzed by novel carbon-based solid strong acid catalyst. *Chinese Science Bulletin, 52*(21), 2892-2895.

Guo, H., Qi, X., Li, L. Smith, R. L. (2012). Hydrolysis of cellulose over functionalized glucose-derived carbon catalyst in ionic liquid. *Bioresource technology, 116*, 355-359.

Hanmoungjai, P., Pyle, D. Niranjan, K. (2001). Enzymatic process for extracting oil and protein from rice bran. *Journal of the American Oil Chemists' Society, 78*(8), 817-821.

Hara, M. (2010). Biomass conversion by a solid acid catalyst. *Energy & Environmental Science, 3*(5), 601-607.

Harry, I., Ibrahim, H., Thring, R. Idem, R. (2014). Catalytic subcritical water liquefaction of flax straw for high yield of furfural. *Biomass and Bioenergy, 71*, 381-393.

Hata, S., Wiboonsirikul, J., Maeda, A., Kimura, Y. Adachi, S. (2008). Extraction of defatted rice bran by subcritical water treatment. *Biochemical Engineering Journal, 40*(1), 44-53.

Herrero, M., Castro-Puyana, M., Rocamora, L., Ferragut, J. A., Cifuentes, A. Ibáñez, E. (2012). Formation of 5-(hydroxymethyl) furfural During Subcritical Water Extraction of Natural Matrices. Is It Bioactivity-Relevant?

Hoekman, S. K., Broch, A. Robbins, C. (2011). Hydrothermal carbonization (HTC) of lignocellulosic biomass. *Energy & Fuels, 25*(4), 1802-1810.

Inada, M., Enomoto, N., Hojo, J. Hayashi, K. (2017). Structural analysis and capacitive properties of carbon spheres prepared by hydrothermal carbonization. *Advanced Powder Technology, 28*(3), 884-889.

Iryani, D. A., Kumagai, S., Nonaka, M., Sasaki, K. Hirajima, T. (2013). Production of 5-hydroxymethyl Furfural from Sugarcane Bagasse under Hot Compressed Water. *Procedia Earth and Planetary Science, 6*, 441-447.

Islam, M. A., Kabir, G., Asif, M. Hameed, B. (2015). Combustion kinetics of hydrochar produced from hydrothermal carbonisation of Karanj (Pongamia pinnata) fruit hulls via thermogravimetric analysis. *Bioresource technology, 194*, 14-20.

Jeong, G. H., Kim, E. G., Kim, S. B., Park, E. D. Kim, S. W. (2011). Fabrication of sulfonic acid modified mesoporous silica shells and their catalytic performance with dehydration reaction of d-xylose into furfural. *Microporous and mesoporous materials, 144*(1), 134-139.

Jongjareonrak, A., Srikok, K., Leksawasdi, N. Andreotti, C. (2015). Extraction and functional properties of protein from de-oiled rice bran. *Chiang Mai University Journal of Neural Sciences, 14*(2), 163-174.

Kang, S., Li, X., Fan, J. Chang, J. (2012). Characterization of hydrochars produced by hydrothermal carbonization of lignin, cellulose, D-xylose, and wood meal. *Industrial & Engineering Chemistry Research, 51*(26), 9023-9031.

Kang, S., Ye, J., Zhang, Y. Chang, J. (2013). Preparation of biomass hydrochar derived sulfonated catalysts and their catalytic effects for 5-hydroxymethylfurfural production. *RSC Advances, 3*(20), 7360-7366.

Karimi, K., Kheradmandinia, S. Taherzadeh, M. J. (2006). Conversion of rice straw to sugars by dilute-acid hydrolysis. *Biomass and Bioenergy, 30*(3), 247-253.

Kataki, S., Hazarika, S. Baruah, D. (2017). Assessment of by-products of bioenergy systems (anaerobic digestion and gasification) as potential crop nutrient. *Waste management, 59*, 102-117.

Kim, D., Yoshikawa, K. Park, K. Y. (2015). Characteristics of Biochar Obtained by Hydrothermal Carbonization of Cellulose for Renewable Energy. *Energies, 8*(12), 14040-14048.

Kim, S. M., Dien, B. S., Tumbleson, M., Rausch, K. D. Singh, V. (2016). Improvement of sugar yields from corn stover using sequential hot water pretreatment and disk milling. *Bioresource technology, 216*, 706-713.

Kruse, A. Dinjus, E. (2007). Hot compressed water as reaction medium and reactant: properties and synthesis reactions. *The Journal of Supercritical Fluids, 39*(3), 362-380.

Laboratoryinfo.com. High Performance Liquid Chromatography (HPLC): Principle, Types, Instrumentation and Applications. [Cited 2017 5 December]; Available from:*http://laboratoryinfo.com/hplc/*.

Lakkakula, N. R., Lima, M. Walker, T. (2004). Rice bran stabilization and rice bran oil extraction using ohmic heating. *Bioresource technology, 92*(2), 157-161.

Lanzafame, P., Temi, D., Perathoner, S., Spadaro, A. Centi, G. (2012). Direct conversion of cellulose to glucose and valuable intermediates in mild reaction conditions over solid acid catalysts. *Catalysis today, 179*(1), 178-184.

Lee, H., Hamid, S. Zain, S. (2014). Conversion of Lignocellulosic Biomass to Nanocellulose: Structure and Chemical Process. *The Scientific World Journal, 2014*.

Lei, Y., Su, H. Tian, R. (2016). Morphology evolution, formation mechanism and adsorption properties of hydrochars prepared by hydrothermal carbonization of corn stalk. *RSC Advances, 6*(109), 107829-107835.

Li, M., Li, W. Liu, S. (2011). Hydrothermal synthesis, characterization, and KOH activation of carbon spheres from glucose. *Carbohydrate research, 346*(8), 999-1004.

Li, M., Li, W., Lu, Y., Jameel, H., Chang, H.-m. Ma, L. (2017). High conversion of glucose to 5-hydroxymethylfurfural using hydrochloric acid as a catalyst and sodium chloride as a promoter in a water/γ-valerolactone system. *RSC Advances, 7*(24), 14330-14336.

Li, X., Li, X., Qi, W., Shi, J., Zhang, J., Xu, Y. Pang, J. (2015). Preparation of Magnetic Biomass-based Solid Acid Catalyst and Effective Catalytic Conversion of Cellulose into High Yields of Reducing Sugar. *BioResources, 10*(4), 6720-6729.

Libra, J. A., Ro, K. S., Kammann, C., Funke, A., Berge, N. D., Neubauer, Y., Titirici, M.-M., Fühner, C., Bens, O. Kern, J. (2011). Hydrothermal carbonization of biomass residuals: a comparative review of the chemistry, processes and applications of wet and dry pyrolysis. *Biofuels, 2*(1), 71-106.

Liu, M., Jia, S., Gong, Y., Song, C. Guo, X. (2013). Effective hydrolysis of cellulose into glucose over sulfonated sugar-derived carbon in an ionic liquid. *Industrial & Engineering Chemistry Research, 52*(24), 8167-8173.

Liu, T., Li, Z., Li, W., Shi, C. Wang, Y. (2013). Preparation and characterization of biomass carbon-based solid acid catalyst for the esterification of oleic acid with methanol. *Bioresource technology, 133*, 618-621.

Liu, X.-Y., Huang, M., Ma, H.-L., Zhang, Z.-Q., Gao, J.-M., Zhu, Y.-L., Han, X.-J. Guo, X.-Y. (2010). Preparation of a carbon-based solid acid catalyst by sulfonating activated carbon in a chemical reduction process. *Molecules, 15*(10), 7188-7196.

Lu, X., Pellechia, P. J., Flora, J. R. Berge, N. D. (2013). Influence of reaction time and temperature on product formation and characteristics associated with the hydrothermal carbonization of cellulose. *Bioresource technology, 138*, 180-190.

Machado, G., Leon, S., Santos, F., Lourega, R., Dullius, J., Mollmann, M. E. Eichler, P. (2016). Literature review on furfural production from Lignocellulosic biomass. *Natural Resources, 7*(03), 115.

Malins, K., Kampars, V., Brinks, J., Neibolte, I. Murnieks, R. (2015). Synthesis of activated carbon based heterogenous acid catalyst for biodiesel preparation. *Applied Catalysis B: Environmental, 176*, 553-558.

Mamidipally, P. K. Liu, S. X. (2004). First approach on rice bran oil extraction using limonene. *European Journal of Lipid Science and Technology, 106*(2), 122-125.

Mardhiah, H. H., Ong, H. C., Masjuki, H. H., Lim, S. Pang, Y. L. (2017). Investigation of carbon-based solid acid catalyst from Jatropha curcas biomass in biodiesel production. *Energy Conversion and Management, 144*, 10-17.

Miller, G. L. (1959). Use of dinitrosalicylic acid reagent for determination of reducing sugar. *Analytical chemistry, 31*(3), 426-428.

Mo, X., Lotero, E., Lu, C., Liu, Y. Goodwin, J. G. (2008). A novel sulfonated carbon composite solid acid catalyst for biodiesel synthesis. *Catalysis Letters, 123*(1-2), 1-6.

Montané, D., Salvadó, J., Torras, C. Farriol, X. (2002). High-temperature dilute-acid hydrolysis of olive stones for furfural production. *Biomass and Bioenergy, 22*(4), 295-304.

Nakajima, K., Hara, M. Hayashi, S. (2007). Environmentally Benign Production of Chemicals and Energy Using a Carbon-Based Strong Solid Acid. *Journal of the American Ceramic Society, 90*(12), 3725-3734.

Nakhate, A. V. Yadav, G. D. (2016). Synthesis and Characterization of Sulfonated Carbon-Based Graphene Oxide Monolith by Solvothermal Carbonization for Esterification and Unsymmetrical Ether Formation. *ACS Sustainable Chemistry & Engineering, 4*(4), 1963-1973.

Nata, I. F. Lee, C. K. (2010). Novel carbonaceous nanocomposite pellicle based on bacterial cellulose. *Green Chemistry, 12*(8), 1454-1459.

Nata, I. F., Putra, M. D., Irawan, C. Lee, C.-K. (2017). Catalytic performance of sulfonated carbon-based solid acid catalyst on esterification of waste cooking oil for biodiesel production. *Journal of Environmental Chemical Engineering, 5*(3), 2171-2175.

National Institute of Standards and Technology. 5-(Hydroxymethyl)furfural. [Cited 2017 5 December]; Available from: *http://webbook.nist.gov/cgi/cbook.cgi?Name=HMF&Units=SI.*

National Institute of Standards and Technology. Furfural. [Cited 2017 5 December]; Available from: *http://webbook.nist.gov/cgi/cbook.cgi?Name=furfural&Units=SI.*

O'Driscoll, Á., Leahy, J. Curtin, T. (2017). The influence of metal selection on catalyst activity for the liquid phase hydrogenation of furfural to furfuryl alcohol. *Catalysis today, 279*, 194-201.

Okamura, M., Takagaki, A., Toda, M., Kondo, J. N., Domen, K., Tatsumi, T., Hara, M. Hayashi, S. (2006). Acid-catalyzed reactions on flexible polycyclic aromatic carbon in amorphous carbon. *Chemistry of Materials, 18*(13), 3039-3045.

Ormsby, R., Kastner, J. R. Miller, J. (2012). Hemicellulose hydrolysis using solid acid catalysts generated from biochar. *Catalysis today, 190*(1), 89-97.

Parveen, F., Patra, T. Upadhyayula, S. (2016). Hydrolysis of microcrystalline cellulose using functionalized Bronsted acidic ionic liquids–A comparative study. *Carbohydrate polymers, 135*, 280-284.

Pileidis, F. D., Tabassum, M., Coutts, S. Titirici, M.-M. (2014). Esterification of levulinic acid into ethyl levulinate catalysed by sulfonated hydrothermal carbons. *Chinese Journal of Catalysis, 35*(6), 929-936.

Pourali, O., Asghari, F. S. Yoshida, H. (2009). Sub-critical water treatment of rice bran to produce valuable materials. *Food chemistry, 115*(1), 1-7.

Proctor, A. Bowen, D. (1996). Ambient-temperature extraction of rice bran oil with hexane and isopropanol. *Journal of the American Oil Chemists' Society, 73*(6), 811-813.

Qi, X., Lian, Y., Yan, L. Smith, R. L. (2014). One-step preparation of carbonaceous solid acid catalysts by hydrothermal carbonization of glucose for cellulose hydrolysis. *Catalysis Communications, 57*, 50-54.

Qi, X., Liu, N. Lian, Y. (2015). Carbonaceous microspheres prepared by hydrothermal carbonization of glucose for direct use in catalytic dehydration of fructose. *RSC Advances, 5*(23), 17526-17531.

Qi, X., Watanabe, M., Aida, T. M. Smith, R. L. (2008). Catalytical conversion of fructose and glucose into 5-hydroxymethylfurfural in hot compressed water by microwave heating. *Catalysis Communications, 9*(13), 2244-2249.

Quispe, I., Navia, R. Kahhat, R. (2017). Energy potential from rice husk through direct combustion and fast pyrolysis: A review. *Waste management, 59*, 200-210.

Reza, M. T., Andert, J., Wirth, B., Busch, D., Pielert, J., Lynam, J. G. Mumme, J. (2014). Hydrothermal carbonization of biomass for energy and crop production. *Applied Bioenergy, 1*(1).

Reza, M. T., Nover, J., Wirth, B. Coronella, C. J. (2016). Hydrothermal carbonization of glucose in saline solution: sequestration of nutrients on carbonaceous materials. *AIMS Energy, 4*(1), 173-189.

Röhrdanz, M., Rebling, T., Ohlert, J., Jasper, J., Greve, T., Buchwald, R., von Frieling, P. Wark, M. (2016). Hydrothermal carbonization of biomass from landscape management–Influence of process parameters on soil properties of hydrochars. *Journal of environmental management, 173*, 72-78.

Roldán, L., Pires, E., Fraile, J. M. García-Bordejé, E. (2015). Impact of sulfonated hydrothermal carbon texture and surface chemistry on its catalytic performance in esterification reaction. *Catalysis today, 249*, 153-160.

Rosatella, A. A., Simeonov, S. P., Frade, R. F. Afonso, C. A. (2011). 5-Hydroxymethylfurfural (HMF) as a building block platform: Biological properties, synthesis and synthetic applications. *Green Chemistry, 13*(4), 754-793.

Salak Asghari, F. Yoshida, H. (2006). Acid-catalyzed production of 5-hydroxymethyl furfural from D-fructose in subcritical water. *Industrial & Engineering Chemistry Research, 45*(7), 2163-2173.

Sasaki, M. Goto, M. (2008). Recovery of phenolic compounds through the decomposition of lignin in near and supercritical water. *Chemical Engineering and Processing: Process Intensification, 47*(9), 1609-1619.

Sereewatthanawut, I., Prapintip, S., Watchiraruji, K., Goto, M., Sasaki, M. Shotipruk, A. (2008). Extraction of protein and amino acids from deoiled rice bran by subcritical water hydrolysis. *Bioresource technology, 99*(3), 555-561.

Serrano-Ruiz, J. C. Dumesic, J. A. (2011). Catalytic routes for the conversion of biomass into liquid hydrocarbon transportation fuels. *Energy & Environmental Science, 4*(1), 83-99.

Sevilla, M. Fuertes, A. B. (2009a). Chemical and structural properties of carbonaceous products obtained by hydrothermal carbonization of saccharides. *Chemistry-A European Journal, 15*(16), 4195-4203.

Sevilla, M. Fuertes, A. B. (2009b). The production of carbon materials by hydrothermal carbonization of cellulose. *Carbon, 47*(9), 2281-2289.

Shi, H. (2017). Sulfonation mechanism of benzene with SO3 in sulfuric acid or oleum or aprotic solvent: Obeying the transition state theory via a trimolecular electrophilic substitution clarified by density functional theory calculation. *Computational and Theoretical Chemistry, 1112*(1), 111-122.

Shu, Q., Zhang, Q., Xu, G., Nawaz, Z., Wang, D. Wang, J. (2009). Synthesis of biodiesel from cottonseed oil and methanol using a carbon-based solid acid catalyst. *Fuel Processing Technology, 90*(7), 1002-1008.

Sinyoung, S., Kunchariyakun, K., Asavapisit, S. MacKenzie, K. J. (2017). Synthesis of belite cement from nano-silica extracted from two rice husk ashes. *Journal of environmental management, 190*, 53-60.

Sobrosa, F., Stochero, N., Marangon, E. Tier, M. (2017). Development of refractory ceramics from residual silica derived from rice husk ash. *Ceramics International, 43*(9), 7142-7146.

Son, P. A., Nishimura, S. Ebitani, K. (2012). Synthesis of levulinic acid from fructose using Amberlyst-15 as a solid acid catalyst. *Reaction Kinetics, Mechanisms and Catalysis, 106*(1), 185-192.

Sophisticated Analytical Instrument Facility, IIT Bombay. (CHNS(O) Analyzer. [Cited 2017 5 December]; Available from: *http://www.rsic.iitb.ac.in/chn.html.*

Suganuma, S., Nakajima, K., Kitano, M., Yamaguchi, D., Kato, H. Hayashi, S. (2008). Hydrolysis of cellulose by amorphous carbon bearing SO3H, COOH, and OH groups. *Journal of the American Chemical Society, 130*(38), 12787-12793.

Suganuma, S., Nakajima, K., Kitano, M., Yamaguchi, D., Kato, H., Hayashi, S. Hara, M. (2010). Synthesis and acid catalysis of cellulose-derived carbon-based solid acid. *Solid State Sciences, 12*(6), 1029-1034.

Sun, Y. Cheng, J. (2002). Hydrolysis of lignocellulosic materials for ethanol production: a review. *Bioresource technology, 83*(1), 1-11.

Sunphorka, S., Chavasiri, W., Oshima, Y. Ngamprasertsith, S. (2012). Protein and sugar extraction from rice bran and de-oiled rice bran using subcritical water in a semi-continuous reactor: optimization by response surface methodology. *International Journal of Food Engineering, 8*(3).

Tang, S., Hettiarachchy, N. S. Shellhammer, T. H. (2002). Protein extraction from heat-stabilized defatted rice bran. 1. Physical processing and enzyme treatments. *Journal of Agricultural and Food Chemistry, 50*(25), 7444-7448.

Tian, S.-Q., Wang, X.-W., Zhao, R.-Y. Ma, S. (2016). Effect of doping pretreated corn stover conditions on yield of bioethanol in immobilized cell systems. *Renewable Energy, 86*, 858-865.

Titirici, M.-M., Antonietti, M. Baccile, N. (2008). Hydrothermal carbon from biomass: a comparison of the local structure from poly-to monosaccharides and pentoses/hexoses. *Green Chemistry, 10*(11), 1204-1212.

Titirici, M.-M., White, R. J., Falco, C. Sevilla, M. (2012). Black perspectives for a green future: hydrothermal carbons for environment protection and energy storage. *Energy & Environmental Science, 5*(5), 6796-6822.

Toda, M., Takagaki, A., Okamura, M., Kondo, J. N., Hayashi, S., Domen, K. Hara, M. (2005). Green chemistry: biodiesel made with sugar catalyst. *Nature, 438*(7065), 178-178.

Tran, T. T. V., Kaiprommarat, S., Kongparakul, S., Reubroycharoen, P., Guan, G., Nguyen, M. H. Samart, C. (2016). Green biodiesel production from waste cooking oil using an environmentally benign acid catalyst. *Waste management, 52*, 367-374.

TutorVista.com. Reverse Phase HPLC. [Cited 2017 5 December]; Available from: *http://chemistry.tutorvista.com/analytical-chemistry/reverse-phase-hplc.html.*

Viriya-Empikul, N., Wiboonsirikul, J., Kobayashi, T. Adachi, S. (2012). Effects of temperature and flow rate on subcritical-water extraction from defatted rice bran. *Food Science and Technology Research, 18*(3), 333-340.

Wang, J., Xu, W., Ren, J., Liu, X., Lu, G. Wang, Y. (2011). Efficient catalytic conversion of fructose into hydroxymethylfurfural by a novel carbon-based solid acid. *Green Chemistry, 13*(10), 2678-2681.

Wang, L. H., Liu, H. Li, L. (2015). Carbon-based acid catalyst from waste seed shells: preparation and characterization. *Polish Journal of Chemical Technology, 17*(4), 37-41.

Wang, M., Wu, W.-W., Wang, S.-S., Shi, X.-Y., Wu, F.-A. Wang, J. (2015). Preparation and Characterization of a Solid Acid Catalyst from Macro Fungi Residue for Methyl Palmitate Production. *BioResources, 10*(3).

Wang, Y., Guo, W., Cheng, C.-L., Ho, S.-H., Chang, J.-S. Ren, N. (2016). Enhancing bio-butanol production from biomass of Chlorella vulgaris JSC-6 with sequential alkali pretreatment and acid hydrolysis. *Bioresource technology, 200*, 557-564.

Wang, Y., Wang, D., Tan, M., Jiang, B., Zheng, J., Tsubaki, N. Wu, M. (2015). Monodispersed Hollow SO3H-Functionalized Carbon/Silica as Efficient Solid Acid Catalyst for Esterification of Oleic Acid. *ACS applied materials & interfaces, 7*(48), 26767-26775.

Watanabe, M., Aida, T. M. Smith, R. L. (2014). Review of Biomass Conversion in High Pressure High Temperature Water (HHW) Including Recent Experimental

Results (Isomerization and Carbonization). *Application of Hydrothermal Reactions to Biomass Conversion*, 249-274).

Wataniyakul, P., Pavasant, P., Goto, M. Shotipruk, A. (2012). Microwave pretreatment of defatted rice bran for enhanced recovery of total phenolic compounds extracted by subcritical water. *Bioresource technology, 124*, 18-22.

Watchararuji, K., Goto, M., Sasaki, M. Shotipruk, A. (2008). Value-added subcritical water hydrolysate from rice bran and soybean meal. *Bioresource technology, 99*(14), 6207-6213.

Wiboonsirikul, J., Kimura, Y., Kadota, M., Morita, H., Tsuno, T. Adachi, S. (2007). Properties of extracts from defatted rice bran by its subcritical water treatment. *Journal of Agricultural and Food Chemistry, 55*(21), 8759-8765.

Wu, Y., Fu, Z., Yin, D., Xu, Q., Liu, F., Lu, C. Mao, L. (2010). Microwave-assisted hydrolysis of crystalline cellulose catalyzed by biomass char sulfonic acids. *Green Chemistry, 12*(4), 696-700.

Xiao, L.-P., Shi, Z.-J., Xu, F. Sun, R.-C. (2012). Hydrothermal carbonization of lignocellulosic biomass. *Bioresource technology, 118*, 619-623.

Yan, L., Liu, N., Wang, Y., Machida, H. Qi, X. (2014). Production of 5-hydroxymethylfurfural from corn stalk catalyzed by corn stalk-derived carbonaceous solid acid catalyst. *Bioresource technology, 173*, 462-466.

Yang, L., Liu, Y., Ruan, R., Wang, Y., Zeng, W., Liu, C. Zhang, J. (2011). Advances in production of 5-hydroxymethylfurfural from starch. *Modern Chemical Industry, 1*, 014.

Yang, Z., Huang, R., Qi, W., Tong, L., Su, R. He, Z. (2015). Hydrolysis of cellulose by sulfonated magnetic reduced graphene oxide. *Chemical Engineering Journal, 280*, 90-98.

Yu, J. T., Dehkhoda, A. M. Ellis, N. (2010). Development of biochar-based catalyst for transesterification of canola oil. *Energy & Fuels, 25*(1), 337-344.

Yue, Z., Ma, D., Peng, S., Zhao, X., Chen, T. Wang, J. (2016). Integrated utilization of algal biomass and corn stover for biofuel production. *Fuel, 168*, 1-6.

Zhang, K., Pei, Z. Wang, D. (2016). Organic solvent pretreatment of lignocellulosic biomass for biofuels and biochemicals: A review. *Bioresource technology, 199*, 21-33.

Zhang, M., Yang, H., Liu, Y., Sun, X., Zhang, D. Xue, D. (2012). First identification of primary nanoparticles in the aggregation of HMF. *Nanoscale research letters, 7*(1), 38.

Zhang, T., Li, W., Xu, Z., Liu, Q., Ma, Q., Jameel, H., Chang, H.-m. Ma, L. (2016). Catalytic conversion of xylose and corn stalk into furfural over carbon solid acid catalyst in γ-valerolactone. *Bioresource technology, 209*, 108-114.

Zhao, J., Zhou, C., He, C., Dai, Y., Jia, X. Yang, Y. (2016). Efficient dehydration of fructose to 5-hydroxymethylfurfural over sulfonated carbon sphere solid acid catalysts. *Catalysis today, 264*, 123-130.

Zheng, X., Gu, X., Ren, Y., Zhi, Z. Lu, X. (2016). Production of 5-hydroxymethyl furfural and levulinic acid from lignocellulose in aqueous solution and different solvents. *Biofuels, Bioproducts and Biorefining, 10*(6). 917-931.

Zong, M.-H., Duan, Z.-Q., Lou, W.-Y., Smith, T. J. Wu, H. (2007). Preparation of a sugar catalyst and its use for highly efficient production of biodiesel. *Green Chemistry*, *9*(5), 434-437.

APPENDIX

APPENDIX A
EXPERIMENTAL AND DATA ANALYSIS

A1 Standard calibration curve from Shodex SUGAR SH1011 column

Table A-1: Standard calibration curve for HPLC analysis of HMF

Peak area	Concentration of HMF (mg/ml)
4028	0.05
64075	0.2
171431	0.5
276848	0.8
351172	1

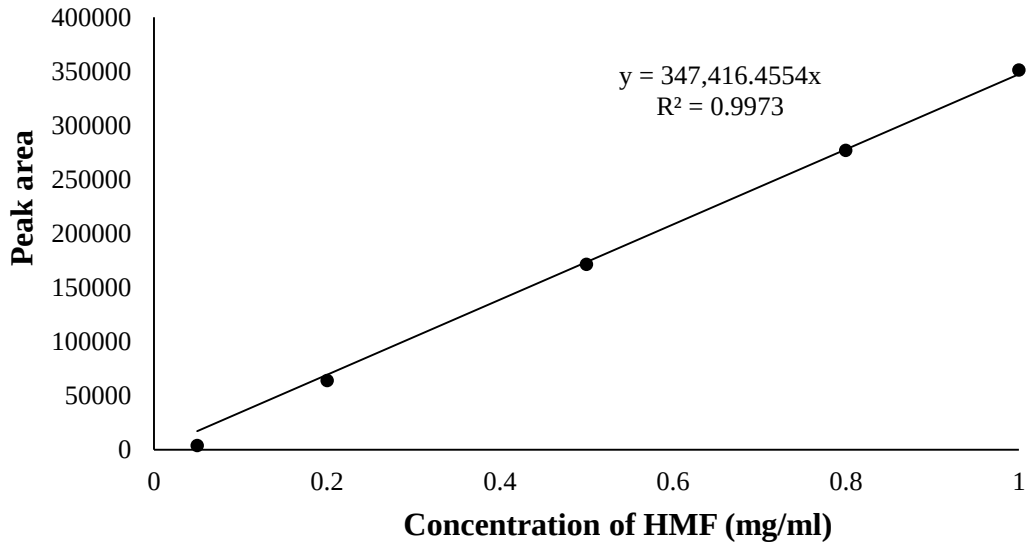

Figure A-1: Standard calibration curve of HMF

Table A-2: Standard calibration curve for HPLC analysis of furfural

Peak area	Concentration of furfural (mg/ml)
2466	0.05
57205	0.2
167115	0.5
269768	0.8
349148	1

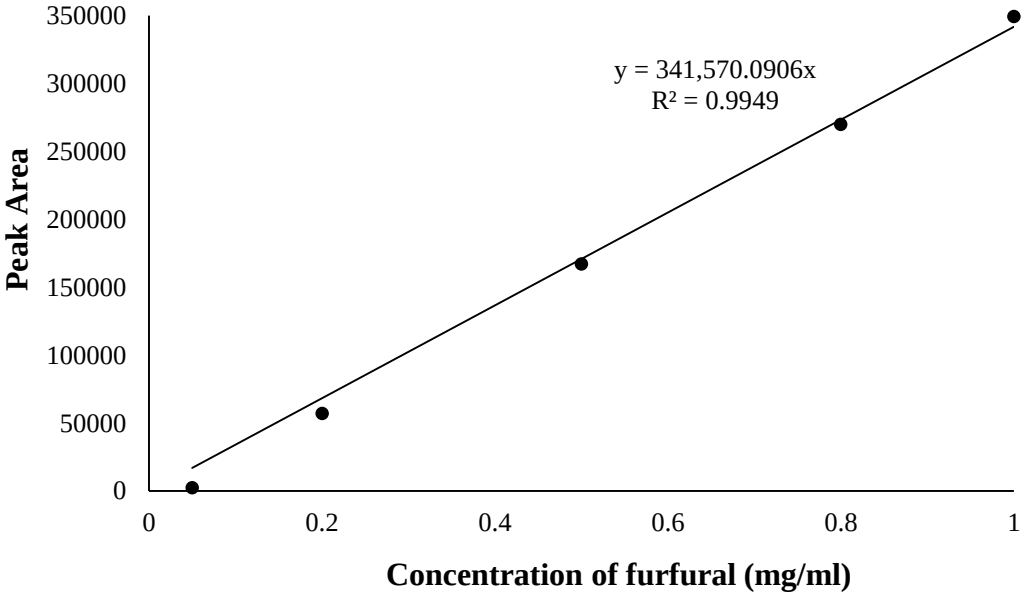

Figure A-2: Standard calibration curve for HPLC analysis of furfural

Table A-3: Standard calibration curve for HPLC analysis of levulinic acid

Peak area (UV detector at 210 nm)	Concentration of levulinic acid (mg/ml)
1854	0.05
88289	0.5
319008	2
816871	5
1565800	10
2402527	15
3287849	20

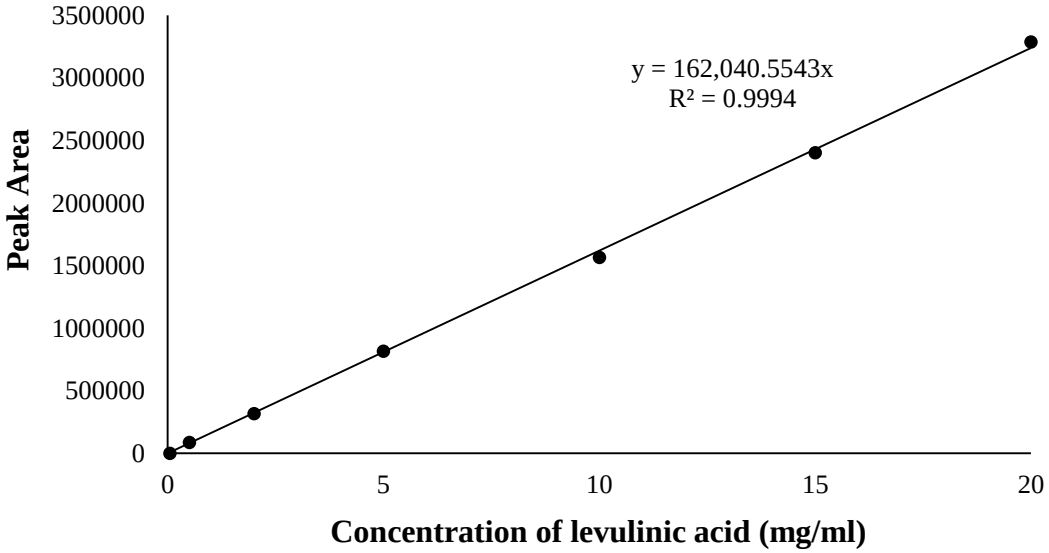

Figure A-3: Standard calibration curve for HPLC analysis of levulinic acid

Table A-4: Standard calibration curve for HPLC analysis of formic acid

Peak area (UV detector at 210 nm)	Concentration of formic acid (mg/ml)
17298	0.05
261899	0.5
1105050	2
2854425	5
5837738	10
8789228	15
11398890	20

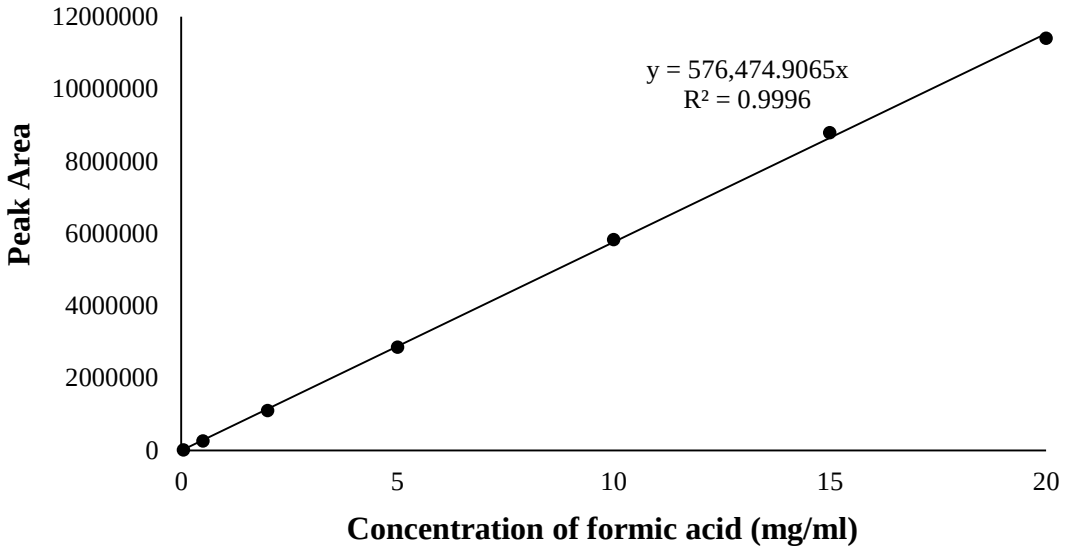

Figure A-4: Standard calibration curve for HPLC analysis of formic acid

Table A-5: Standard calibration curve for HPLC analysis of glucose

Peak area	Concentration of glucose (mg/ml)
1628207	5
3633801	10
5409210	15
7518492	20
9552869	25

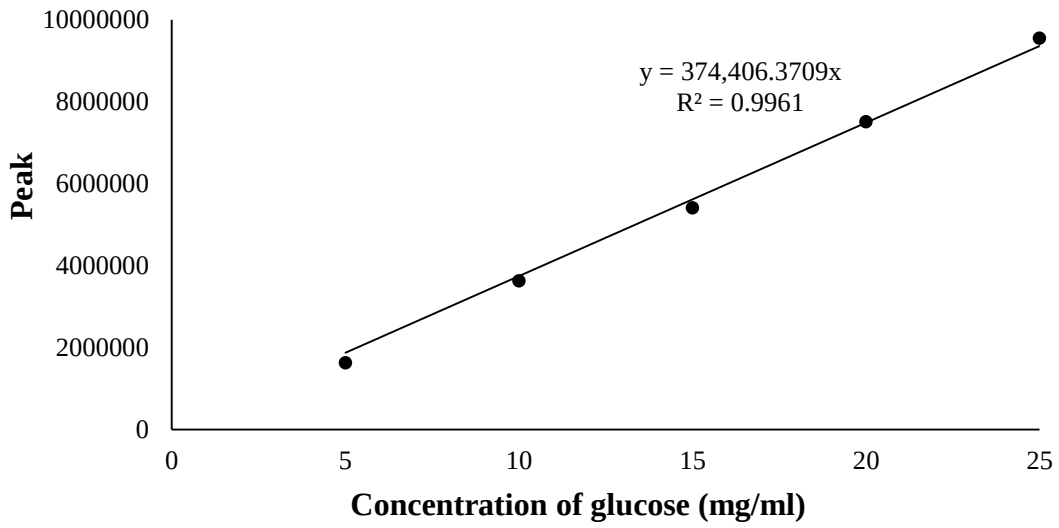

Figure A-5: Standard calibration curve for HPLC analysis of glucose

A2 Standard calibration curve from Rezex RPM Monosaccharide Pb+2 column

Table A-6: Standard calibration curve for HPLC analysis of HMF

Peak area	Concentration of HMF (mg/ml)
25693192	0.1
91171456	0.3
135840624	0.5
183575168	0.7
257350992	1.0

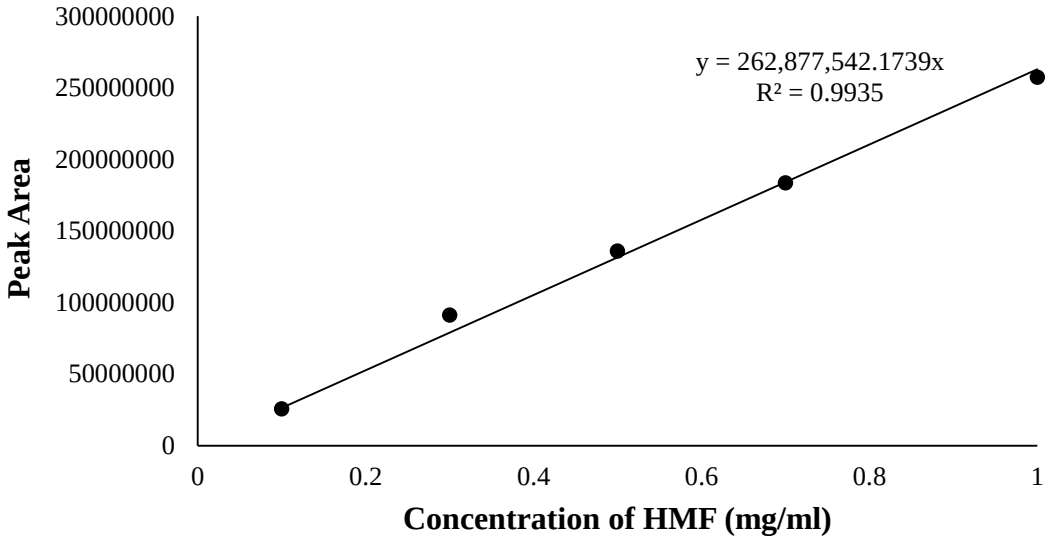

Figure A-6: Standard calibration curve for HPLC analysis of HMF

Table A-7: Standard calibration curve for HPLC analysis of furfural

Peak area	Concentration of furfural (mg/ml)
29449178	0.1
90232632	0.3
159215744	0.5
226371712	0.7
304448992	1.0

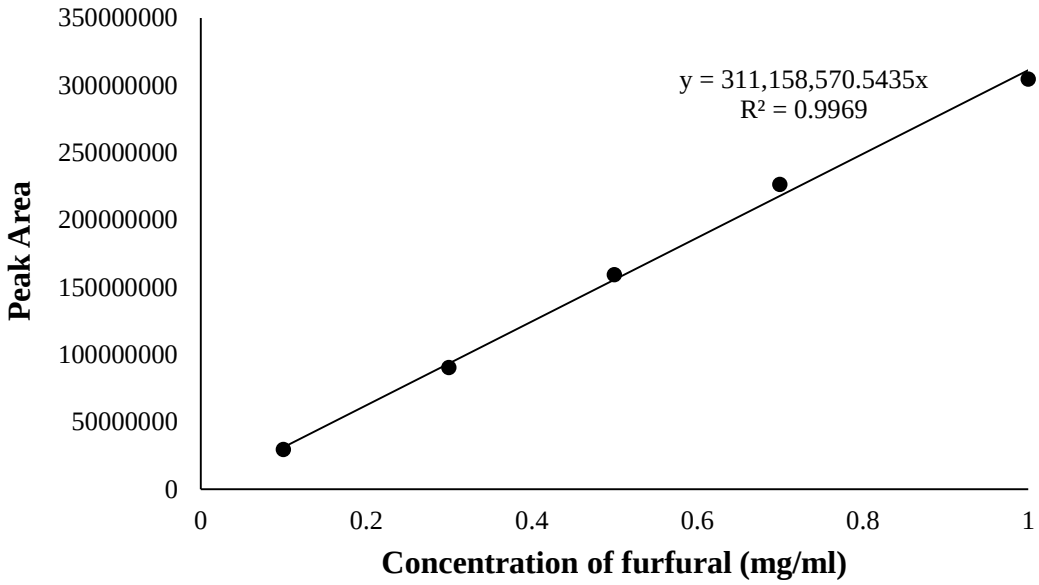

Figure A-7: Standard calibration curve for HPLC analysis of furfural

Table A-8: Standard calibration curve for HPLC analysis of glucose

Peak area	Concentration of glucose (mg/ml)
200	0.1
879	0.3
1709	0.5
2551	0.7
4243	1.0

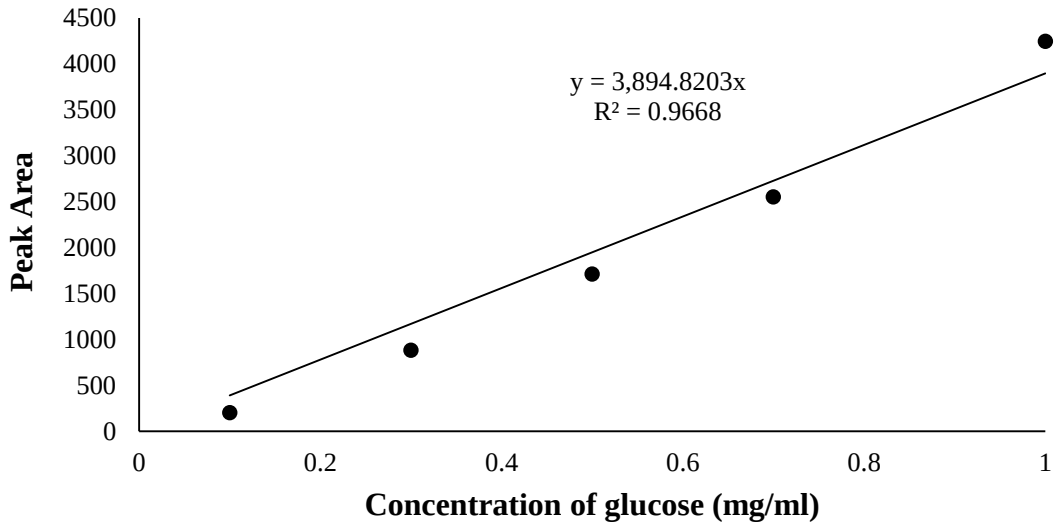

Figure A-8: Standard calibration curve for HPLC analysis of glucose

Table A-9: Standard calibration curve for HPLC analysis of fructose

Peak area	Concentration of fructose (mg/ml)
174	0.1
1001	0.3
1564	0.5
2416	0.7
3442	1.0

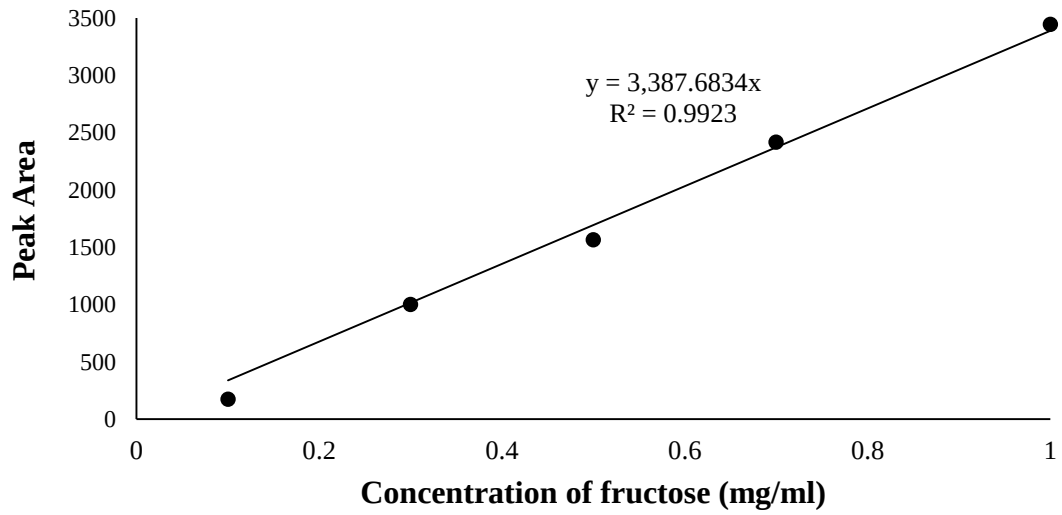

Figure A-9: Standard calibration curve for HPLC analysis of fructose

APPENDIX B
EXPERIMENTAL DATA

Table B-1: Amounts of HMF, furfural, levulinic acid, and formic acid in liquid fraction from catalyst leaching test under microwave

Catalysts	Product yields (wt.%)			
	HMF	Furfural	Levulinic Acid	Formic Acid
HTCG220-1-SO_3H	0.0514	1.0877	27.1285	5.0327
HTCG220-3-SO_3H	0.0328	0.0680	18.6134	2.7670
HTCDRB220-1-SO_3H	0.0012	0.0158	3.9607	0.8192
HTCDRB220-3-SO_3H	0.0007	0.0039	1.7497	0.4296

Table B-2: Total reducing sugar (TRS) as well as glucose conversion and HMF yield of liquid products after hydrothermal carbonization at various temperatures and times

Sample name	Conditions		Glucose conversion	Product yields (wt.%)	
	T (°C)	t (h)	(wt.%)	TRS	HMF
HTCG180-6	180	6	54.4056	61.5673	4.4859
HTCG180-12	180	12	75.4060	32.1149	3.4985
HTCG180-18	180	18	88.5224	15.5719	1.7594
HTCG180-24	180	24	95.0304	9.3323	0.7441
HTCG220-6	220	6	100.0000	3.2283	0.0000
HTCG220-12	220	12	100.0000	2.8056	0.0000
HTCG220-18	220	18	100.0000	2.5068	0.0000
HTCG220-24	220	24	100.0000	2.2875	0.0000
HTCG250-6	250	6	100.0000	2.9238	0.0000
HTCG250-12	250	12	100.0000	2.8309	0.0000
HTCG250-18	250	18	100.0000	2.0308	0.0000
HTCG250-24	250	24	100.0000	2.6739	0.0000

Table B-3: Glucose, HMF, and furfural yields obtained in liquid product of cellulose hydrolysis in subcritical water at 180°C and 5 min without and with various catalysts (0.005 g catalyst loading)

Catalysts	Glucose (wt.%)			SD
	Exp. 1	Exp. 2	Average	
No Catalyst	2.9742	1.0141	1.9941	1.3860
HTCDRB220-3	4.6977	2.0584	3.3781	1.8663
HTCG220-6	6.9195	7.0693	6.9944	0.1059
HTCDRB220-3-SO_3H	52.8692	46.3748	49.6220	4.5922
HTCG220-6-SO_3H	42.4863	44.7797	43.6330	1.6217
Graphene Oxide	44.9300	45.4194	45.1747	0.3461
Amberlyst 16 WET	43.9501	39.4774	41.7137	3.1626
Catalysts	**HMF (wt.%)**			**SD**
	Exp. 1	**Exp. 2**	**Average**	
No Catalyst	0.3048	0.2278	0.2663	0.0544
HTCDRB220-3	0.4567	0.3257	0.3912	0.0926
HTCG220-6	0.4990	0.6169	0.5580	0.0834
HTCDRB220-3-SO_3H	1.5316	1.5170	1.5243	0.0103
HTCG220-6-SO_3H	1.3505	1.2451	1.2978	0.0745
Graphene Oxide	1.0433	1.2207	1.1320	0.1255
Amberlyst 16 WET	1.1375	0.9575	1.0475	0.1273
Catalysts	**Furfural (wt.%)**			**SD**
	Exp. 1	**Exp. 2**	**Average**	
No Catalyst	0.0232	0.0216	0.0224	0.0012
HTCDRB220-3	0.0418	0.0364	0.0391	0.0038
HTCG220-6	0.0668	0.0719	0.0693	0.0036
HTCDRB220-3-SO_3H	0.1024	0.1062	0.1043	0.0027
HTCG220-6-SO_3H	0.0979	0.0923	0.0951	0.0040
Graphene Oxide	0.1064	0.1250	0.1157	0.0132
Amberlyst 16 WET	0.1156	0.0920	0.1038	0.0167

Table B-4: Fructose conversion, HMF and furfural yields obtained in liquid product of fructose dehydration in subcritical water at 180°C and 5 min without and with various catalysts (0.005 g catalyst loading)

Catalysts	Fructose conversion (wt.%)			SD
	Exp. 1	Exp. 2	Average	
No Catalyst	58.2173	54.1691	56.1932	2.8625
HTCG220-6	79.5771	76.8909	78.2340	1.8994
HTCG220-6-SO_3H	87.2958	87.8194	87.5576	0.3702
Graphene Oxide	74.8998	81.8439	78.3718	4.9102
Amberlyst 16 WET	73.8964	80.8280	77.3622	4.9014
Catalysts	**HMF (wt.%)**			**SD**
	Exp. 1	**Exp. 2**	**Average**	
No Catalyst	14.1653	14.3862	14.2757	0.1562
HTCG220-6	17.9671	17.6669	17.8170	0.2123
HTCG220-6-SO_3H	21.0555	19.5188	20.2871	1.0866
Graphene Oxide	18.0378	18.0472	18.0425	0.0066
Amberlyst 16 WET	16.1433	16.5815	16.3624	0.3098
Catalysts	**Furfural (wt.%)**			**SD**
	Exp. 1	**Exp. 2**	**Average**	
No Catalyst	0.6321	0.5403	0.5862	0.0649
HTCG220-6	0.6960	0.7313	0.7136	0.0250
HTCG220-6-SO_3H	1.0054	0.9370	0.9712	0.0484
Graphene Oxide	0.9255	0.8563	0.8909	0.0489
Amberlyst 16 WET	0.5893	0.7186	0.6540	0.0914

Table B-5: Fructose conversion, HMF and furfural yields obtained in liquid product of fructose dehydration in subcritical water at 180°C and 5 min with recycle catalyst

Recycles	Fructose conversion (wt.%)			SD
	Exp. 1	Exp. 2	Average	
Run 1	87.2958	87.8194	87.5576	0.3702
Run 2	76.7562	70.4450	73.6006	4.4627
Run 3	54.2855	60.9157	57.6006	4.6883
Run 4	53.2859	60.1255	56.7057	4.8363
Run 5	57.4670	51.6883	54.5777	4.0861
Recycles	**HMF (wt.%)**			**SD**
	Exp. 1	**Exp. 2**	**Average**	
Run 1	19.7212	19.5188	19.6200	0.1431
Run 2	16.4652	17.0938	16.7795	0.4445
Run 3	15.7620	15.6294	15.6957	0.0937
Run 4	15.8608	14.9347	15.3977	0.6548
Run 5	14.1509	14.0598	14.1053	0.0645
Recycles	**Furfural (wt.%)**			**SD**
	Exp. 1	**Exp. 2**	**Average**	
Run 1	0.8900	0.9370	0.9135	0.0332
Run 2	0.7316	0.7168	0.7242	0.0105
Run 3	0.6675	0.6144	0.6410	0.0376
Run 4	0.7233	0.5581	0.6407	0.1168
Run 5	0.5849	0.5643	0.5746	0.0146

APPENDIX C
CHARACTERIZATION TECHNIQUES

Characteristics of catalysts such morphological structure and surface characteristics, as well as chemical composition, are important determinants of the catalytic activity. In Appendix C, general description of several characterization techniques and the conditions employed are described.

C1 Scanning Electron Microscopy (SEM) (Cabús Llauradó, 2007)

External morphology of heterogenous organic and inorganic materials on a nanometer (nm) to micrometer (μm) scale can be observed and characterized by scanning electron microscopy (SEM, obtaining magnified three-dimensional-like images of their surfaces.

SEM is a microscope which uses electrons to illuminate a sample, instead of visible light used in optical microscope. When an electron beam strikes the sample, a variety of signals are generated. The three signals performing the task in SEM are secondary electrons, backscattered electrons and X-rays. Secondary electrons (SE) provide fine structure topographical feature of sample surface, while backscattered electrons (BE) are used to discriminate areas of different atomic number elements and X-rays are used to identify the composition and measure the amount of elements in the sample. The SEM operates in high vacuum so the living samples, liquids and anything that contains liquids must be dried before being observed. The SEM model JSM-7610F is Schottky field emission gun which provide high resolution, 1.0 nm at 15 kV and 1.5 nm at 1 kV, and high magnification x25 to x1,000,000. There are two SE (upper and lower) and 1 BE detectors. The application mode, gentle beam (GB) can reduce the incident electron penetration and the beam damage to the sample. Additional EDS is equipped for qualitative and quantitative, mapping and line scan elemental analysis. EDS limitations include the inabilityto detect elements below B, X-ray detection limit of 1,000-2,000 ppm (0.1-0.2 %wt.) depending on the element and the samples must not contain fluids.

Measurement Conditions

The measurements were carried out in a Field Emission Scanning Electron Microscopy (FESEM) using a FEI Quanta 200 microscope (Eindhoven, Netherlands) operated at an accelerating voltage in the 2 kV.

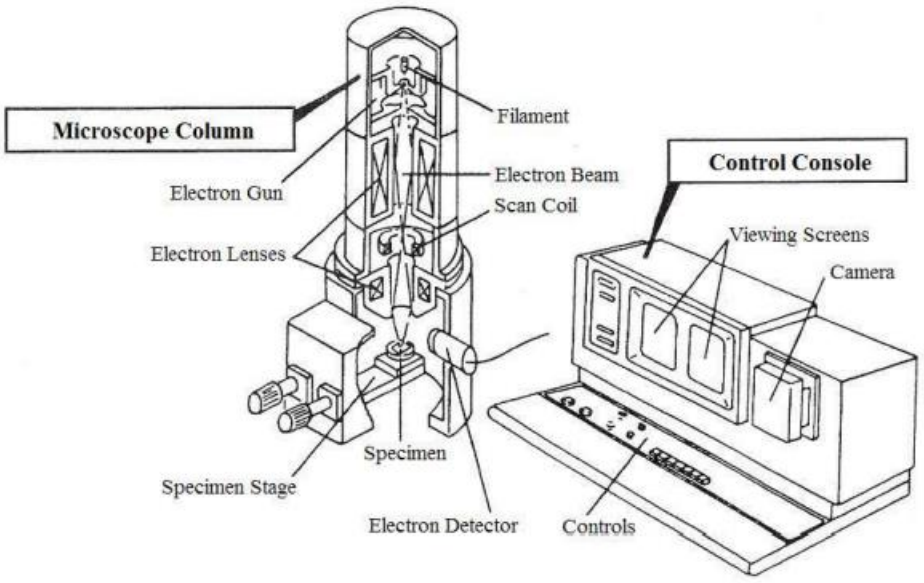

Figure C-1: Two major parts of SEM: electron column and electronics console.

The specimen support used for mounting samples consisted of aluminium alloy-stub. One side of the stub was covered by a double sided-adhesive carbon tape, where the specimen was mounted. If the specimen was non-conductive, a thin coating layer of gold would need to be applied by sputtering.

C2 X-Ray Powder Diffraction (XRD) (Cabús Llauradó, 2007)

X-ray powder diffraction plays a critical role in material research and development. Among its applications is the identification of the present phases in a multiphase specimen, the unit cell metrics, microstructure analysis of polycrystalline materials, etc.

X-rays are diffracted by the crystals. This diffraction represents the interference between X-ray scattered by the electrons in the various atoms at different locations in

the unit cell. The diffracted beam is ‘reflected’ from a plane passing through points of the crystal lattice in a manner that makes this crystal-lattice planes analogous to mirrors, so the angle of incidence is equal to the angle of reflection. The diffraction from a crystal is described by the equation known as Bragg’s law:

$$n\lambda = 2\mathbf{d}_{hkl}\sin\theta_{hkl} \qquad \text{Eq. C-1}$$

Therefore, if λ (x-ray wavelength) and θ_{hkl} (one-half the diffraction angle) are known, the perpendicular spacing between lattice planes $\mathbf{d}_{hkl}$ and consequently, the unit cells dimensions and the indices *h, k, l* of those crystal planes can be determined. A powder pattern contains a set of diffraction peak at 2θ positions which correspond to the interplanar spacing in the crystal. A schematic of x-ray powder diffractometer is shown in **Figure C-2**.

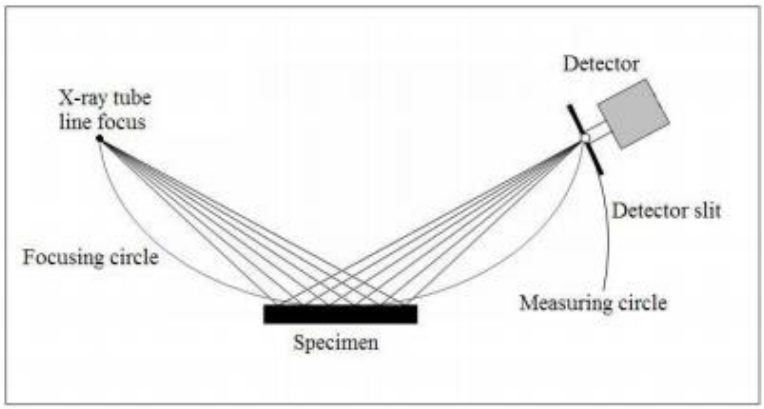

Figure C-2: Schematics of a x-ray powder diffractometer with a Bragg-Brentano parafocusing geometry.

Experimental Conditions

X-ray powder diffraction patterns of our samples were collected in a RINT 2100 diffractometer with Bragg-Brentano geometry using nickel-filtered Cu-Kα radiation (λ=0.15406 nm). Data were collected in the 2θ rang of 2-60 degrees with an angular step of each sample scanned in the range of 2-90 degrees with an angular step of 0.058

at 3 s per step. The crystalline phases were identified using the diffraction patterns of Joint Committee on Powder Diffraction Standards (JCPDS) of the International Centre for Diffraction Data (ICDD).

C3 Fourier-transform Infrared Spectroscopy (FTIR) (Cabús Llauradó, 2007)

One of the principal uses of Fourier-transform infrared spectroscopy (FTIR) is the identification of unknown substances or the characterization of their chemical structure. A spectrum of a material is its fingerprint. Sometimes it is not possible to totally identify a material from its spectrum, but the presence or absence of certain groups can be correlated with the presence or absence of absorption at specific wavelengths.

IR spectroscopy refers to radiation between two vibration states, whose wavelength (λ) is in the range 30 to 3μ ($1\mu=10^{-3}$mm) of the electromagnetic spectrum and the energy differences are in the range between 1-10 kcal mol^{-1}. The IR spectra usually present a plot of absorption (% of transmission) as a function of wavelength (cm^{-1})

FTIR spectroscopy is an interferometric method. It is a measurement technique whereby spectra are collected based on measurement of the temporal coherence of an irradiative source, using time-domain measurements of the electromagnetic radiation or other type of radiation. A schematic representation of FTIR spectrometer is presented in **Figure C-3**.

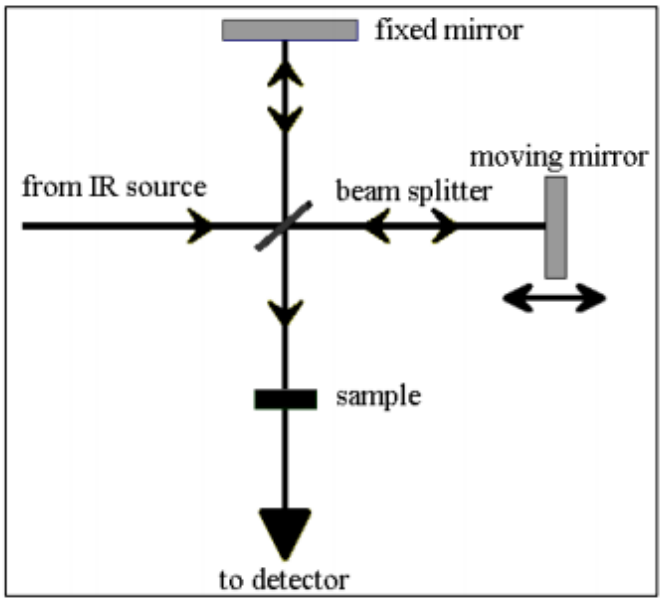

Figure C-3: Schematic set up of a FTIR spectrometer.

Experimental Conditions

The system used was a Jasco FT-IR-4100 spectrometer. Prior to each measurement, the sample was grounded into fine particles and mixed with KBr to prepare disks. The spectra were obtained directly at room temperature. The spectra were recorded in wavenumber from 4000-500 cm^{-1} with the resolution of 4 cm^{-1}.

C4 **Physisoption of Nitrogen** (Cabús Llauradó, 2007)

Adsorption occurs wherever a solid surface is exposed to fluid. It means the enrichment of one or more components in an interfacial layer. Particularly, gas adsorption has become a wide-used procedure to determine the surface area and pore size distribution of porous materials and powders. Porous solid are those solids with cavities or channels which are deeper than their widths. The pores are arbitrarily classified depending on their diameters in micropores (< 20 Å), mesoporous (20-50 Å) and macrospores (>50 Å).

Physisorption is a general phenomenon with a low degree of specificity, whose force is the same as those responsible for the condensation of vapors and the deviation from ideal gas behavior. The molecule of fluid keeps its identity along the adsorption-desorption process. It is always exothermic, and the low interactions involved are of Van der Waals type. At high pressures, it generally occurs as a multilayer (molecules of adsorbate superposed and are not in contact with adsorbent) and achieves equilibrium fairly rapidly.

Nitrogen physisorption has extensively been used, since its weak interaction with the adsorbent is suitable for physisorption phenomenon. Adsorption isotherms are the relation between the amount of adsorbed and equilibrium pressure at constant temperature. When adsorption and desorption curves are not coincident, hysteresis occurs. It appears in the multilayer range of physisorption isotherm and it is generally associated with capillary condensation. These curves have a wide variety of forms. Nevertheless, the majority may conveniently be grouped into six classes in the IUPAC classifications. Brunauer, Emmett and Teller were able to extend the Langmuir mechanism, which is a theory for monolayer molecular adsorption, to multilayer adsorption. The hypotheses of this theory are basically: (a) gas molecules physically adsorb on a solid in layers infinitely, (b) in the second and all higher layers, the energy of the adsorption has the same value as the liquefaction energy of the liquid adsorbate, (c) there is no interaction between each adsorption layer and (d) the Langmuir theory can be applied to each layer. The resulting BET equation is expressed by Eq. C-2:

$$\frac{p}{n(p_o-p)} = \frac{1}{n_m c} + \frac{C-1}{n_m C} \times \frac{p}{p_o} \qquad \text{Eq. C-2}$$

where n is the specific amount of gas adsorbed at the equilibrium pressure p, n_m is the monolayer capacity and p_o is the saturated pressure. C is a constant, which is often assumed to be exponentially related to the adsorption energy. Thus, the BET plot should be a straight line with slope of $(C-1)/n_m$ and intercept of $1/n_mC$. Then, the specific surface area, a(BET), can be obtained from the BET monolayer capacity, n_m, by applying the following simple relation (Eq. C-3):

$$a(BET)=n_mL\sigma \quad \text{Eq. C-3}$$

where L is the Avogrado constant and σ is the average area occupied by each molecule in the complete monolayer.

Although BET method has become an extremely popular method for determining the surface area of adsorbents over the past 60 years, it presents important limitations and is applicable in a restricted p/p_o range (typically between 0.05 and 0.3). Therefore, other procedures (e.g. the α_s-method) should be used, when there is significant primary micropore filling contribution and when the structure of the completed monolayer varies from one surface to another.

Experimental Conditions

N_2 adsorption and desorption isotherms at 77 K were measured on a Belsorp-mini (BEL Japan, Tokyo, Japan). Before analysis, the samples were degassed in vacuum at 150 °C for 3 h. The gas used was N_2. The surface area was calculated according to the BET method and the pore size distribution was determined by using the Barrett-Joyner-Halenda (BJH) method.

C5 Temperature Programmed Desorption (TPD) (Cabús Llauradó, 2007)

Temperature-Programmed Desorption (TPD) is one of the most widely used and flexible techniques for characterizing the acid sites on oxide surfaces.

Determining the quantity and strength of the acid sites on alumina, amorphous silica-alumina, and zeolites is crucial to understanding and predicting the performance of a catalyst. For several significant commercial reactions (such as n-hexane cracking, xylene isomerization, propylene polymerization, methanol-to-olefins reaction, toluene disproportionation, and cumene cracking), all reaction rates increase linearly with Al content (acid sites) in H-ZSM-5. The activity depends on many factors, but the Brønsted-acid site density is usually one of the most crucial parameters.

There are three types of molecular probes commonly used for characterizing acid sites using TPD:

- Ammonia
- Non-reactive vapors
- Reactive vapors

Adsorption

The sample is saturated with the basic probe at 120°C; this temperature is used to minimize physisorption of the ammonia. For ammonia, two techniques are available to saturate the sample: pulsing the ammonia using the loop or continuously flowing ammonia. Pulsing the ammonia allows the user to compare the quantity of ammonia adsorbed (via pulse adsorption) to the quantity desorbed for the subsequent TPD. Using the organic amines requires the use of a vapor generator; the sample must be saturated by using the built-in loop and pulse adsorption. The AutoChem vapor generator contains a temperature-controlled valve, reflux condenser, and flask for the probe liquid. Temperature-control allows precise control of vapor composition. Its use is imperative for liquids with high vapor pressures. The temperature zones for the AutoChem should be altered to reflect the use of vapors in the system; in particular, the temperature for the valves should be set to 110°C. While using organic amines the vapor valve zone temperature should also be set to 110°C to prevent condensation. The temperature of the condenser controls the liquid vapor pressure (and concentration of the vapor in the loop). An appropriate temperature can be obtained using the Antoinne equation to calculate the temperature required to obtain a vapor pressure or 0.1 to 0.2 bar which translates to 10 to 20% vapor composition by Dalton's equation for partial pressures (Eq. C-4).

$$\log_{10}(P_v)=A-\frac{B}{T+C} \quad \text{or} \quad T=\frac{B}{A-\log_{10}(P_v)}-C \qquad \text{Eq. C-4}$$

where: P_v = the vapor pressure in bar (1 bar=750.0615613 mmHg), T = the condenser temperature in Kelvin.

Desorption

The temperature-programmed desorption is easily performed by ramping the sample temperature at 10°C/minute to 500°C. It is a good rule of thumb that the end temperature during the TPD not exceed the maximum temperature used in the preparation of the sample. Exceeding the maximum preparation temperature may liberate additional species from the solid unrelated to the probe molecule and cause spurious results. During the TPD of ammonia, the built-in thermal conductivity detector (TCD) will monitor the concentration of the desorbed species.

Experimental Conditions

Samples are degassed at 100 °C for one hour in flowing helium to remove water vapor and to avoid pore damage from steaming which may alter the structure of zeolites. The samples are then temperature programmed to 500 ºC at a ramp rate of 10 °C/minute and held at that temperature for two hours to remove strongly bound species and activate the sample. Finally, the sample is cooled to 120 °C in a stream of flowing helium.

C6 Thermogravimetric analysis (TGA) (Gabbott, 2008)

Thermogravimetric analysis (TGA) is an experimental technique in which the weight or, strictly speaking, the mass of a sample is measured as a function of sample temperature or time. The sample is typically heated at a constant heating rate (so-called dynamic measurement) or held at a constant temperature (isothermal measurement), but may also be subjected to non-linear temperature programs such as those used in sample controlled TGA (so-called SCTA) experiments. The choice of temperature program will depend upon the type of information required about the sample. Additionally, the atmosphere used in the TGA experiment plays an important role and can be reactive, oxidising or inert. Changes in the atmosphere during a measurement may also be made. The results of a TGA measurement are usually displayed as a TGA curve in which mass or per cent mass is plotted against temperature and/or time. An

alternative and complementary presentation is to use the first derivative of the TGA curve with respect to temperature or time. This shows the rate at which the mass changes and is known as the differential thermogravimetric or DTG curve. Mass changes occur when the sample loses material in one of several different ways or reacts with the surrounding atmosphere. This produces steps in the TGA curve or peaks in the DTG curve. Different effects can cause a sample to lose, or even gain, mass and so produce steps in the TGA curve. These include the following:

- Evaporation of volatile constituents; drying; desorption and adsorption of gases, moisture and other volatile substances; loss of water of crystallization. See **Figure C-4**.
- Oxidation of metals in air or oxygen.
- Oxidative decomposition of organic substances in air or oxygen.
- Thermal decomposition in an inert atmosphere with the formation of gaseous products. With organic compounds, this process is known as pyrolysis or carbonization.
- Heterogeneous chemical reactions in which a starting material is taken up from the atmosphere, for example reduction reactions with a purge gas containing hydrogen. Furthermore, reactions in which a product is evolved, for example decarboxylation or condensation reactions.
- Ferromagnetic materials. The magnetic properties of some materials change with temperature (Curie transition). If the sample is measured in an inhomogeneous magnetic field, the change in magnetic attraction at the transition generates a TGA signal. The magnetic field is produced by placing a permanent magnet in close proximity to the furnace close to the sample.
- Uptake or loss of water in a humidity controlled experiment.

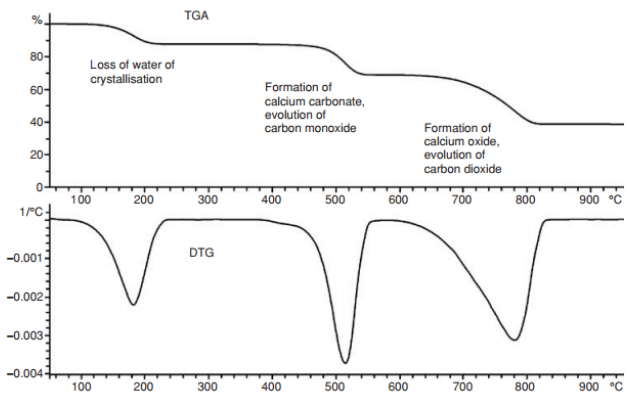

Figure C-4: Stepwise decomposition of calcium oxalate monohydrate: sample mass 19 mg, heating rate 30 K/min, nitrogen. The TGA curve has been normalized (divided by the sample weight) and therefore begins at 100%. The temperature range of the three mass losses is particularly clear in the normalized first derivative or DTG curve.

Experimental Conditions

Non-isothermal combustion of samples was conducted in the furnace of the TGA system under a nitrogen gas atmosphere at a flow rate of 10 ml/min and a heating rate of 10 °C/min from the starting temperature of 45 °C to 500 °C. The sample weight loss was continuously recorded under the experimental conditions.

C7 **Elemental Analyzer** (Source: Sophisticated Analytical Instrument Facility, IIT Bombay; http://www.rsic.iitb.ac.in/chn.html)

The CHNS(O) Analyzer find utility in determining the percentages of Carbon, Hydrogen, Nitrogen, Sulphur and Oxygen of organic compounds, based on the principle of "Dumas method" which involves the complete and instantaneous oxidation of the sample by "flash combustion". The combustion products are separated by a chromatographic column and detected by the thermal conductivity detector (T.C.D.), which gives an output signal proportional to the concentration of the individual components of the mixture.

There are different techniques for the determination of CHN\CHNS\O. It brings a new level of precision, accuracy, speed of analysis and ease of operation. The built in chromatographic column converts the compound and elutes it in the form of NO_2, CO_2, SO_2, H_2O which are then detected with the help of Thermal Conductivity Detector.

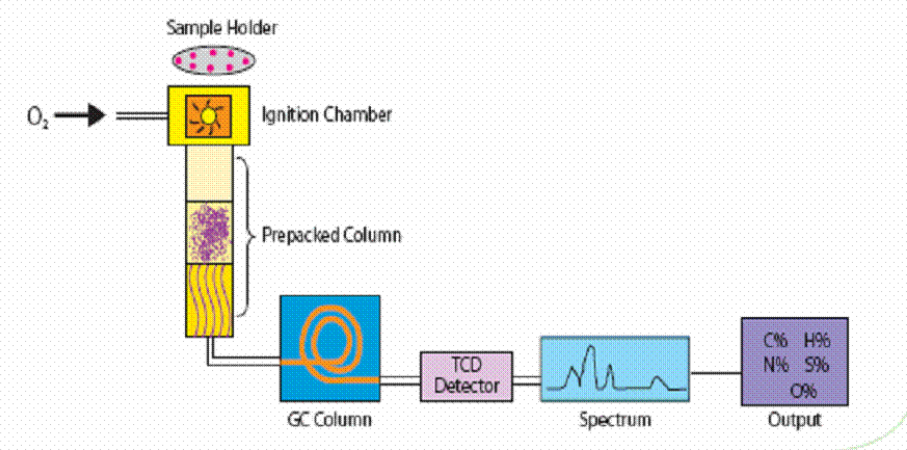

Figure C-5: Elemental analysis principle

The instrument is calibrated with the analysis of standard compounds using the K-factors calculations. Thus, the instrument ensures maximum reliability of the results because the combustion gases are not split or diluted but directly carried to build in GC system simultaneous determination of CHNS can be done in less than 10 min. This method finds greatest utility in finding out percentages of C, H, N, S, (O) in organic compounds which are generally combustible at 1800 ^oC. Key components of CHNS are auto sampler, combustion reactors, chromatographic column, and T.C.D. detector.

Experimental Conditions

The elemental compositions of samples were carried out using two equipments. For carbon, hydrogen, and nitrogen content of samples were carried out using CHN analyzer (J-Science Lab Micro Corder JM10). The sulfur content was carried out using Sulphur analyzer (J-Science Lab Micro Corder JMSU10). The oxygen content was calculated by subtraction of C, H, N, and S from 100%.

C8 High Performance Liquid Chromatography (HPLC) (Source: laboratoryinfo.com; http://laboratoryinfo.com/hplc/)

HPLC or high pressure liquid chromatography is an advance technique for the separation of components in the mixture. It can be classified as normal and reverse phase HPLC. Out of these, reversed phase HPLC is the most commonly used form of HPLC. In High performance liquid chromatography, the stationary phase can be porous solid surface active material or a liquid that is coated on an inert solid support like silica. The mobile phase moves through the packed stationary phase in the column at high pressure.

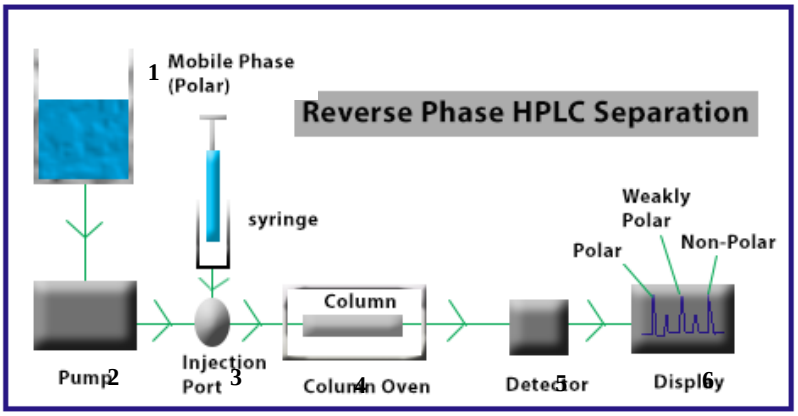

Figure C-6: The schematic diagram of HPLC system (Source: TutorVista.com; http://chemistry.tutorvista.com/analytical-chemistry/reverse-phase-hplc.html)

As shown in the schematic diagram in **Figure C-6**, HPLC instrumentation includes a pump, injector, column, detector and integrator or acquisition and display system. The heart of the system is the column where separation occurs.

1. **Solvent Reservoir**: Mobile phase contents are contained in a glass resorvoir. The mobile phase, or solvent, in HPLC is usually a mixture of polar and non-polar liquid components whose respective concentrations are varied depending on the composition of the sample.
2. **Pump**: A pump aspirates the mobile phase from the solvent reservoir and forces it through the system's column and detector. Depending on a number of factors

including column dimensions, particle size of the stationary phase, the flow rate and composition of the mobile phase, operating pressures of up to 42000 kPa (about 6000 psi) can be generated.

3. **Sample Injector**: The injector can be a single injection or an automated injection system. An injector for an HPLC system should provide injection of the liquid sample within the range of 0.1-100 mL of volume with high reproducibility and under high pressure (up to 4000 psi).
4. **Columns**: Columns are usually made of polished stainless steel, are between 50 and 300 mm long and have an internal diameter of between 2 and 5 mm. They are commonly filled with a stationary phase with a particle size of 3–10 µm. Columns with internal diameters of less than 2 mm are often referred to as microbore columns. Ideally the temperature of the mobile phase and the column should be kept constant during an analysis.
5. **Detector**: The HPLC detector, located at the end of the column detects the analytes as they elute from the chromatographic column. Commonly used detectors are UV-spectroscopy, fluorescence, mass-spectrometric and electrochemical detectors.
6. **Data Collection Devices**: Signals from the detector may be collected on chart recorders or electronic integrators that vary in complexity and in their ability to process, store and reprocess chromatographic data. The computer integrates the response of the detector to each component and places it into a chromatograph that is easy to read and interpret.

The sample is injected within the column and mixed with the mobile phase followed by being pumped under high pressure. The analytes in the sample mixture interact with the stationary phase within the column differently depending on their chemical nature. Some might be retained for a longer time as compared to others and will be hence eluted at a later stage. Finally, all the eluted components are recorded by the detector and expressed in the form of a chromatogram. This chromatogram depicts each analyte within the mixture in the form of a peak plotted against the retention time (RT). The area under the curve (AUC) is generally depictive of the concentration of the analyte.

Experimental Conditions

In this research, we used three columns to quantify the components: (i) Shodex SUGAR SH1011 column, (ii) Rezex RPM Monosaccharide Pb+2 column, and (iii) Varian C18 column.

(i) **Shodex SUGAR SH1011 column**: This column contains cross-linked polymer as a stationary phase. We used this column to quantify glucose and HMF components. Perchoric acid ($HClO_4$) was used as a mobile phase. Glucose and HMF were analyzed with detected by the refractive index (RI) detector and the UV detector at 220 nm, respectively.

(ii) **Rezex RPM Monosaccharide Pb+2 column**: Rezex columns are Ion-exclusion columns for sugar, organic acid, and alcohol analysis. In columns contain sulfonated styrene-divinylbenzene spheres in 4 and 8% cross-link forms as well as various ionic forms, including calcium, sodium, potassium, hydrogen, lead and silver. We connected this column with evaporative light scattering detector (ELSD) detector to quantify and identify glucose and fructose. This method saves the cost of operation because water is used as a mobile phase.

(iii) **Varian C18 column**: C18 is strongly hydrophobic silica-based bonded phase; used to adsorb analytes of even weak hydrophobicity from aqueous solutions; typical applications include drugs and their metabolites in serum, plasma or urine, desalting of peptides, trace organics in environmental water samples, organic acid in beverages. We used C18 to analyze the amount of HMF and furfural. A 90% (1% aq. Acetic acid):10% methanol used as an eluent and HMF as well as furfural were detected by UV absorbance detector at 285 nm.

VITA

Miss Piyaporn Wataniyakul was born February 13, 1986 in Nakhon Si Thammarat, Thailand. She finished high school from Triam Udom Suksa School of the South, Nakhon Si Thammarat in 2005. She received the Bachelor's Degree in Chemical Engineering from Department of Chemical Engineering, Faculty of Engineering, King Mongkut's University of Technology Thonburi (KMUTT) in April 2009. During her undergraduate study, she received final support from Thailand Research Fund (TRF) through the Industrial Projects for Undergraduate Students (IPUS). She completed the requirements for Master's Degree in Chemical Engineering, Faculty of Engineering, Chulalongkorn University in 2011. During her Master's Degree study, she received a scholarship from Thailand Research Fund (TRF) through the TRF Master Research Grants (TRF-MAG). Her Master's thesis was on "Hydrothermal extraction of protein and total phenolics from defatted rice bran: effect of pretreatment with microwave heating". The work was published in Bioresource Technology. After graduation, between 2011 and 2012, she worked as a process engineer at B.S.T. Elastomers Company Limited.

Ms. Piyaporn continued to pursuing her Doctor of Engineering degree in 2013 at Chulalongkorn University. During the Doctor of Engineering program, under three sources of research funding: e-ASIA Joint Research Program (e-ASIA JRP), the 100th Anniversary Chulalongkorn University Fund for Doctoral Scholarship, and the Japan Student Services Organization (JASSO) Scholarship.